

ABSTRACT

Title of Document: CLIMATE FORCING OF PHYTOPLANKTON
DYNAMICS IN CHESAPEAKE BAY

William David Miller, Doctor of Philosophy, 2006

Directed By: Professor Lawrence W. Harding, Jr.
Horn Point Laboratory, UMCES
Marine Estuarine Environmental Science

Climate has long been recognized as an important driver of phytoplankton dynamics. In Chesapeake Bay, climate variability is manifest as differences in timing and magnitude of freshwater flow. Interannual differences of freshwater flow influence phytoplankton through effects on light and nutrient distributions. Understanding how climate forces temporal and spatial patterns of phytoplankton biomass (Chla) and primary productivity (PP) is an important area of research as we attempt to predict effects of climate change and nutrient enrichment on estuarine ecosystems. This Dissertation describes climate forcing of Chla and PP using a synoptic climatology to quantify climate variability and ocean color remote sensing to assess phytoplankton variability. I developed a synoptic climatology using surface sea-level pressure data for the eastern United States to characterize regional climate because large-scale climate indices are not strongly expressed in this region. The long time series (1989-2004) of remotely sensed ocean color measurements provided high

spatial and temporal resolution that allowed me to resolve interannual differences of Chla and PP. I show that the frequency-of-occurrence of synoptic-scale weather patterns during winter explained 54% of the variance in spring freshwater flow to Chesapeake Bay through interannual differences in precipitation and water storage in the basin as snow and ice. Winter weather patterns were also linked to interannual variability of several characteristics of the spring phytoplankton bloom (timing, position, magnitude) through their effects on precipitation and freshwater flow. Multiple linear regression models of winter weather pattern frequencies on regional Chla explained between 23-89% of the variance of the time series. Climate variability in winter-spring also influenced summer and annual integral production through nutrient loading associated with the spring freshet, explaining between 43-62% of the variance of integral production. Finally, I quantified the effects of Hurricane Isabel on Chesapeake Bay phytoplankton dynamics and showed that event-scale climate perturbations can have significant impacts on ecosystem dynamics as well as seasonal and regional carbon cycling. Together these analyses highlight the importance of climate forcing of Chla and PP in Chesapeake Bay and support predictive models that explain significant amounts of the variance of these important ecosystem properties.

CLIMATE FORCING OF PHYTOPLANKTON DYNAMICS IN
CHESAPEAKE BAY

By

William David Miller

Dissertation submitted to the Faculty of the Graduate School of the
University of Maryland, College Park, in partial fulfillment
of the requirements for the degree of
Doctor of Philosophy
2006

Advisory Committee:

Professor Lawrence W. Harding, Jr., Chair

Professor Raleigh R. Hood

Professor Edward D. Houde

Professor Ming Li

Professor Thomas C. Malone

Dr. Charles R. McClain

Professor James A. Carton, Dean's Representative

© Copyright by
William David Miller
2006

Dedication

To my wife.

Acknowledgements

There is no way to adequately thank or acknowledge all the people that have helped me during my time at Horn Point, but this will serve as my best effort. I have undoubtedly forgotten some of you and I am sorry. Horn Point provides a unique environment to conduct research. If you don't experience the interdisciplinary nature of the Lab then you aren't trying. No task is too large when you have support from the entire community as you do here. Students, housekeeping, maintenance, front office, FRAs and faculty all contribute to make HPL a great place to work. I specifically want to thank all of you who have participated in lunchtime basketball or afternoon soccer with me, they may not have been the prettiest games but I smile when I think about them and I am certain I will miss them greatly.

I am grateful to my committee (Tom Malone, Ed Houde, Chuck McClain, Raleigh Hood, and Ming Li) for all their efforts and encouragement throughout this process. They have been more involved in my work than most committees and I believe my work has benefited significantly from their input. There were also a number of other faculty members who were not on my committee but were equally generous with their time and resources; particularly Diane Stoecker, Michael Kemp, Mike Roman, Bill Boicourt, and Jeff Cornwell. Anyone familiar with my work is aware that it has been a collaborative effort and that Dave Kimmel has been an essential part of my educational experience. I cannot begin to express my appreciation for the time and effort Dave has devoted to me and the interests we share.

My Dissertation has benefited from the work conducted by many members of the Harding Lab including Mike Mallonee, Jason Adolf, Christy Yeager, Andrea

Magnuson, and Kathleen Cone. I was fortunate to be part of this group and learned not only from Larry, but from everyone in the group. I would specifically like to thank Mikie. Not only is he the best technician around, he is a better person and I for one fail to recognize that enough. I would also like to thank Jason for constantly helping me to think about things, his excitement about science should be a model for us all. Lastly, I thank my research advisor, Larry Harding. I have learned a lot from Larry, and he has provided me with ample guidance, support, and opportunity. He has also shown exceptional patience and perseverance in trying to teach me how to write. I am grateful for his efforts.

The chlorophyll data I used for the majority of my dissertation required not only an airplane to collect, but skilled pilots who were willing to endure countless, mechanical, meteorological, and personnel difficulties to get good data. Those pilots include, but are not limited to; Sam White, Richard Aldridge, John Kirby, Gay Williams, Tate Jackson, John Youskaurus, Tom Tofani, Charlie McGowan, Chris Youskaurus, Steve Tomlinson, and John Sherman.

Finally, none of this work could have been accomplished without the financial support for salaries, supplies, travel, cruises, and flight time. It takes a lot of money to keep an aircraft remote sensing program running and the Harding Lab has received funds from NSF, NOAA, NASA, Maryland Sea Grant, NOAA Chesapeake Bay Office, and EPA. I specifically have benefited from HPL Education committee funds for a variety of travel, research, and workshop opportunities as well as NASA's Earth System Science Fellowship Program that supported me for three years.

Thank you all.

Table of Contents

Dedication.....	iii
Acknowledgements.....	iii
Table of Contents.....	v
List of Tables.....	vii
List of Figures.....	viii
Chapter 1: Introduction.....	1
References.....	10
Chapter 2: Predicting Spring Discharge of the Susquehanna River from a Winter Synoptic Climatology for the Eastern United States	14
Abstract.....	15
Introduction.....	16
Methods	18
Results.....	22
Discussion.....	26
Conclusions.....	33
Acknowledgements.....	33
References.....	34
Tables.....	39
Figures	42
Chapter 3: Climate Forcing of the Spring Bloom in Chesapeake Bay	54
Abstract.....	55
Introduction.....	56
Methods	59
Results.....	63
Discussion.....	67
Acknowledgements.....	72
References.....	73
Tables.....	77
Figures	80

Chapter 4: Climate Forcing of Primary Production in Chesapeake Bay	91
Abstract	92
Introduction.....	93
Methods	96
Results.....	99
Discussion.....	104
Conclusions.....	109
Acknowledgements.....	110
References.....	111
Tables.....	114
Figures	116
Chapter 5: Hurricane Isabel generated and unusual fall bloom in Chesapeake Bay	129
Abstract.....	130
Introduction.....	131
Methods	132
Results.....	133
Discussion.....	135
Conclusions.....	138
Acknowledgements.....	138
References.....	139
Tables.....	141
Figures	142
Chapter 6: Conclusions.....	145
References.....	151

List of Tables

2.1	Statistics from the linear regression of winter Niño3.4, NAO, PDO, PNA, Temperature, Precipitation, and combined Temperature + Precipitation variables against average spring flow from the Susquehanna River.....	39
2.2	Pearson’s correlation coefficients for comparisons of winter indices for NAO, ENSO, PDO, and PNA against winter frequency-of-occurrence for each cluster. * indicates significance at the $p > 0.01$ level.	40
2.3	Meteorological characteristics for clusters during winter. Standard deviations in parentheses.	41
3.1	Meteorological characteristics for weather patterns during winter 1989-2004. Wind speed and direction based on data from Baltimore-Washington International airport.	77
3.2	Results from multiple linear regression models of winter weather pattern frequencies on measurements of regional spring phytoplankton standing stock. Units for RMSE are $\text{mg chl } a \text{ m}^{-3}$ for B, $\text{mg chl } a \text{ m}^{-2}$ for B_{eu} and B_{wc} , and metric tons chl <i>a</i> for B_{tot}	78
3.3	Linear regression results of ENSO and NAO winter climate indices and winter-spring (Jan.-Apr.) freshwater flow from the Susquehanna River on regional spring phytoplankton biomass measures, ns indicates the model was not statistically significant ($p > 0.05$).	79
4.1	Meteorological characteristics for weather patterns during winter-spring 1989-2004. Wind speed and direction based on data from Baltimore-Washington International airport.....	114
4.2	Results from multiple linear regression models of winter-spring weather pattern frequencies on measurements of regional SIP and summer Chl <i>a</i> . Units for RMSE are $\text{g C m}^{-2} \text{ summer}^{-1}$ for SIP, $\text{mg chl } a \text{ m}^{-3}$ for Chl <i>a</i> , and $\text{g C m}^{-2} \text{ yr}^{-1}$ for AIP.....	115
5.1	Phytoplankton and hydrographic data before and after Hurricane Isabel.....	141

List of Figures

2.1	Map of synoptic climate region with inset of Suquehanna River Basin showing NOAA climate divisions.....	42
2.2	Flow chart of synoptic climatology methods, after Yarnal (1993).....	43
2.3	Average sea-level pressure maps for each cluster. Cluster number in upper left-hand corner.....	44
2.4	Monthly average frequency-of-occurrence by cluster. Cluster number in upper left-hand corner.....	45
2.5	Monthly temperature anomaly by cluster. Cluster number in upper left-hand corner.....	46
2.6	Monthly precipitation anomaly by cluster. Cluster number in upper left-hand corner.....	47
2.7	Time series of deviation (in days) from long-term average winter frequency-of-occurrence for each cluster. Cluster number in upper left-hand corner.....	48
2.8	Regression of observed average spring freshwater flow from the Susquehanna River on modeled flow predicted from winter cluster frequency-of-occurrence using the complete (n = 52) dataset.....	49
2.9	Plot of residuals by year from multiple linear regression model shown in figure 8.....	50
2.10	Regression of observed average spring freshwater flow from the Susquehanna River on modeled flow, predicted from winter cluster frequency-of-occurrence using the modified dataset (n = 46) with 6 outliers removed.....	51

2.11	Planktonic response in spring to years of contrasting winter weather patterns. a) weather pattern anomalies for winter 1984-5, b) weather pattern anomalies for winter 1997-8, c) phytoplankton biomass anomalies for spring 1985 in three geographical regions d) phytoplankton biomass anomalies for spring 1998 in three geographical regions, e) copepod abundance anomalies for spring 1985 in two geographical regions, f) copepod abundance anomalies for spring 1998 in two geographical regions. Error bars indicate standard error.....	52
2.12	Maps of spring phytoplankton biomass (mg m^{-3}) for long-term average condition, dry year of 1985, and wet year of 1998. Maps interpolated from Chesapeake Bay Program station data (n=49). Black bars demarcate upper, mid-, and lower Bay regions used in analyses..	53
3.1	Map of Chesapeake Bay showing flight lines from CBRSP, regions noted with heavy black lines and large numbers, and CBP stations as open circles. Regions are delineated as 1, 36.95-37.40°N; 2, 37.41-37.80°N; 3, 37.81-38.40°N; 4, 38.41-38.80°N; 5, 38.81-39.10°N; 6, 39.11-39.66°N.....	80
3.2	Average sea-level pressure maps for each cluster. Weather pattern number in upper left-hand corner. H and L indicate centers of high and low pressure regions, respectively. Black lines delineate regions of constant pressure (mb).....	81
3.3	Time series (1989-2004) of winter (December-February) frequency-of-occurrence for each cluster. Weather pattern number in upper left-hand corner. Horizontal dashed lines indicate the LTA for each weather pattern.....	82
3.4	a) Winter weather pattern deviations from LTA frequency-of-occurrence for contrasting climate extremes for years dominated by a) warm/wet weather patterns and b) cool/dry weather patterns..	83
3.5	Regional water column properties for warm/wet (black bars), LTA (open bars), and cool/dry years (gray bars) for a) Z_p and b) surface DIN. Error bars indicate standard error. Regions progress from freshwater (6) to saltwater (1).....	84

3.6	Regional mean a) B, b) B_{eu} , and c) B_{wc} for warm/wet (black circles), LTA (open diamonds), and cool/dry (gray squares) years. Error bars indicate standard error. Regions progress from freshwater (6) to saltwater (1)..	85
3.7	Percent difference from LTA for 6 regions during warm/wet years a) B, c) B_{eu} , and e) B_{wc} and cool/dry years b) B, d) B_{eu} , and f) B_{wc} . Regions progress from freshwater (6) to saltwater (1)..	86
3.8	Timing of maximum B_{tot} for warm/wet (black circles), LTA (open diamonds), and cool/dry (gray squares) years average over two week intervals.....	87
3.9	Spatially explicit maps of B for a) warm/wet, b) LTA, and c) cool/dry years.....	88
3.10	Comparison of predicted versus observed results from regional multiple linear regression models predicting spring a) B, b) B_{eu} , c) B_{wc}	89
3.11	Time series of regional predicted (open circles) and observed (black circles) results from multiple linear regression models and residuals for B, B_{eu} , B_{wc} . Horizontal dashed lines indicate the LTA for each region. Black bars indicate residuals. Region shown in upper right hand corner.....	90
4.1	Map of Chesapeake Bay showing regions used in analyses. Regions are delineated as polyhaline, 36.95°-37.80°N; mesohaline, 37.81°-38.80°N; oligohaline, 38.81°-39.66°N.....	116
4.2	Time series (1989-2004) of monthly PP estimated from CBPM for 3 regions and whole Bay. Dashed lines indicate 5 and 95% confidence intervals.....	117
4.3	Time series (1989-2004) of AIP and SIP for 3 regions and whole Bay. Pie chart shows the fraction of total production accounted for by each region.	118

4.4	Linear regression of AIP on SIP.....	119
4.5	Results of monthly Mann-Kendall trend test for 3 regions and whole Bay. Bars indicate the direction and magnitude of relationship between monthly PP estimate and year. Shading of the bars indicates the significance of the relationship.....	120
4.6	Time series (1989-2004) of SIP for 3 regions and whole Bay showing linear downward trend line. Grey bars represent residuals from that regression line.....	121
4.7	Time series (1989-2004) of summer Z_p for 3 regions and whole Bay showing linear downward trend line.....	122
4.8	Average sea-level pressure maps for 10 dominant weather patterns. Weather pattern number in upper left-hand corner. H and L indicate centers of high and low pressure regions, respectively. Black lines delineate regions of constant pressure (mb).....	123
4.9	Time series (1989-2004) of winter-spring (January-April) weather pattern frequencies-of-occurrence. Weather pattern number in upper left-hand corner. Horizontal dashed lines indicate the LTA for each weather pattern.....	124
4.10	Winter-spring weather pattern deviations from LTA frequency-of-occurrence for contrasting climate extremes for years dominated by a) warm/wet weather patterns and b) cool/dry weather patterns. Error bars indicate (± 1 SD).....	125
4.11	Phytoplankton response in summer of a) SIP and b) Chl <i>a</i> for contrasting warm/wet (black bars) and cool/dry (open bars) winter-springs. Error bars indicate (± 1 SD).	126
4.12	Moving average of Chl <i>a</i> for 3 regions and whole Bay showing Chl <i>a</i> during warm/wet years (black circles), LTA (grey circles), and cool/dry years (open circles). Error bars indicate (± 1 SD)..	127

4.13	Time series of regional predicted (open circles) and observed (black circles) results from multiple linear regression models of winter-spring weather pattern frequencies on residual SIP for 3 regions and whole Bay. Graphs on the right side show scatter plots of observed versus predicted against the 1:1 line.....	128
5.1	Phytoplankton biomass as Chl <i>a</i> : a) LTA for September 1989-04; b) pre-Isabel, 11 September; c) post-Isabel, 24 September and d) two weeks post-Isabel, 2 October. Diamonds in first panel show CBP stations used in analyses..	142
5.2	Floral composition in bloom region as percent of Chl <i>a</i> : a) LTA for fall (1995-2000); b) pre-Isabel (24 August); c) post-Isabel (3 October).....	143
5.3	a) DIN in the surface layer, and b) bottom layer; c) $\Delta \sigma_t$ from CBP cruises. Hatched area indicates bloom region.....	144

Chapter 1

Introduction

Climate has long been recognized as an important driver of phytoplankton dynamics on a variety of spatial and temporal scales (Cushing and Dickson, 1976). In the mid-Atlantic, climate is highly variable (Yarnal and Leather, 1988) and leads to commensurate variability at a number of trophic levels (Harding, 1994; Kimmel and Roman, 2004; North and Houde, 2003). Freshwater flow in rivers entering estuaries is an important expression of climate variability (Cayan and Peterson, 1993); influencing many aspects of ecosystem structure and function (Kimmerer, 2002). Malone et al. (1988) showed that flow from the Susquehanna River, the major source of freshwater to Chesapeake Bay, explained a significant amount of the variability of phytoplankton biomass (Chl *a*), and that nutrient loading associated with the spring freshet also affected the summer maximum of primary productivity (PP). Harding and Perry (1997) developed simple statistical models of regional Chl *a* from independent variables (freshwater flow, salinity, and temperature) to hind-cast Chl *a* conditions for earlier decades and separate variability associated with climate from a long-term trend linked to nutrient overenrichment. More recently, Harding et al. (2002) showed that interannual variability of annual integral production (AIP) was correlated with freshwater flow and nutrient loading in winter-spring. While these studies give evidence that freshwater flow plays an important role in Chesapeake Bay phytoplankton dynamics, I believe a more direct and comprehensive measure of climate variability may improve our ability to predict Chl *a* and PP. This Ph.D. Dissertation describes studies of climate forcing of Chl *a* and PP, using a synoptic climatology to quantify climate variability and drawing on extensive data from ocean color remote sensing to assess phytoplankton variability. This is an important area of

research as we attempt to predict effects of climate change and nutrient enrichment on estuarine and coastal ecosystems (Cloern, 2001).

Climate, defined as the average weather a region experiences (Stenseth et al., 2003), has both direct and indirect influences on phytoplankton dynamics through temperature, cloud cover, precipitation, and wind. For example, temperature directly affects rate processes i.e., growth, primary productivity (Lomas et al., 2002), but indirectly affects phytoplankton through grazer activity (Smayda et al., 2004). Cloud cover directly affects incoming solar radiation and thereby light availability to phytoplankton (Cushing and Dickson, 1976). Precipitation leads to freshwater flow with concomitant inputs of nutrients and sediment, affecting light and nutrient conditions (Cloern et al., 1983), while also influencing optimal salinity habitat for grazers (Kimmerer, 2002). Wind controls the average light phytoplankton experience via vertical mixing/stratification (Kirk, 1994) and inputs of nutrients from below the nutricline in stratified waters (Venrick et al., 1987). These properties of climate act in combination, possibly synergistically, to influence phytoplankton dynamics.

In Chesapeake Bay, the annual cycle of phytoplankton has been related to interannual differences of freshwater flow (Malone, 1992), primarily through effects on light and nutrient distributions along the north-south axis of the Bay (Harding et al., 1986). The annual maximum of biomass as integrated, water-column Chl *a* is observed during the winter-spring diatom bloom. The timing, position, and magnitude of the bloom all vary as a function of flow during the preceding winter months (Harding, 1994). The summer maximum of PP does not co-occur with the biomass maximum, but is indirectly related to winter-spring flow and associated nutrient

loading through estuarine circulation and benthic-pelagic coupling (Kemp and Boynton, 1984). The observation that Chl *a* is maximal in spring while PP peaks in summer has been attributed to differential responses of the phytoplankton communities (Malone et al., 1988). Growth rates are temperature-limited in spring so that phytoplankton compensate for increased nutrient concentrations by increasing biomass in the absence of strong grazing (biomass compensation; Malone et al., 1996). Conversely, during summer phytoplankton respond to inputs of regenerated nutrients through changes in growth rate at high summer temperatures (rate compensation; Malone et al., 1996). I observe this annual cycle as a Chl *a* maximum consisting of large diatoms in spring that dissipates by summer and is followed by a PP peak composed of flagellates and smaller diatoms in summer.

I recognize the role of freshwater flow in determining spatial and temporal variability of phytoplankton in estuaries generally (San Francisco Bay-Cloern et al., 1983; Neuse River estuary-Rudek et al., 1991; Gulf of Mexico-Justić et al., 2003), and Chesapeake Bay specifically (Malone et al., 1988; Harding, 1994). Climate principally underlies variability of freshwater flow, despite changes imposed by water regulation at dams for power or flood control and water withdrawals for agriculture or human consumption. Unlike flow that is simple to gauge, climate variability and effects on weather patterns cannot be described by a single weather element such as temperature or precipitation. Climate indices provide comprehensive measures of environmental influence that improve on individual weather measurements by consolidating multiple aspects of weather (wind, temperature, precipitation) into a simple diagnostic variable that describes coincident spatial and temporal responses of

those weather parameters (Stenseth et al., 2003). The importance of large-scale climate variability defined by indices such as El Niño/Southern Oscillation (ENSO), North Atlantic Oscillation (NAO), and Pacific Decadal Oscillation (PDO) has gained attention in recent years (Stenseth et al., 2002). These large-scale indices have documented effects on marine ecosystems (phytoplankton and higher trophic levels) in many areas, including the equatorial Pacific (ENSO; Cane, 1983; Barber and Chavez, 1983; Chavez et al., 1999), the North Atlantic (NAO; Hurrell, 1995; Barton et al., 2003; Ottersen et al., 2001), and the North Pacific (PDO; Mantua et al., 1997; Royer et al., 2001). Remotely sensed data on ocean color and temperature have improved our understanding of how these ocean-atmosphere interactions drive phytoplankton dynamics (Behrenfeld et al., 2001). However, in some areas, such as the mid-Atlantic region of the Eastern United States, large-scale climate indices are not strongly expressed and sub-continental processes assume greater importance in forcing local meteorological conditions (Tootle, 2005). This is not to suggest that large-scale climate patterns do not influence the mid-Atlantic, but rather that these forcings are manifested through changes in regional scale weather.

An alternative way to characterize climate variability at smaller spatial (1,000-2,500 km) and temporal scales, while retaining the comprehensive information incorporated in climate indices, is to create a synoptic climatology based on regional atmospheric circulation. Synoptic climatology is a statistical approach to quantify and classify atmospheric circulation patterns and is used as a regional alternative to large-scale climate indices (Yarnal, 1993). The input data are typically daily sea-level pressures, but a variety of other pressure surfaces have been reported in the literature

(Yarnal et al., 2001). This method condenses the large volume of data associated with atmospheric circulation into definable, commonly experienced weather patterns, and integrates the effects of individual meteorological parameters related to each of the patterns.

The overall goal of this dissertation was to develop quantitative relationships between climate and phytoplankton dynamics in Chesapeake Bay. I developed a synoptic climatology using surface sea-level pressure data for the eastern United States to categorize and quantify regional climate variability. Data on phytoplankton Chl *a* and PP were obtained from remotely sensed ocean color measurements spanning nearly two decades of highly variable climate forcing. The long time series and high spatial and temporal resolution of the data allowed me to resolve interannual differences of Chl *a* and PP that were attributable to regional climate forcing. The four research chapters of this dissertation; (1) describe the synoptic climatology and reconcile winter weather patterns with precipitation and freshwater flow using a water balance model; (2) document climate forcing of the spring bloom in Chesapeake Bay by quantifying the effects of winter climate on seasonal and interannual variability of phytoplankton biomass; (3) relate climate variability in winter-spring to PP in summer using integral measures of production (summer, annual); (4) demonstrate how event-scale climate perturbations such as hurricanes significantly impact phytoplankton dynamics with consequences for the ecosystem.

Chapter 2 describes the methods used to create a ‘synoptic climatology’ from surface sea-level pressure data for the eastern United States (Yarnal, 1993) and addresses the question, ‘what scales of climate variability drive interannual

differences in freshwater flow for the Susquehanna River'. I show that the magnitude of spring discharge is not related to large-scale indices of climate variability, such as ENSO or NAO, but rather is quantitatively related to the frequencies and types of 'synoptic-scale' weather patterns affecting the region. Winter weather patterns explained 54% of the variance of spring freshwater flow for the study period (1950-2002). The predictive power of this approach, i.e., winter weather explaining spring freshwater flow, is related to the fact that precipitation falling in the watershed in winter is largely stored in the basin as snow and ice and released in the spring when temperatures increase (Najjar, 1999).

Chapter 3 applies the synoptic climatology to spring bloom dynamics. The working hypothesis was that regional-scale weather patterns would explain a significant amount of the interannual variability of the spring bloom. I used data on four measures of phytoplankton biomass: surface, photic-layer, water column, and total Chl *a* to show that the forcing was expressed in several relevant measures of spring bloom intensity. Phytoplankton data were obtained from remotely sensed ocean color measurements of the Chesapeake Bay Remote Sensing Program (CBRSP) spanning 16 yrs (1989-2004), combined with shipboard data for validation and to generate depth-integrated measures of biomass. Years with more frequent warm/wet weather patterns had spring blooms that: (1) reached peak biomass farther seaward in the estuary; (2) were greater in magnitude; (3) occurred later in the spring; (4) covered a larger area than years with a predominance of cool/dry weather patterns. I also used frequencies of winter weather patterns to forecast spring Chl *a* using

multiple linear regression models that explained 23 to 89% of the variance of regional Chl *a* in spring.

Chapter 4 quantifies climate forcing of PP. I investigated the role of a number of climate time frames as drivers of variability in annual (AIP) and summer integral production (SIP). I used the synoptic scale weather pattern frequencies developed in Chapter 2 to describe climate variability and determine which climate time frame explained the highest amount of variance of PP in the same 16-yr span. To adequately quantify temporal (seasonal, interannual) and spatial variability in PP, I applied a depth-integrated model (DIM) that was calibrated and validated for Chesapeake Bay (Harding et al., 2002) to remotely sensed data to generate a time series of PP. I observed two-fold variability of AIP and SIP over the time series. Years dominated by warm/wet weather patterns in winter-spring showed higher AIP and SIP as well as elevated Chl *a* compared to the long-term average for spring and summer. Years dominated by cool/dry patterns showed the opposite responses, suggesting that climate conditions during winter-spring 'set up' the Chl *a* signal for the balance of the annual cycle. Multiple linear regression models demonstrated that AIP and SIP were more tightly linked to winter-spring weather than to summer conditions, suggesting that interannual differences in the winter-spring loading of nutrients during the spring freshet plays a critical role in driving variability of AIP and SIP.

Chapter 5 presents observations of phytoplankton responses to an event-scale climate perturbation associated with the passage of Hurricane Isabel in September 2003. Ocean color measurements from CBRSP revealed an unusually strong bloom of diatoms covering ~3000 km² of the mid- to lower Bay. This 'fall bloom' occurred in

an exceptionally 'wet year', obscuring the ecosystem response to the hurricane from that associated with high flow. I present evidence to support the hypothesis that wind mixing induced rapid de-stratification of the water column, injecting nitrogen (N) into the photic layer that supported the observed bloom at a time that N is typically limiting (Fisher et al., 1992). The bloom was ephemeral, lasting ~2-3 weeks, but its effects on regional and seasonal carbon cycling and ecosystem dynamics were significant. Particulate organic matter associated with collapse of the bloom may have remained unutilized in the surface sediments over winter due to low temperatures. This labile organic matter appeared to be the substrate for microbial degradation that resulted in an early onset of low dissolved oxygen throughout the Bay in spring 2004.

The final chapter offers general conclusions for the Dissertation, identifies new research questions that have arisen from this work, and suggests improvements and future directions. I begin by explaining how this research expands our understanding of phytoplankton dynamics in the Bay. As with any dissertation, there are more questions than answers and I outline some of them here. I conclude by offering a number of suggestions for synthesis of our knowledge and additional applications of the approach I developed.

References

- Barber, R.T., and F.P. Chavez. 1983. Biological consequences of El Nino. *Science* 222, 1203- 1210.
- Barton, A.D., C.H. Greene, B.C. Monger, and A.J. Pershing. 2003. The continuous plankton recorder survey and the North Atlantic Oscillation: interannual- to multidecadal-scale patterns of phytoplankton variability in the North Atlantic Ocean. *Prog. Oceanogr.*, 58, 337-358.
- Behrenfeld, M.J., J.T. Randerson, C.R. McClain, G.C. Feldman, S.O. Los, C.J. Tucker, P.G. Falkowski, C.B. Field, R. Frouin, W.E. Esaias, D.D. Kolber, and N.H. Pollack. 2001. Biospheric primary production during an ENSO transition. *Science* 291, 2594-2597.
- Cane, M.A. 1983. Oceanographic events during El Nino. *Science* 222, 1189-1195.
- Cayan, D.R., and D.H. Peterson. 1993. Spring climate and salinity in the San Francisco Bay Estuary. *Water Resour. Res.*, 29, 293-303.
- Chavez F.P., P.G. Strutton, G.E. Friederich, R.A. Feely, G.C. Feldman, D.G. Foley, and M.J. McPhaden. 1999. Biological and chemical response of the Equatorial Pacific Ocean to the 1997-1998 El Niño. *Science* 286, 2126-2131.
- Cloern, J.E., A.E. Alpine, B.E. Cole, R.L. Wong, J.F. Arthur, and M.D. Ball. 1983. River discharge controls phytoplankton dynamics in the northern San Francisco Bay estuary. *Est. Coast. Shelf Sci.*, 21, 711-725.
- Cloern, J.E. 2001. Our evolving conceptual model of the coastal eutrophication problem. *Mar. Ecol. Prog. Ser.*, 210, 223-253.
- Cushing, D.H., and R.R. Dickson. 1976. The biological response in the sea to climate changes. *Adv. Mar. Biol.*, 14, 1-122.
- Fisher, T.R., E.R. Peele, J.W. Ammermann, and L.W. Harding, Jr. 1992. Nutrient limitation of phytoplankton in Chesapeake Bay. *Mar. Ecol. Prog. Ser.*, 82, 51-63.
- Harding, Jr., L.W., B.W. Meeson, and T.R. Fisher. 1986. Phytoplankton in two East coast estuaries: photosynthesis-light curves and patterns of carbon assimilation. *Est. Coast. Shelf Sci.*, 23, 773-806.
- Harding, Jr., L.W. 1994. Long-term trends in the distribution of phytoplankton in Chesapeake Bay: roles of light, nutrients, and streamflow. *Mar. Ecol. Prog. Ser.*, 104, 267-291.

- Harding, Jr., L.W., and E.S. Perry. 1997. Long-term increases of phytoplankton biomass in Chesapeake Bay, 1950-1994. *Mar. Ecol. Prog. Ser.*, 157, 39-52.
- Harding, Jr., L.W., M.E. Mallonee, and E.S. Perry. 2002. Toward a predictive understanding of primary productivity in a temperate, partially stratified estuary. *Est. Coast. Shelf Sci.*, 55, 437-463.
- Hurrell, J.W. 1995. Decadal trends in the North Atlantic Oscillation: regional temperatures and precipitation. *Science* 269, 676-679.
- Justić, D., R.E. Turner, and N.N. Rabalais. 2003. Climatic influences on riverine nitrate flux: implications for coastal marine eutrophication and hypoxia. *Estuaries* 26, 1-11.
- Kemp, W.M., and W.R. Boynton. 1984. Spatial and temporal coupling of nutrient inputs to estuarine production: the role of particulate transport and decomposition. *Bull. Mar. Sci.*, 3, 242-247.
- Kirk, J.T.O. 1994. *Light and photosynthesis in aquatic ecosystems*. Cambridge University Press.
- Kimmel, D.G., and M.R. Roman. 2004. Long-term trends in mesozooplankton abundance in Chesapeake Bay, USA: influence of freshwater input. *Mar. Ecol. Prog. Ser.*, 267, 71-83.
- Kimmerer, W.J. 2002. Effects of freshwater flow on abundance of estuarine organisms: physical effects or trophic linkages? *Mar. Ecol. Prog. Ser.*, 243, 39-55.
- Lomas, M.W., P.M. Glibert, F-K. Shiah, and E.M. Smith. 2002. Microbial processes and temperature in Chesapeake Bay: current relationships and potential impacts of regional warming. *Global Change Biology* 8, 51-70.
- Malone, T.C., L.H. Crocker, S.E. Pike, and B.W. Wendler. 1988. Influences of river flow on the dynamics of phytoplankton production in a partially stratified estuary. *Mar. Ecol. Prog. Ser.*, 48, 235-249.
- Malone, T.C. 1992. Effects of water column processes on dissolved oxygen, nutrients, phytoplankton and zooplankton, p. 61-112. In D.E. Smith, M. Leffler, and G. Mackiernan [eds.]. *Oxygen Dynamics in the Chesapeake Bay: A Synthesis of Recent Research*. Maryland Sea Grant Program.
- Malone, T.C., D.J. Conley, T.R. Fisher, P.M. Glibert, L.W. Harding Jr., and K.G. Sellner. 1996. Scales of nutrient-limited phytoplankton productivity in Chesapeake Bay. *Estuaries* 19, 371-385.

- Mantua, N.J., S.R. Hare, Y. Zhang, J.M. Wallace, and R.C. Francis. 1997. A Pacific interdecadal climate oscillation with impacts on salmon production. *Bull. Am. Meteorol. Soc.*, 78, 1069-1079.
- Najjar, R.G. 1999. The water balance of the Susquehanna River Basin and its response to climate change. *J. Hydrol.*, 219, 7-19.
- North, E.W., and E.D. Houde. 2003. Linking ETM physics, zooplankton prey, and fish early-life histories to striped bass *Morone saxatilis* and white perch *M. Americana* recruitment. *Mar. Ecol. Prog. Ser.*, 260, 219-236.
- Ottersen, G., B. Planque, A. Belgrano, E. Post, P.C. Reid, and N.C. Stenseth. 2001. Ecological effects of the North Atlantic Oscillation. *Oecologia* 128, 1-14.
- Royer, T.C., C.E. Grosch, and L.A. Mysak. 2001. Interdecadal variability of Northeast Pacific coastal freshwater and its implications on biological productivity. *Prog. Oceanogr.*, 49, 95-111.
- Rudek J., H.W. Paerl, M.A. Mallin, and P.W. Bates. 1991. Seasonal and hydrological control of phytoplankton nutrient limitation in the lower Neuse River Estuary, North Carolina. *Mar. Ecol. Prog. Ser.*, 75, 133-142.
- Smayda, T.J., D.G. Borkman, G. Beaugrand, and A. Belgrano. 2004. Responses of marine phytoplankton populations to fluctuations in marine climate, p. 49-58. In N.C. Stenseth, G. Ottersen, J.W. Hurrell, and A. Belgrano [eds]. *Marine ecosystems and climate variation: the North Atlantic a comparative perspective*. Oxford University Press.
- Stenseth, N.C., A. Mysterud, G. Ottersen, J.W. Hurrell, K.S. Chan, and M. Lima. 2002. Ecological effects of climate fluctuation. *Science* 297, 1292-1296.
- Stenseth, N.C., G. Ottersen, J.W. Hurrell, A. Mysterud, M. Lima, K.S. Chan, N.G. Yoccoz, and B. Adlandsvik. 2003. Studying climate effects on ecology through the use of climate indices: the North Atlantic Oscillation, El Niño Southern Oscillation and beyond. *Proc. R. Soc. Lond., B* 270, 2087-2096.
- Tootle, G.A., T.C. Piechota, and A. Singh. 2005. Couple oceanic-atmospheric variability and U.S. streamflow. *Water Resour. Res.*, 41. [doi:10.1029/2005WR004381].
- Venrick, E.L., J.A. McGowan, D.R. Cayan, and T.L. Hayward. 1987. Climate and chlorophyll a: long-term trends in the Central north Pacific Ocean. *Science* 238, 70-72.

Yarnal, B., and D.J. Leathers. 1988. Relationships between interdecadal and interannual climatic variations and their effect on Pennsylvania climate. *Annals of the Association of American Geographers* 78, 624-641.

Yarnal, B. 1993. *Synoptic Climatology in Environmental Analysis*, Belhaven Press.

Yarnal, B., A.C. Comrie, B. Frakes, and D.P. Brown. 2001. Developments and prospects in synoptic climatology. *Int. J. Climatol.*, 21, 1923-1950.

Chapter 2

Predicting Spring Discharge of the Susquehanna River from a Winter Synoptic Climatology for the Eastern United States¹

¹Miller, W.D., D.G. Kimmel, and L.W. Harding, Jr. 2006. Predicting Spring Discharge of the Susquehanna River from a Winter Synoptic Climatology for the Eastern United States. *Water Resources Research* 42, W05414, [doi:10.1029/2005WR004270].

Abstract

Seasonal and interannual variations of freshwater flow strongly influence estuarine processes, exemplified by plankton biomass and productivity. The main tributary feeding Chesapeake Bay, the Susquehanna River, has shown 3-fold variability of spring flow in the last 52 years. The magnitude of spring discharge from the Susquehanna River is associated with the frequency and type of weather patterns transiting the Eastern United States during winter and is related to the precipitation stored in the basin as snow and ice. Large-scale indices of climate variability, such as El Niño/Southern Oscillation (ENSO) and the North Atlantic Oscillation (NAO), have not proven to be strong predictors of freshwater flow in the mid-Atlantic. I developed a synoptic climatology as an alternative way to quantify and classify regional weather, focusing on the types and frequency-of-occurrence of patterns I identified for winter. This approach was used to predict freshwater flow in spring and explained 54% of the variance of spring discharge after extreme outliers were removed. Responses of Chesapeake Bay plankton to contrasting years of weather pattern frequencies and associated freshwater flow were examined to illustrate ecosystem response to climatic forcing.

Introduction

Freshwater flow into an estuary affects important physical and chemical processes, including circulation, stratification, sedimentation, nutrient loading, light attenuation, and dissolved oxygen (Schubel and Pritchard, 1986). The distribution and abundance of many ecologically and economically important estuarine organisms, such as phytoplankton and zooplankton, are also strongly influenced by freshwater flow (Kimmerer, 2002). Phytoplankton and zooplankton are key components of estuarine systems that are being used as indicators of ecosystem status (Paerl et al., 2003). To detect change in ecosystems using plankton as indicators, we must understand how the indicators respond to environmental variability, driven largely by changes in freshwater flow. Ecosystem responses to freshwater flow have been documented for estuaries and coastal systems including San Francisco Bay (Cloern et al., 1983; Kimmerer, 2004), the Gulf of Mexico (Riley, 1937; Justić et al., 2003), and the Hudson River estuary (Malone, 1977; Howarth et al., 2000). Freshwater flow into Chesapeake Bay has been related to dissolved oxygen (Boicourt, 1992; Hagy et al., 2004), phytoplankton biomass (Malone et al., 1988; Harding and Perry, 1997), zooplankton abundance (Kimmel and Roman, 2004), and larval fish recruitment (Wood, 2000; North and Houde, 2003; Jung and Houde, 2003).

During the last 52 years, the Susquehanna River as the major source of freshwater to Chesapeake Bay has experienced 3-fold variability of spring flow (range = 988 – 3366 m³ s⁻¹). Interannual differences in the types and frequencies of atmospheric circulation patterns that transit the Susquehanna River basin influence regional temperature and precipitation, and thereby strongly affect freshwater flow (Yarnal and Frakes, 1997). Najjar (1999) showed that much of the streamflow increase that

occurs during spring could be attributed to release of winter precipitation that is stored in the basin over winter as snow. A number of studies have addressed the relationship of atmospheric circulation to precipitation and freshwater flow (Peterson et al., 1989; Cayan and Peterson, 1989, 1993; McCabe and Ayers, 1989; Wilby, 1993), and specifically for the Susquehanna River (Crane and Hewitson, 1998; Lakhtakia et al., 1998; Yu et al., 1999; Najjar, 1999). Despite the overriding influence of flow on ecosystem structure and function in this important estuary (Malone et al., 1988; Kimmel and Roman, 2004), a predictive link between freshwater flow and variability in atmospheric circulation has not been developed.

Large-scale indices of climate variability, such as El Niño/Southern Oscillation (ENSO) and the North Atlantic Oscillation (NAO), have strong effects on marine ecosystems, such as the equatorial Pacific (Cane, 1983; Barber and Chavez, 1983; Stenseth et al., 2002) and the North Atlantic (Hurrell, 1995; Ottersen et al., 2001; Stenseth et al., 2002), but their influence in the mid-Atlantic region is ambiguous (Read, 2002; Stenseth et al., 2003). This is not to suggest that large-scale climate indices do not influence the Mid-Atlantic, but rather that these forcings are manifest through changes in regional scale weather. An alternative way to characterize climate variability at smaller spatial (1,000-2,500 km) and temporal (interannual) scales is to create a synoptic climatology that is based on regional atmospheric circulation. Yarnal (1993) defines synoptic climatology as the relationship between atmospheric circulation and the surface environment. It is a statistical approach to classify and quantify predominant weather patterns in a region. This procedure condenses the large volume of data associated with atmospheric circulation into definable,

commonly experienced weather patterns, and integrates the effects of the individual meteorological parameters related to each of the patterns.

I developed a synoptic climatology for the Eastern United States in order to describe the climatic variability in the region. I postulated that defining and quantifying the climatic drivers of freshwater flow would support analyses of the causes and scales of variability in estuarine ecosystems. This paper: 1) describes and quantifies the predominant synoptic-scale weather patterns in the Eastern United States over the last 52 years; 2) identifies anomalies in the frequency-of-occurrence of these synoptic-scale weather patterns that underlie interannual differences in spring discharge; 3) predicts spring flow from synoptic-scale weather patterns in winter; 4) addresses how this predictive capability will improve our understanding of estuarine responses to climate variability, climate change, and anthropogenic perturbations, expressed in planktonic processes.

Methods

Data

Twice daily (0 and 1200 h GMT), 5° latitude by 5° longitude gridded sea level pressure (SLP; mb) data were acquired from the National Center for Atmospheric Research (NCAR; <http://dss.ucar.edu>). These data were averaged to produce 19,358 daily maps of SLP for the study period, 1 January 1950 through 31 December 2002. Gridded data have biases that must be acknowledged (Reid et al., 2001), but they provide the best source of data for these analyses (Yarnal, 1993). Daily and monthly data on temperature and precipitation for use in regression models and descriptions of synoptic-scale weather patterns were obtained from the National Climate Data Center

(NCDC; <http://cdo.ncdc.noaa.gov>). Divisional data from the eight climatic regions within the Susquehanna River basin (Pennsylvania divisions 4, 5, 6, 7, 8; Maryland division 6; New York divisions 1, 2; Fig. 2.1 inset) were weighted by area to produce a single estimate of temperature or precipitation for the basin. Climate division data were used because they provide comprehensive measures of temperature and precipitation from all stations in a division (Guttman and Quayle, 1996). Freshwater flow ($\text{m}^3 \text{s}^{-1}$) for the Susquehanna River was obtained from the United States Geological Survey gauging station at Harrisburg, Pennsylvania (USGS-01570500; 100 km from mouth; <http://waterdata.usgs.gov>), and extrapolated to the entire watershed based on the relationship between flow at Harrisburg and the Conowingo Dam (USGS-01578310; 15 km from mouth; Harrisburg flow * 1.125 = Conowingo flow) to generate a continuous flow record for the entire period of analysis, as data for Conowingo only extended back to 1967. Data for the plankton analyses were obtained from the Chesapeake Bay Program monitoring cruises (CBP; <http://www.chesapeakebay.net>). Geographical regions for planktonic responses are defined as; upper $> 38.8^\circ \text{N}$, middle $38.8^\circ \text{N} - 37.8^\circ \text{N}$, lower $< 37.8^\circ \text{N}$.

Synoptic Climatology

Surface SLP data were used to describe atmospheric circulation patterns following an eigenvector-based, map-pattern classification procedure outlined in Yarnal (1993) and Wood (2000) (Fig. 2.2). A 48-point (6x8) grid of SLP data covering the area 25° to 50°N latitude and 65° to 100°W longitude was identified as the region of interest (Fig. 2.1). Next, an S-mode eigenvector analysis (principal component analysis; PCA) was performed on a correlation matrix of SLP station data

against time (days) to reduce spatial variability in the data set from the original 48 points to a smaller number of new, statistically independent (orthogonal) variables (PC scores) that explained 90% of the variance in the original data set. The number of variables to retain (7) was determined in two ways: 1) a 'scree' test in which a major break in the plot of eigennumber versus eigenvalue establishes the number of variables to retain and 2) the N-rule test (eigenvalues > 1) (Yarnal, 1993). Comparison of rotated and unrotated PC scores gave similar results and thereafter unrotated results were used for the analyses. The saved scores from the PCA were then submitted to a two-stage clustering procedure to identify similarly occurring modes of variance related to atmospheric circulation patterns. The first stage employed an agglomerative, hierarchical cluster analysis (average-linkage) to maximize the between-cluster variance which was used to determine the number of clusters (10) comprising a significant fraction of the total number of days ($>2\%$), and to provide 'seed' values for a subsequent *k*-means clustering procedure. This second clustering procedure regrouped the retained PC scores into one of 10 dominant 'seed' clusters identified previously. Once all days were categorized into one of 10 clusters, the average SLP from each grid point within each cluster was determined, and average SLP maps were generated for visualization. These clusters represent the prevailing weather patterns experienced in the region. Monthly frequency-of-occurrence for each weather pattern was then determined for use in regression models.

Data Analyses

All analyses were performed using S-PLUS 6.2 (Insightful Corp.) statistical software. Pearson's correlations were used to determine relationships between the frequency-of-occurrence of synoptic-scale weather patterns during winter (December-January-February) and the winter NAO index defined as the normalized SLP difference between the Azores and Iceland (Hurrell, 1995), the winter ENSO index defined as sea-surface temperature anomaly in the Niño3.4 region (5° N-5° S, 170°-120° W; Trenberth and Stepaniak, 2001), the winter Pacific Decadal Oscillation index (PDO) defined as the leading eigenvector of North Pacific sea-surface temperature (Mantua et al., 1997), and the winter Pacific/North America pattern (PNA) defined as the dominant rotated empirical orthogonal function of 500 hPa geopotential height anomalies for the Northern Hemisphere (Barnston and Livezey, 1987). Anomalies were calculated as the difference between monthly/seasonal conditions and the long-term average for weather patterns (1950-2002), temperature (1950-2002), precipitation (1950-2002) and planktonic responses (1985-2002). Simple linear regression models were used to determine the strength of relationships between average spring freshwater flow (March-April-May) and the winter climate indices for NAO, ENSO, PDO, PNA, and basin-wide temperature and precipitation. Using the complete 52 year dataset, a multiple linear regression model was developed to predict spring Susquehanna River flow from winter cluster frequencies-of-occurrence with limited success. A robust least trimmed squares regression model (Rousseeuw, 1984) was used to determine outliers from the freshwater flow data set. These outliers were removed and a second regression model was developed from the modified dataset. The ten clusters used as explanatory variables were not statistically independent from

one another, violating an assumption of the regression model. However, this violation only affects the interpretation of the regression coefficients, not the r^2 , significance, or reliability of the predicted values and therefore, the model still provides valuable information (Shaw, 2003). No interpretation of the coefficients was attempted in these analyses. Differences in planktonic response during example years and the long-term average were determined by t-test (Zar, 1984).

Results

Climate Indices and Weather Variables

Climate indices for NAO, ENSO, PDO, and PNA during winter explained less than 8% of the variance of Susquehanna River flow during spring and were not significant at the 0.05 level (Table 2.1). Regressions of regional average temperature and precipitation, individually and multiple regressions of temperature and precipitation combined, explained a maximum of 16.7% of the variance in spring flow, with precipitation and combined precipitation and temperature producing significant models (Table 2.1). Pearson's correlation coefficients between the frequency-of-occurrence of individual clusters and climate indices (NAO, ENSO, PDO, and PNA) revealed weak to moderate relationships for many of the variables, with strongest associations to the Niño3.4 index (Table 2.2). The correlations reached a maximum of 0.466 and were both positive and negative in sign.

Synoptic Climatology

I identified ten significant weather patterns (Fig. 2.3), each occurring 3.9 to 16.8% of the days in the study period during winter (Table 2.3). Several maps showed very recognizable weather patterns, including the Bermuda High in cluster 1 and the Nor-

easter in cluster 4. The environmental conditions associated with each cluster are shown in Table 2.3, indicating whether the conditions are warm or cold, or wet or dry on days when the patterns occurred. For instance, when cluster 2 occurred during winter it was on average 3.0 °C colder and received 0.9 mm day⁻¹ less precipitation than the long-term average for December, January, and February in the Susquehanna River basin. Alternatively when cluster 4 occurred, conditions tended to be 2.0 °C warmer and the basin received 2.7 mm day⁻¹ more precipitation than average.

Each daily observation was associated with a map pattern, supporting computation of the frequency-of-occurrence for each weather pattern for specific time periods. Several map patterns were identified, using the monthly frequency-of-occurrence that had distinct seasonal signals (Table 2.3; Fig. 2.4). Weather patterns captured by clusters 1, 8, and 9 occurred commonly throughout the year, were predominant in summer, and comprised over 60% of June and July days, associated with positive temperature anomalies (Fig. 2.5). Clusters more common in winter, including 2, 7, and 10, had a summer minimum and a winter maximum of up to 50% of January days, associated with negative temperature anomalies and low precipitation (Figs. 2.5, 2.6). While cluster 4 did not occur commonly in any season, it may be disproportionately important due to potentially heavy precipitation that accompanies this pattern in winter and spring (Table 2.3; Figs. 2.4, 2.6).

Deviations from the long-term frequency-of-occurrence during winter showed large changes for several clusters, including clusters 2, 7, and 10 (Fig. 2.7), while others, such as clusters 1, 8, and 9, showed little variation (Fig. 2.7), coinciding with winter and summer dominant clusters respectively. Trends in cluster frequency-of-

occurrence during winter were tested with a Mann-Kendall trend test. There were no significant changes in cluster frequency-of-occurrence during winter (1950-2002), except for cluster 5 which had a small but significant positive increase.

Weather Pattern-Flow Relationship

The multiple linear regression model developed using the complete 52 year dataset produced a non-significant model ($p = 0.32$) with limited success in predicting spring freshwater flow ($r^2 = 0.22$; $RMSE = 520 \text{ m}^3 \text{ s}^{-1}$) from winter weather patterns (Fig. 2.8). A robust least trimmed squares regression model identified six points as being more than 2.5 standard deviations from the regression line of winter cluster frequency-of-occurrence and spring flow (Fig. 2.9). These points were the first (1995), second (1981), and fifth (1969) driest and the first (1993), second (1994), and fourth (1972) wettest springs in the data set (1950-2002). After removal of these extreme points, the modified dataset ($n = 46$) produced a new, highly significant model ($p < 0.001$) with a substantial improvement in variance explained ($r^2 = 0.54$) and reduction in error ($RMSE = 329 \text{ m}^3 \text{ s}^{-1}$) (Fig. 2.10).

Planktonic Response

Planktonic responses in Chesapeake Bay to strongly contrasting freshwater flow and associated weather patterns were exemplified by the conditions in 1985 and 1998 (Fig. 2.11a-f). During winter of 1984-5, two of the patterns that occurred more frequently than average (clusters 2 and 10) were the driest (Table 2.3; Fig. 2.6), while the patterns that occurred less frequently than average (clusters 3 and 4) often produced high precipitation in winter (Table 2.3; Fig. 2.6); this led to spring flow $552 \text{ m}^3 \text{ s}^{-1}$ (28.9%) below average (Fig. 2.11a). Alternatively, the winter of 1997-8 saw

wet weather patterns (clusters 3, 4, and 8) occur 32 days more frequently than average, while drier patterns (clusters 2 and 10) occurred 23 days less frequently than average (Table 2.3); resulting in spring flow $559 \text{ m}^3 \text{ s}^{-1}$ (29.0%) above average (Fig. 2.11b).

Observations of phytoplankton biomass in 1985 and 1998 showed conditions significantly different from average, particularly in the middle portion of Chesapeake Bay (Fig. 2.11c, d; Fig. 2.12). Long-term average biomass for the Bay, in spring, reaches a maximum in the mid-Bay (9.5 mg m^{-3}) with slightly lower concentrations in the upper (7.7 mg m^{-3}) and lower Bay (7.3 mg m^{-3} ; Fig. 2.12). During the low flow conditions of 1985, biomass was significantly (t-test; $p < 0.01$) greater than average in both the upper (14.8 mg m^{-3}) and mid-Bay (14.6 mg m^{-3}), while the lower Bay showed a non-significant 1.9 mg m^{-3} decrease (Figs. 2.11c, 2.12). In 1998, high flow caused below average biomass in the upper Bay (6.0 mg m^{-3}), along with significantly above average biomass in the mid-Bay (t-test; $p < 0.02$; 13.8 mg m^{-3}) and a modest increase of 1.0 mg m^{-3} in the lower Bay (Fig. 2.11d).

Eurytemora affinis, a dominant calanoid copepod and major food source for larval fish, responded strongly to differences in spring flow (Figs. 2.11e, f). Average *E. affinis* abundance for spring is higher in the upper Bay (mean= 18159 no. m^{-3}) relative to the mid-Bay (mean= 3684 no. m^{-3}). Zooplankton abundance was significantly (t-test; $p < 0.001$) below the long-term average for both the upper and middle regions of the Bay in 1985 (Fig. 2.11e). In the high flow year of 1998, upper Bay *E. affinis* abundance was close to the long-term average (16005 no. m^{-3}); while mid-Bay values were 10444 no. m^{-3} above average (Fig. 2.11f). Due to small sample size ($n=3$) and

high variance (s.d.=20582), the 1998 mid-Bay observations were not significantly different from the long-term average (t-test; $p>0.20$).

Discussion

Climate interacts with ecology through local weather patterns (Stenseth et al. 2003). Freshwater flow acts as an integrator of climate variability by reducing the short-term noise associated with local temperature and precipitation (Cayan and Peterson, 1989). Hypothesized responses of estuarine ecosystems to climate change in the mid-Atlantic are strongly coupled to changes in freshwater flow (Najjar et al., 2000; Neff et al., 2000; Gibson and Najjar, 2000). The primary goal of this paper was to describe a quantitative link between climate variability and estuarine plankton dynamics through freshwater flow. I have shown that large-scale climate indices are limited in predicting freshwater flow from the Susquehanna River. I developed an alternative methodology to classify and quantify regional climate variability with a synoptic climatology. This approach to quantifying climate variability provided us with a tool to predict spring freshwater flow with a reasonable degree of confidence. Finally I showed how these interannual variations in spring flow from the Susquehanna River influence plankton dynamics in Chesapeake Bay.

Climate Indices

Large-scale climate indices, such as NAO and ENSO, provide an integrated measure of climate variability over broad spatial and temporal scales (Stenseth et al. 2002). They are correlated to a limited extent with local weather patterns in the Eastern United States (Table 2.2), but these indices do not support prediction of spring flow from the Susquehanna River (Table 2.1). Read (2002) identified ‘modest’

correlations between NAO and flow for several smaller watersheds within the Susquehanna River basin during winter and spring, however, this analyses was limited to smaller watersheds with no anthropogenic impacts on flow (i.e. dams and urban development). In addition, Read (2002) looked at correlations between variables from the same season; I am interested in lagged flow in spring related to precipitation stored in the basin over winter as snow-pack. Indices of ENSO have been used to successfully predict lagged flow in rivers of the Western US with contrasting patterns in the Pacific Northwest and Southwestern US (Redmond and Koch, 1991). While the relationships are not as strong in the Mid-Atlantic, the positive correlation with ENSO (Table 2.1) may be related to increased storm frequency during El Niño years (Hirsch et al., 2001). Stenseth et al. (2003) suggested that the lack of strong correlations between local weather patterns and large-scale climate indices can be related to a number of factors; including: i) variation in local response depending upon geographic location, ii) variation in the intensity of the index with season, iii) change in the relationship between local weather and climate indices over time, iv) nonlinear response of local weather to indices, or v) simply that any given index may only explain a small fraction of the variance in a region's weather. Therefore our results of no strong correlation between large-scale climate indices and Susquehanna River flow are not unexpected.

Water Balance

Another approach to predicting freshwater flow is to develop a water balance model that estimates flow from the difference between input and loss terms. Precipitation and temperature are two of the most important parameters for prediction

of freshwater flow from water balance models (Thorntwaite, 1948). Najjar (1999) developed a water balance model for the Susquehanna River basin using precipitation and temperature that successfully estimated monthly flow, however, the model used real-time precipitation and temperature to predict freshwater flow, providing limited forecasting ability. Our linear regression models using winter precipitation and temperature alone and combined to predict spring flow, while significant, did not explain a large portion of the variance in spring flow (Table 2.1). I believe this approach had limited success because, although important meteorological parameters, temperature and precipitation do not provide a comprehensive description of weather variability (Davis and Kalkstein, 1990).

Synoptic Climatology

To address the limitations of climate indices and water balance models in predicting freshwater flow from the Susquehanna River, I developed a synoptic climatology of the region using maps of SLP. I quantified 52 years of synoptic-scale weather patterns affecting the Eastern U.S. for the purpose of understanding how climate variation affects freshwater flow to Chesapeake Bay. These patterns agree well with literature descriptions of common weather patterns for the region in terms of map structure, seasonality in frequency-of-occurrence, and the weather conditions associated with each pattern (Hayden, 1981; Yarnal and Leathers, 1988; Davis et al., 1993; Davis et al., 1997). High pressure patterns, such as clusters 1, 2, 7, and 9, and their average frequencies coincide well with seasonally distinct modes of the North Atlantic subtropical anticyclone described by Davis et al. (1997). Interannual variations in the frequency-of-occurrence of these ‘summer’ (warm and moist) or

‘winter’ (cold and dry) modes, during winter, have implications for spring freshwater flow through changes in storage within the watershed. Due to their tendency to produce high wind, waves, and precipitation, much research has focused on the frequency, track, generation location, and path of Atlantic Coast 'Nor-Easters' (Hayden, 1981; Davis et al., 1993; Zielinski, 2002). Cluster 4 (Fig. 2.3) represents the completion of a typical Nor-easter track. Passage of this cluster is often associated with heavy precipitation in the Susquehanna River watershed (Fig. 2.6). While relatively rare in frequency-of-occurrence these patterns are extremely important because of their potential to deposit significant amounts of snow over much of the watershed during winter. This snow often stays locked in the basin as ‘storage’ until the warmer spring temperatures release the water as part of the spring freshet (Najjar, 1999).

Weather Pattern-Flow Relationship

I have successfully downscaled from the frequency-of-occurrence of synoptic-scale weather patterns during the winter to spring Susquehanna River flow, explaining 54% of the variance in the modified dataset. Removal of six ‘outliers’ was necessary to obtain this result. The rationale for that decision is discussed below. First, the least trimmed squares regression identified these six points as being more than 2.5 standard deviations from the mean; these points were having a large influence on the regression results. Second these points were hydrologic extremes as the first, second, and fifth driest (lowest flow) and first, second and fourth wettest (highest flow) springs. While the prediction of extremes is important, this model is better suited to forecast the more typical interannual variations in flow that still have

significant impacts on Chesapeake Bay plankton. Finally several of the wet extreme years (1993 and 1994) had exceptional events (blizzards) in March which were outside the time frame identified in these analyses for the climate forcing of freshwater flow. Similarly, during the dry years drought conditions prior to the winter time frame influenced the spring flow. Models developed with winter climate as the independent variables cannot be expected to predict flow that is dominated by events before or after that time frame. Because this model does not predict extremes well, inclusion of the outliers (using the entire dataset) resulted in a substantial decrease ($r^2 = 0.22$) in variance explained and a non-significant model ($p = 0.32$).

There are several potential mechanistic explanations for why the winter weather patterns predict spring freshwater flow better than other variables. In large river basins, there is often a time lag between precipitation and basin flow, and that lag can often be as great 50% of the precipitation on monthly time scales (Gleick, 1987). Precipitation falling during the winter is often retained in the higher elevations of a basin as snow and is not released until spring temperatures melt it (Najjar, 1999). The amount of water stored in this reservoir depends not only on the amount of precipitation falling, but also on winter temperature (Cayan and Peterson, 1993). The synoptic-scale weather patterns used in these analyses take into account the cumulative effects of the weather associated with each pattern, including parameters such as wind speed and direction, cloud cover, and dew point all of which influence storage (Davis and Kalkstein, 1990). Finally, large-scale climate oscillations influence local environmental conditions through changes in local weather patterns (Stenseth et al., 2003). Therefore, use of the regional weather patterns, described by

the synoptic climatology, to predict a local environmental response eliminates one potential source of variability in the linkage.

Potential reasons for the unexplained variance in our regression include; a lack of ability to address the magnitude of precipitation for certain weather patterns, disconnects between the artificial delineation of seasons used in the model, and large precipitation events in the spring that have immediate impacts on freshwater flow. For instance, small variations in the track of cluster 4 can produce large differences in the amount and type of precipitation the watershed experiences (Zielinski, 2002). As mentioned previously, the forecasting ability of this model is largely related to the storage of winter precipitation as snowpack (Najjar, 1999), therefore forecasting during other seasons is likely to be less successful. Due to the relationship between freshwater flow and Chesapeake Bay plankton dynamics, this model provides information that will be useful to managers of both water resources and estuarine ecosystems. This approach can be used to separate variability from trends in highly dynamic datasets by quantifying a climate signal that can be extracted. Future work will incorporate this technique and expand on the relationships between atmospheric circulation and Chesapeake Bay plankton discussed here.

Planktonic Response

Chesapeake Bay phytoplankton dynamics in spring are described well by the interplay of light and nutrients, driven by variations in freshwater flow (Fig. 2.12) (Malone et al., 1988; Harding, 1994). Lower than average flow in 1985 resulted in reduced input of nutrients and sediment to the Bay. Greater than average phytoplankton biomass was observed in the upper and mid-Bay during the spring due

to increased photic depth (126% of LTA) associated with below average river-born sediment delivery (Fisher et al., 1988). Negative phytoplankton anomalies were observed in the lower Bay because lower than average flow exacerbated nutrient limitations (55% of LTA; Fig. 2.11c). Alternatively, high nutrient and sediment loading associated with high flows in 1998 created shallower than average photic depth (87% of LTA) in the upper Bay and concomitant decreased phytoplankton biomass. The mid-Bay saw positive biomass anomalies related to increased nutrient loading (130% of LTA), while the lower Bay showed a slight biomass increase (Fig. 2.11d) (Harding et al., 1986).

Zooplankton, exemplified by the copepod *E. affinis* respond strongly to variations in freshwater input through changes in preferred low salinity and low temperature habitat, and changes in the size of estuarine turbidity maximum (an area of plankton and fish aggregation located near the head of the estuary) (Kimmel and Roman, 2004). During the spring of 1985 *E. affinis* abundance was well below average in the upper Bay due to above average salinities (131% of LTA), low turbidity and reduced size of the estuarine turbidity maximum despite preferred below average temperatures (Roman et al., 2001), while above average salinities (119% of LTA) also reduced biomass in the mid-Bay region (Fig. 2.11e). In 1998, estuarine conditions were favorable for *E. affinis* in the mid-Bay, where low salinities (61% of LTA) and high turbidity resulted in an expanded estuarine turbidity maximum in this region, while exceptionally high flows pushed favorable habitat conditions out of the upper Bay resulting in below average *E. affinis* concentrations (Fig. 2.11f).

Conclusions

A large portion of the physical and biological variability in an estuary can be related to changes in freshwater flow (Schubel and Pritchard, 1986; Kimmerer, 2002). Impacts of climate change on estuarine ecosystems are expected to be driven largely by changes in freshwater flow (Najjar et al., 2000). Our ability to separate natural variability from anthropogenic trends in many key ecosystem indicators is strongly influenced by freshwater flow (Boicourt, 1992; Harding, 1994; Kimmel and Roman, 2004; Jung and Houde, 2003). This paper has shown that the frequency-of-occurrence of winter weather patterns, described by a synoptic climatology, can be used to forecast spring freshwater flow with the caveat that extreme conditions may not be predicted well. Quantifying the link between regional climate and freshwater flow provides the information necessary to forecast ecosystem response to changing environmental conditions.

Acknowledgements. The authors thank Bob Wood and Brent Yarnal for helpful discussions and Ming Li, Ed Houde, and Tom Malone for constructive reviews. WDM was supported by a NASA Earth System Science Fellowship. Although the research described in this article has been funded in part by the United States Environmental Protection Agency through cooperative agreement R82867701 to Atlantic Coast Estuaries Indicators Consortium, it has not been subject to the Agency's required peer and policy review and therefore does not necessarily reflect the views of the Agency and no official endorsement should be inferred. Contribution no. 3928 of Horn Point Laboratory, University of Maryland Center for Environmental Science.

References

- Barber, R.T., and F.P. Chavez. 1983. Biological consequences of El Nino. *Science* 222, 1203-1210.
- Barnston, A.G., and R.E. Livezey. 1987. Classification, seasonality and persistence of low-frequency atmospheric circulation patterns. *Mon. Weather Rev.*, 115, 1083-1126.
- Boicourt, W.C. 1992. Influence of circulation processes on dissolved oxygen in the Chesapeake Bay, p. 7-59. In D.E. Smith, M. Leffler, and G. Mackiernan [eds.]. *Oxygen Dynamics in the Chesapeake Bay: A Synthesis of Recent Research*. Maryland Sea Grant Program.
- Cane, M.A. 1983. Oceanographic events during El Nino. *Science* 222, 1189-1195.
- Cayan, D.R., and D.H. Peterson. 1989. The influence of North Pacific atmospheric circulation on riverflow in the West, p. 375-397. In D.H. Peterson [ed.]. *Aspects of climate variability in the Pacific and the Western Americas*. American Geophysics Union.
- Cayan, D.R., and D.H. Peterson. 1993. Spring climate and salinity in the San Francisco Bay Estuary. *Water Resour. Res.*, 29, 293-303.
- Cloern, J.E., A.E. Alpine, B.E. Cole, R.L. Wong, J.F. Arthur, and M.D. Ball. 1983. River discharge controls phytoplankton dynamics in the northern San Francisco Bay estuary. *Est. Coast. Shelf Sci.*, 21, 711-725.
- Crane, R.G., and B.C. Hewitson. 1998. Doubled CO₂ precipitation changes for the Susquehanna basin: downscaling from the genesis general circulation model. *Int. J. Climatol.*, 18, 65-76.
- Davis, R.E., and L.S. Kalkstein. 1990. Development of an automated spatial synoptic climatological classification. *Int. J. Climatol.*, 10, 769-794.
- Davis, R.E., B.P. Hayden, D.A. Gay, W.L. Phillips, and G.V. Jones. 1997. The North Atlantic subtropical anticyclone. *J. Clim.*, 10, 728-744.
- Davis, R.E., R. Dolan, and G. Demme. 1993. Synoptic climatology of Atlantic coast north-easters. *Int. J. Climatol.*, 13, 171-189.
- Fisher, T.R., L.W. Harding, Jr., D.W. Stanley, and L.G. Ward. 1988. Phytoplankton, nutrients, and turbidity in the Chesapeake, Delaware, and Hudson estuaries. *Est. Coast. Shelf Sci.*, 27, 61-93.

- Gibson, J.R., and R.G. Najjar. 2000. The response of Chesapeake Bay salinity to climate-induced changes in streamflow. *Limnol. Oceanogr.*, 45, 1764-1772.
- Gleick, P.H. 1987. The development and testing of a water balance model for climate impact assessment: modeling the Sacramento Basin. *Water Resour. Res.*, 23, 1049-1061.
- Guttman, N.B., and R.G. Quayle. 1996. A historical perspective of U.S. climate divisions. *Bull. Am. Meteorol. Soc.*, 77, 293-303.
- Hagy, J.D., W.R. Boynton, C.W. Keefe, and K.V. Wood. 2004. Hypoxia in Chesapeake Bay, 1950-2001: Long-term changes in the relation to nutrient loading and river flow. *Estuaries* 27, 634-658.
- Harding, Jr., L.W., B.W. Meeson, and T.R. Fisher. 1986. Phytoplankton in two East coast estuaries: photosynthesis-light curves and patterns of carbon assimilation. *Est. Coast. Shelf Sci.*, 23, 773-806.
- Harding, Jr., L.W. 1994. Long-term trends in the distribution of phytoplankton in Chesapeake Bay: roles of light, nutrients, and streamflow. *Mar. Ecol. Prog. Ser.*, 104, 267-291.
- Harding, Jr., L.W., and E.S. Perry. 1997. Long-term increases of phytoplankton biomass in Chesapeake Bay, 1950-1994. *Mar. Ecol. Prog. Ser.*, 157, 39-52.
- Hayden, B.P. 1981. Secular variation in Atlantic coast extratropical cyclones. *Mon. Weather Rev.*, 109, 159-167.
- Hirsch, M.E., A.T. DeGaetano, and S.J. Colucci. 2001. An East Coast winter storm climatology. *J. Clim.*, 14, 882-899.
- Howarth, R.W., D.P. Swaney, T.J. Butler, and R. Marino. 2000. Climatic control on eutrophication of the Hudson River estuary. *Ecosystems* 3, 210-215.
- Hurrell, J.W. 1995. Decadal trends in the North Atlantic Oscillation: regional temperatures and precipitation. *Science* 269, 676-679.
- Jung, S., and E.D. Houde. 2003. Spatial and temporal variabilities of pelagic fish community structure and distribution in Chesapeake Bay, USA. *Est. Coast. Shelf Sci.*, 58, 335-351.
- Justić, D., R.E. Turner, and N.N. Rabalais. 2003. Climatic influences on riverine nitrate flux: implications for coastal marine eutrophication and hypoxia. *Estuaries* 26, 1-11.

- Kimmel, D.G., and M.R. Roman. 2004. Long-term trends in mesozooplankton abundance in Chesapeake Bay, USA: influence of freshwater input. *Mar. Ecol. Prog. Ser.*, 267, 71-83.
- Kimmerer, W.J. 2002. Effects of freshwater flow on abundance of estuarine organisms: physical effects or trophic linkages? *Mar. Ecol. Prog. Ser.*, 243, 39-55.
- Kimmerer, W. J. 2004. Open water processes of the San Francisco Estuary: from physical forcing to biological responses. *San Francisco Estuary and Watershed Science* 2, 1-140.
- Lakhtakia, M.N., B. Yarnal, D.L. Johnson, R.A. White, D.A. Miller, and Z. Yu. 1998. A simulation of river-basin response to mesoscale meteorological forcing: the Susquehanna River basin experiment (SRBEX). *Journal of the American Water Resources Association* 34, 921-937.
- Malone, T.C. 1977. Environmental regulation of phytoplankton productivity in the Lower Hudson estuary. *Est. Coast. Mar. Sci.*, 5, 157-171.
- Malone, T.C., L.H. Crocker, S.E. Pike, and B.W. Wendler. 1988. Influences of river flow on the dynamics of phytoplankton production in a partially stratified estuary. *Mar. Ecol. Prog. Ser.*, 48, 235-249.
- Mantua, N.J., S.R. Hare, Y. Zhang, J.M. Wallace, and R.C. Francis. 1997. A Pacific interdecadal climate oscillation with impacts on salmon production. *Bull. Am. Meteorol. Soc.*, 78, 1069-1079.
- McCabe, G.J., and M.A. Ayers. 1989. Hydrologic effects of climate change in the Delaware River basin. *Water Resour. Bull.*, 25, 1231-1242.
- Najjar, R.G. 1999. The water balance of the Susquehanna River Basin and its response to climate change. *J. Hydrol.*, 219, 7-19.
- Najjar, R.G., H.A. Walker, P.J. Anderson, E.J. Barron, R.J. Bord, J.R. Gibson, V.S. Kennedy, C.G. Knight, J.P. Megonigal, R.E. O'Connor, C.D. Polsky, N.P. Psuty, B.A. Richards, L.G. Sorenson, E.M. Steele, and R.S. Swanson. 2000. The potential impacts of climate change on the mid-Atlantic coastal region. *Clim. Res.*, 14, 219-233.
- Neff, R., H. Chang, C. G. Knight, R. G. Najjar, B. Yarnal, and H. Walker. 2000. Impact of climate variation and change on Mid-Atlantic region hydrology and water resources. *Clim. Res.*, 14, 207-218.
- North, E.W., and E.D. Houde. 2003. Linking ETM physics, zooplankton prey, and fish early-life histories to striped bass *Morone saxatilis* and white perch *M. Americana* recruitment. *Mar. Ecol. Prog. Ser.*, 260, 219-236.

- Ottersen, G., B. Planque, A. Belgrano, E. Post, P.C. Reid, and N.C. Stenseth. 2001. Ecological effects of the North Atlantic Oscillation. *Oecologia* 128, 1-14.
- Paerl, H.W., L.M. Valdes, J.L. Pinckney, M.F. Piehler, J. Dyble, and P.H. Moisander. 2003. Phytoplankton photopigments as indicators of estuarine and coastal eutrophication. *BioScience* 53, 953-964.
- Peterson, D., D.R. Cayan, J.F. Festa, F.H. Nichols, R.A. Walters, J.V. Slack, S.E. Hager, and L.E. Schemel. 1989. Climate variability in an estuary: effects of streamflow on San Francisco Bay, p. 419-442. In D.H. Peterson [ed.]. *Aspects of climate variability in the Pacific and the Western Americas*. American Geophysics Union.
- Read, M.R. 2002. The influence of the North Atlantic Oscillation on streamflow in the Chesapeake Bay watershed. MS Thesis. Pennsylvania State University.
- Redmond, K.T., and R.W. Koch. 1991. Surface climate and streamflow variability in the Western United States and their relationship to large-scale circulation indices. *Water Resour. Res.*, 27, 2381-2399.
- Reid, P.A., P.D. Jones, O. Brown, C.M. Goodness, and T.D. Davies. 2001. Assessments of the reliability of NCEP circulation data and relationships with surface climate by direct comparisons with station based data. *Clim. Res.*, 17, 247-261.
- Riley, G.A. 1937. The significance of the Mississippi River drainage for biological conditions in the Northern Gulf of Mexico. *J. Mar. Res.*, 1, 60-74.
- Roman, M.R., D.V. Holliday, and L.P. Sanford. 2001. Temporal and spatial patterns of zooplankton in the Chesapeake Bay turbidity maximum. *Mar. Ecol. Prog. Ser.*, 213, 215-227.
- Rousseeuw, P.J. 1984. Least median of squares regression. *Journal of the American Statistical Association* 79, 871-880.
- Schubel, J.R., and D.W. Pritchard. 1986. Response of upper Chesapeake Bay to variations in discharge of the Susquehanna River. *Estuaries* 9, 236-249.
- Shaw, P.J.A. 2003. *Multivariate Statistics for the Environmental Sciences*, Arnold Publishers.
- Stenseth, N.C., A. Mysterud, G. Ottersen, J.W. Hurrell, K.S. Chan, and M. Lima. 2002. Ecological effects of climate fluctuation. *Science* 297, 1292-1296.

- Stenseth, N.C., G. Ottersen, J.W. Hurrell, A. Mysterud, M. Lima, K.S. Chan, N.G. Yoccoz, and B. Adlandsvik. 2003. Studying climate effects on ecology through the use of climate indices: the North Atlantic Oscillation, El Niño Southern Oscillation and beyond. *Proc. R. Soc. Lond.*, B 270, 2087-2096.
- Thornthwaite, C.W. 1948. An approach toward a rational classification of climate. *The Geographical Review* 38, 55-94.
- Trenberth, K.E., and D.P. Stepaniak. 2001. Indices of El Niño evolution. *J. Clim.*, 14, 1697-1701.
- Wilby, R.L. 1993. The influence of variable weather patterns on river water quantity and quality regimes. *Int. J. Climatol.*, 13, 227-241.
- Wood, R.J. 2000. Synoptic scale climate forcing of multispecies fish recruitment patterns in Chesapeake Bay. PhD. Dissertation. College of William and Mary.
- Yarnal, B. 1993. *Synoptic Climatology in Environmental Analysis*, Belhaven Press.
- Yarnal, B., and D.J. Leathers. 1988. Relationships between interdecadal and interannual climatic variations and their effect on Pennsylvania climate. *Annals of the Association of American Geographers* 78, 624-641.
- Yarnal, B., and B. Frakes. 1997. Using synoptic climatology to define representative discharge events. *Int. J. Climatol.*, 17, 323-341.
- Yu, Z., M.N. Lakhtakia, B. Yarnal, Y.A. White, D.A. Miller, B. Frakes, E.J. Barron, C. Duffy, and F.W. Schwartz. 1999. Simulating the river-basin response to atmospheric forcing by linking a mesoscale meteorological model and hydrologic model system. *J. Hydrol.*, 218, 72-91.
- Zar, J.H. 1984. *Biostatistical Analysis*, 2nd ed. Prentice Hall.
- Zielinski, G.A. 2002. A classification scheme for winter storms in the eastern and central United States with emphasis on "Nor'easters". *Bull. Am. Meteorol. Soc.*, 83, 37-51.

Table 2.1. Statistics from the linear regression of winter Niño3.4, NAO, PDO, PNA, Temperature, Precipitation, and combined Temperature+Precipitation variables against average spring flow from the Susquehanna River.

Variable	p-value	r ²
Niño3.4	0.068	0.073
NAO	0.621	0.006
PDO	0.578	0.007
PNA	0.625	0.005
Temp	0.116	0.055
Precip	0.028	0.104
Temp+Precip	0.019	0.167

Table 2.2. Pearson's correlation coefficients for comparisons of winter indices for NAO, ENSO, PDO, and PNA against winter frequency-of-occurrence for each cluster. * indicates significance at the $p > 0.01$ level.

Cluster	NAO	ENSO	PDO	PNA
1	-0.031	-0.235	-0.031	0.114
2	0.158	-0.354*	0.135	0.109
3	-0.289	0.297	-0.026	-0.117
4	-0.429*	0.375	-0.034	0.072
5	0.380*	-0.337*	-0.086	-0.209
6	-0.125	0.456*	0.066	0.042
7	-0.418*	0.397*	-0.101	0.045
8	-0.127	0.383*	0.145	0.036
9	0.452*	-0.311	-0.025	-0.075
10	0.215	-0.294	-0.061	-0.041

Table 2.3. Meteorological characteristics for clusters during winter. Standard deviations in parentheses.

Cluster	Days of Occurrence	%	Temperature Anomaly (°C)	Precipitation Anomaly (mm day ⁻¹)	Wind Direction	Wind Speed (m s ⁻¹)	Seasonality
1 ^a	353	7.4	3.2 (±4.6)	0.9 (±4.9)	W	3.3 (±1.4)	summer
2 ^b	802	16.8	-3.0 (±5.2)	-0.9 (±3.2)	NW	3.8 (±1.5)	winter
3	346	7.2	-0.6 (±4.3)	0.7 (±4.9)	NW	3.2 (±1.8)	spring/fall
4 ^c	245	5.1	2.0 (±4.6)	2.7 (±7.0)	W	3.9 (±1.7)	winter/spring
5	698	14.6	2.4 (±4.9)	0.1 (±4.2)	W	2.9 (±1.2)	summer
6	344	7.2	-0.4 (±4.8)	-0.4 (±3.9)	E	2.2 (±1.5)	fall
7	681	14.2	-1.9 (±4.6)	-0.1 (±4.1)	W	4.9 (±1.7)	winter
8	188	3.9	2.9 (±4.7)	1.5 (±4.9)	E	2.4 (±1.4)	spr/sum/fall
9	423	8.8	2.2 (±5.1)	-0.1 (±3.9)	S	2.3 (±1.1)	winter/spring
10	692	14.5	-1.0 (±5.2)	-0.9 (±2.9)	S	2.3 (±1.1)	winter

^a Bermuda High

^b Ohio Valley High

^c Nor'easter

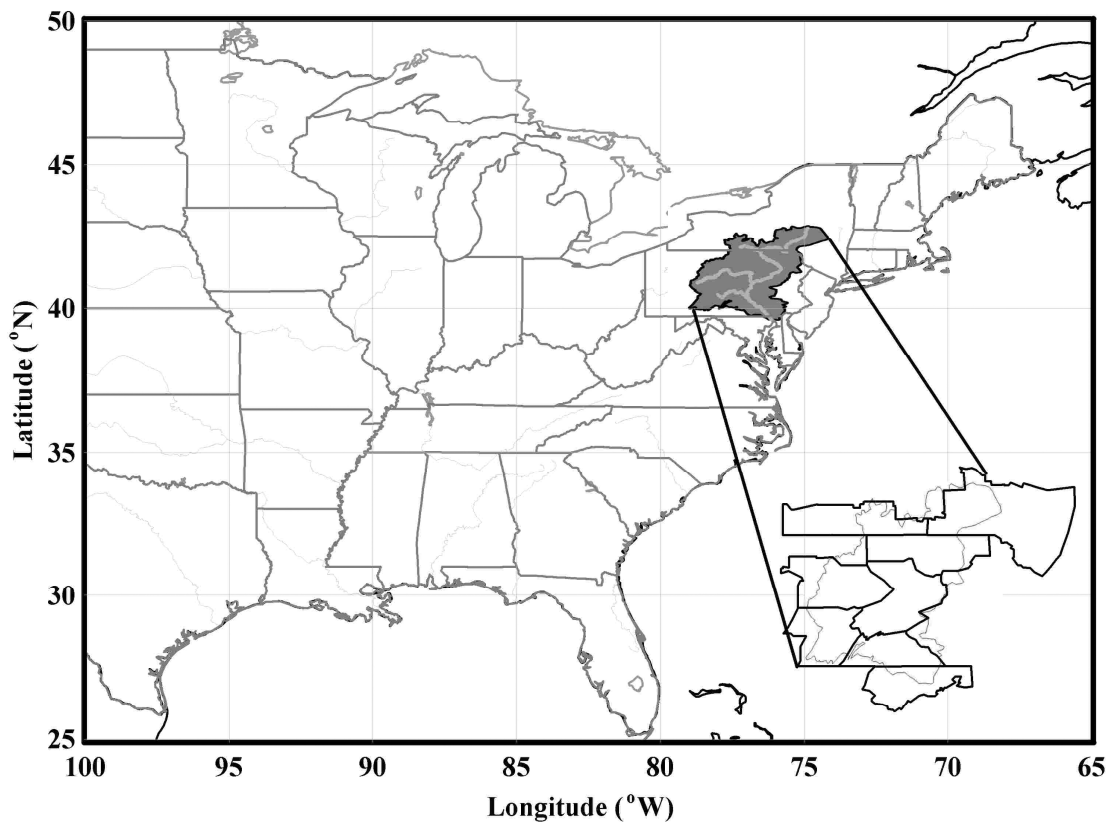


Fig. 2.1. Map of synoptic climate region with inset of Suquehanna River Basin showing NOAA climate divisions.

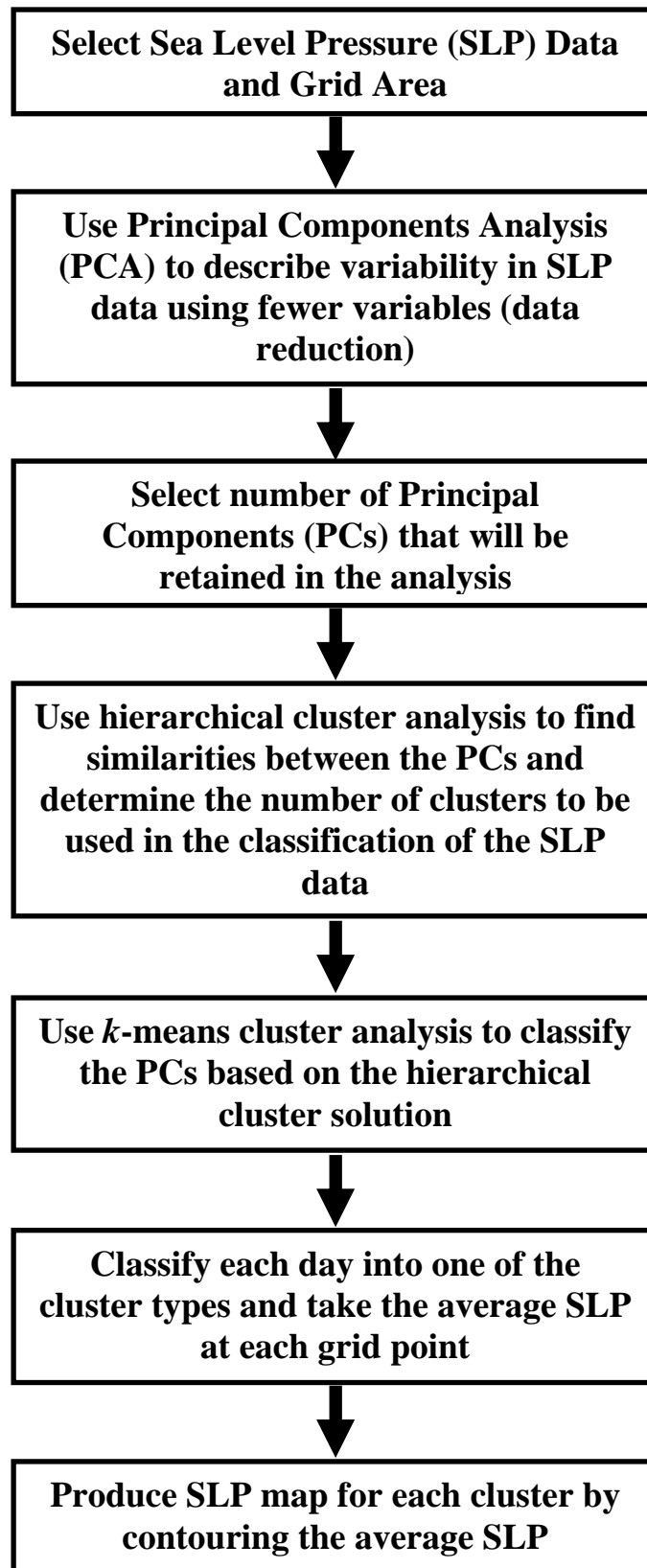


Fig. 2.2. Flow chart of synoptic climatology methods, after Yarnal (1993).

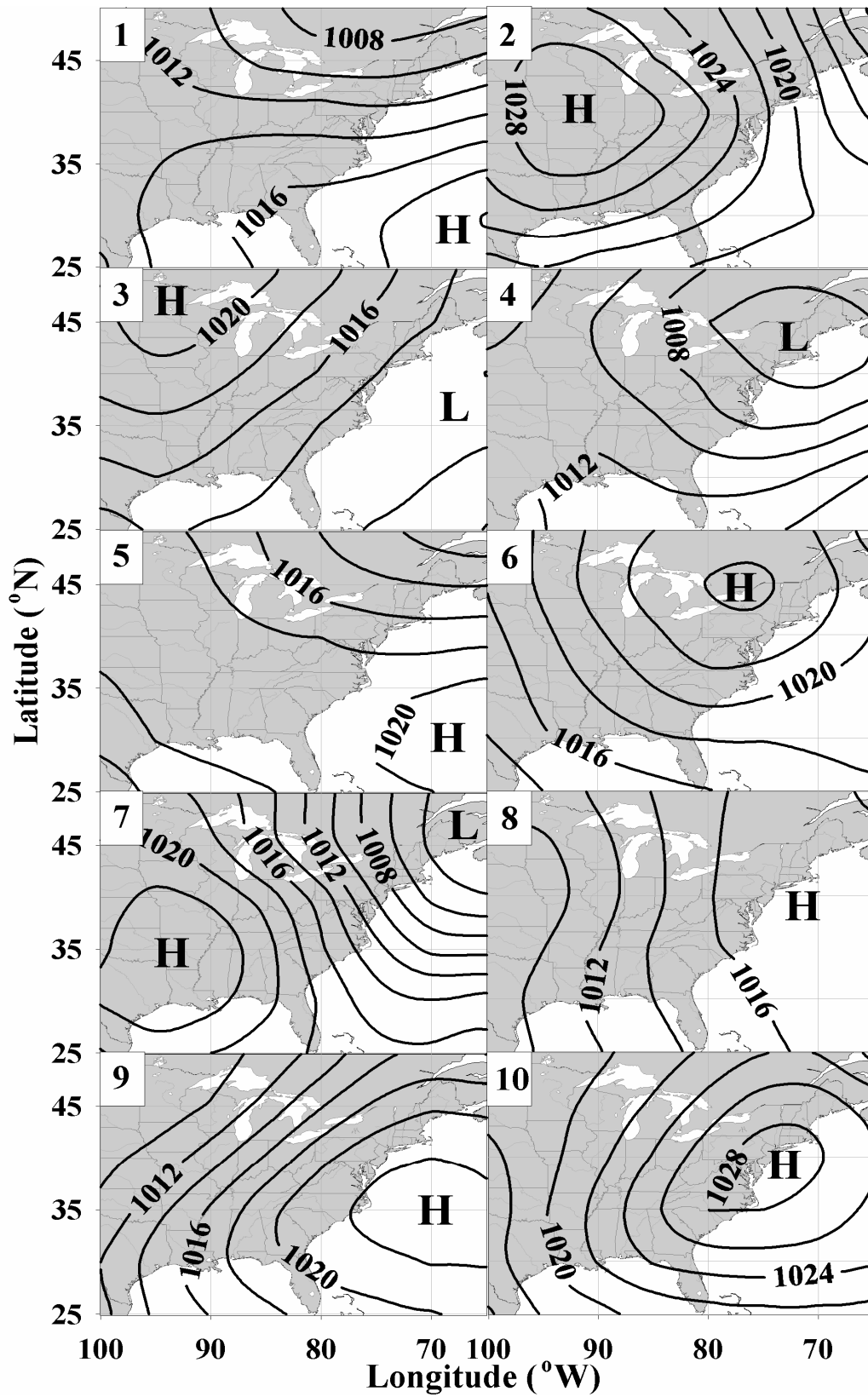


Fig. 2.3. Average sea-level pressure maps for each cluster. Cluster number in upper left-hand corner.

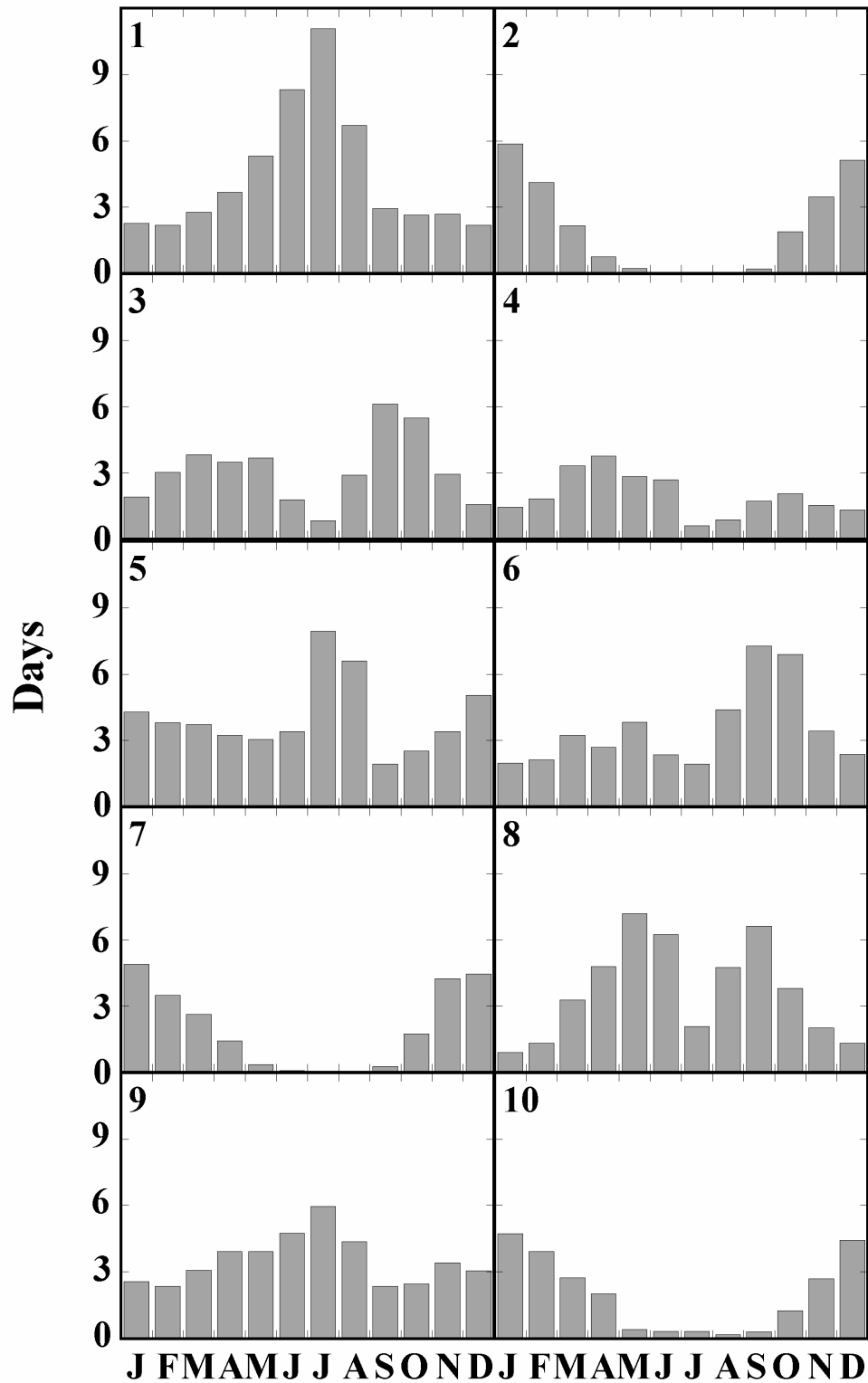


Fig. 2.4. Monthly average frequency-of-occurrence by cluster. Cluster number in upper left-hand corner.

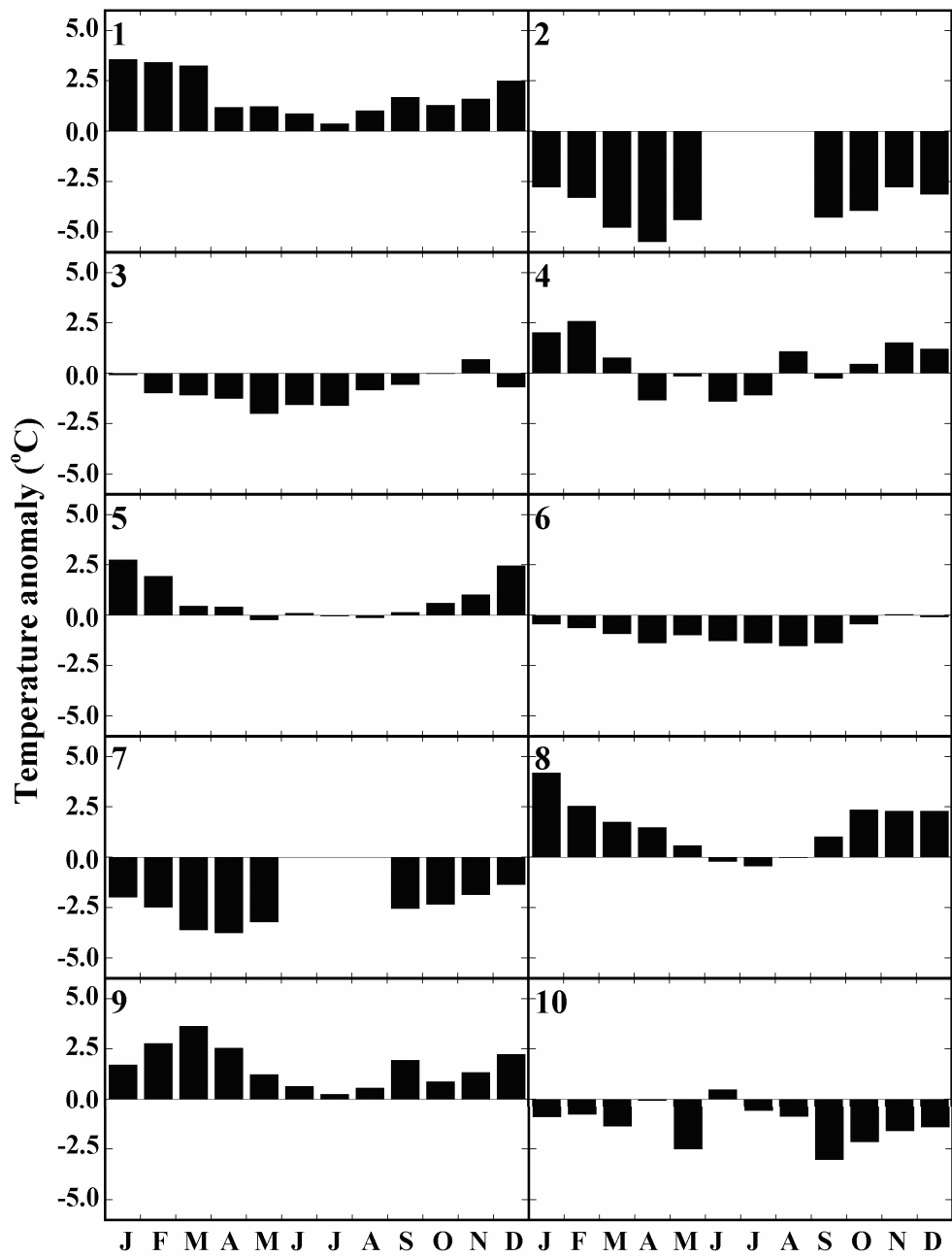


Fig. 2.5. Monthly temperature anomaly by cluster. Cluster number in upper left-hand corner.

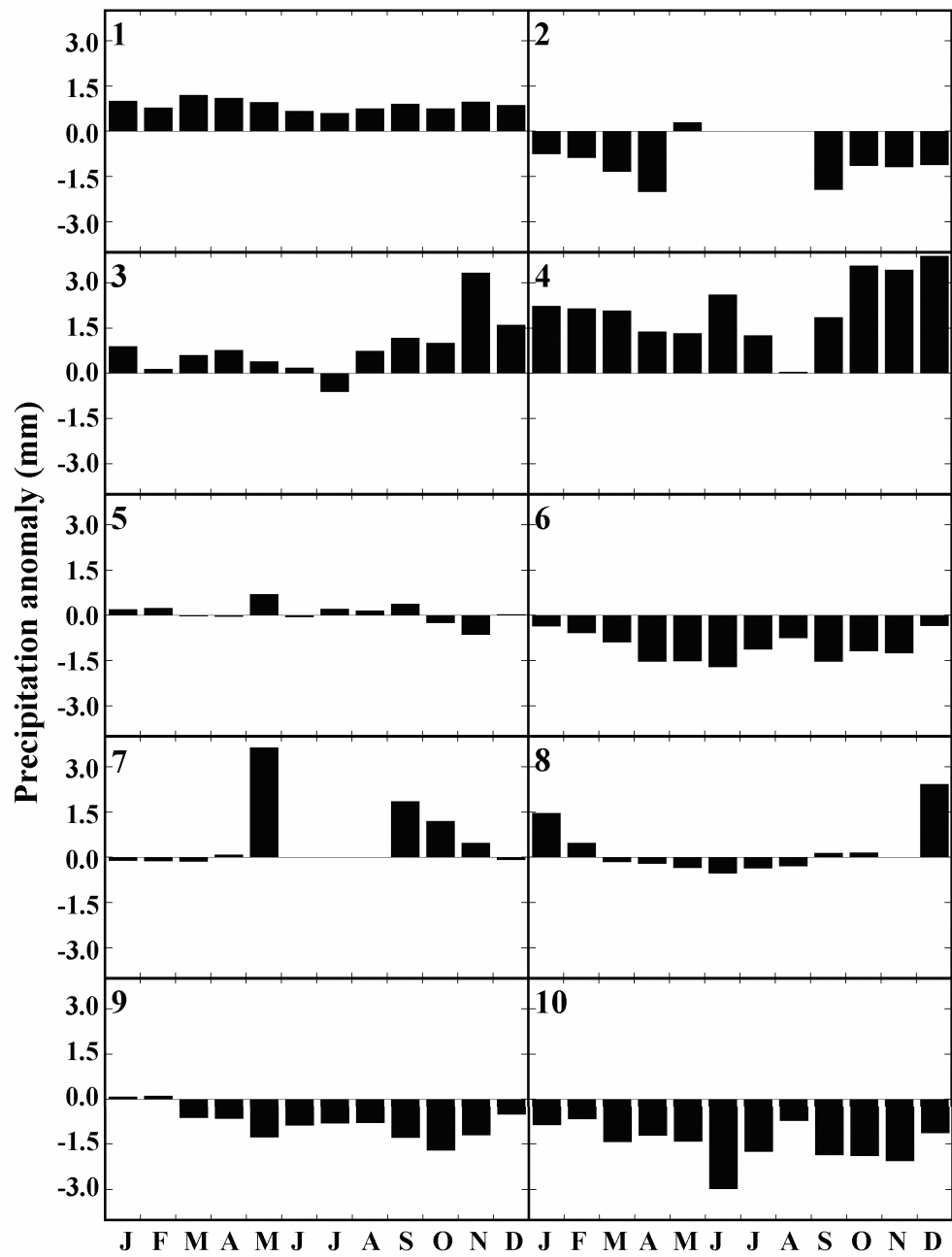


Fig. 2.6. Monthly precipitation anomaly by cluster. Cluster number in upper left-hand corner.

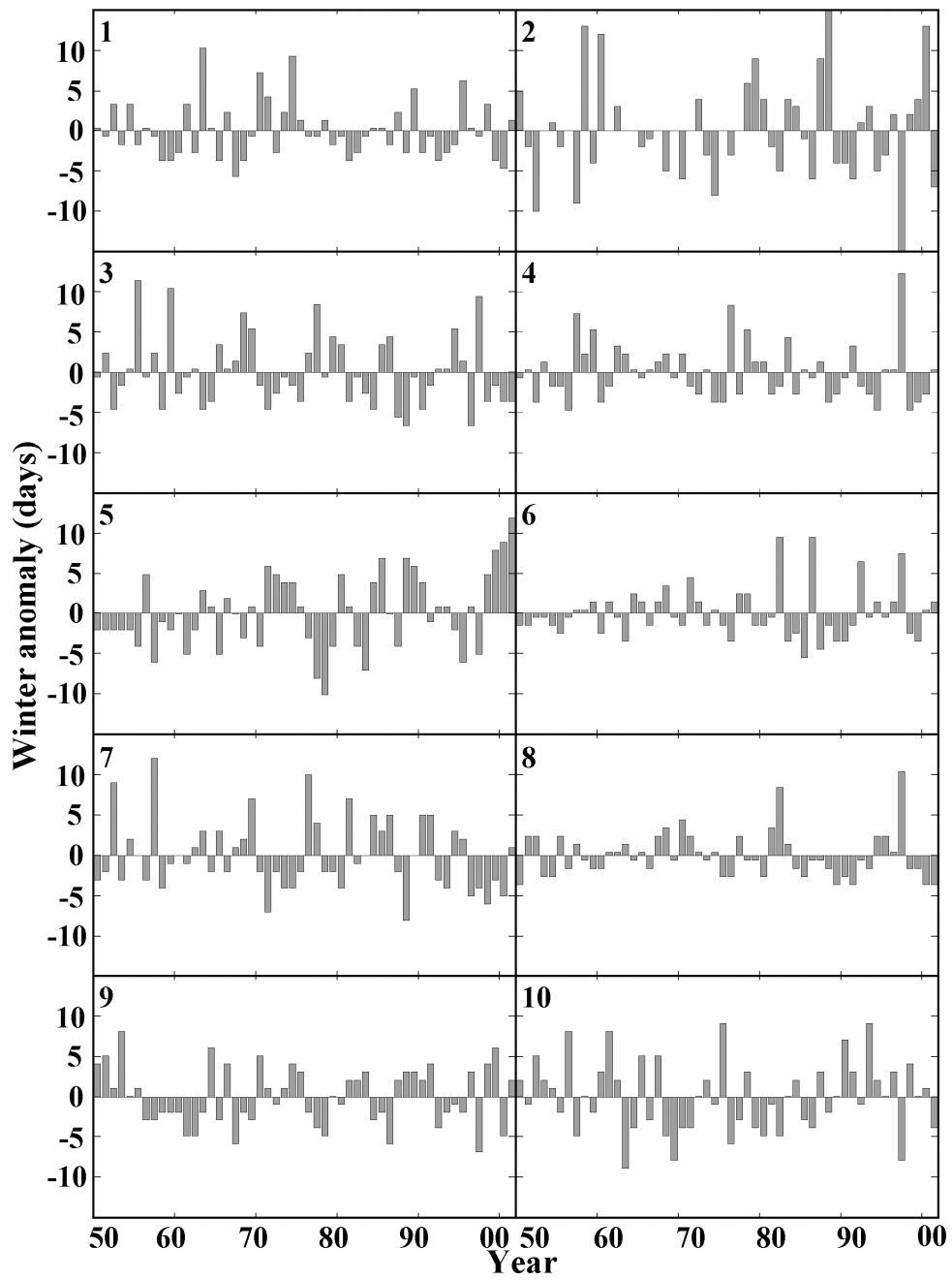


Fig. 2.7. Time series of deviation (in days) from long-term average winter frequency-of-occurrence for each cluster. Cluster number in upper left-hand corner.

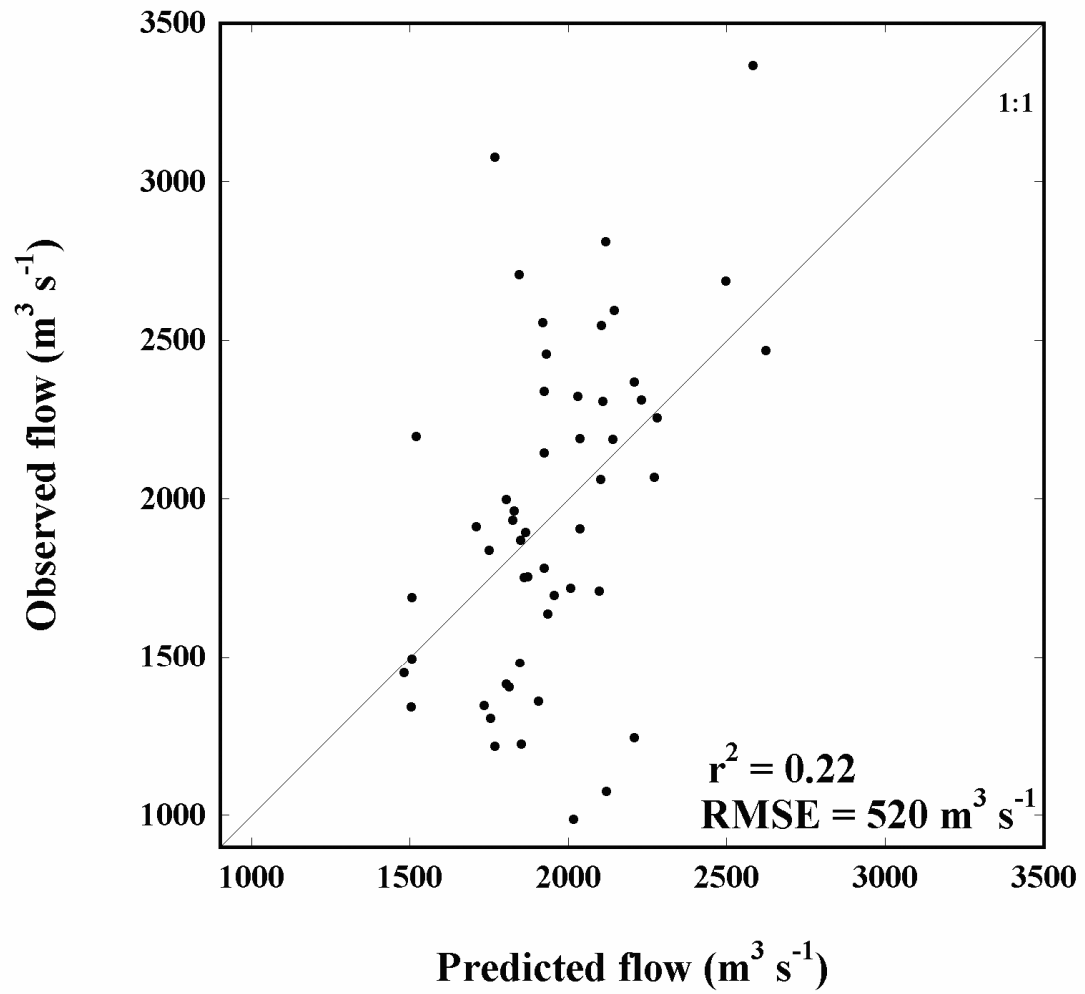


Fig. 2.8. Regression of observed average spring freshwater flow from the Susquehanna River on modeled flow predicted from winter cluster frequency-of-occurrence using the complete ($n = 52$) dataset.

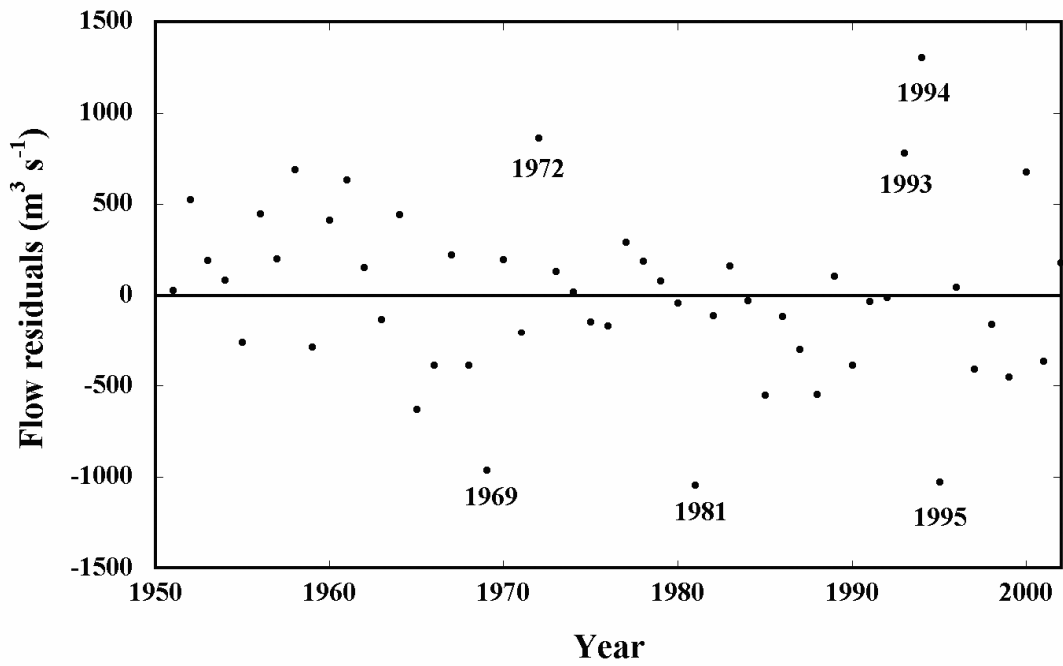


Fig. 2.9. Plot of residuals by year from multiple linear regression model shown in figure 8.

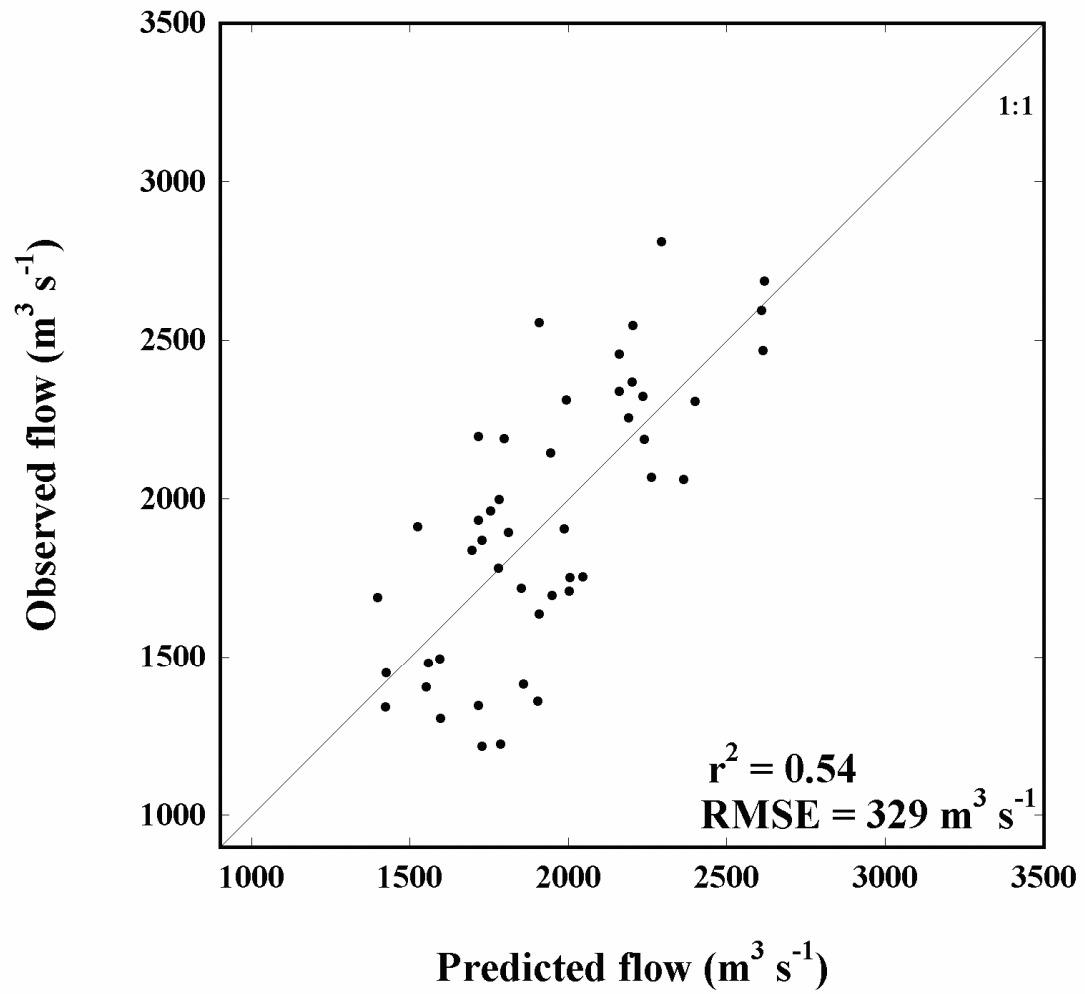


Fig. 2.10. Regression of observed average spring freshwater flow from the Susquehanna River on modeled flow, predicted from winter cluster frequency-of-occurrence using the modified dataset ($n = 46$) with 6 outliers removed.

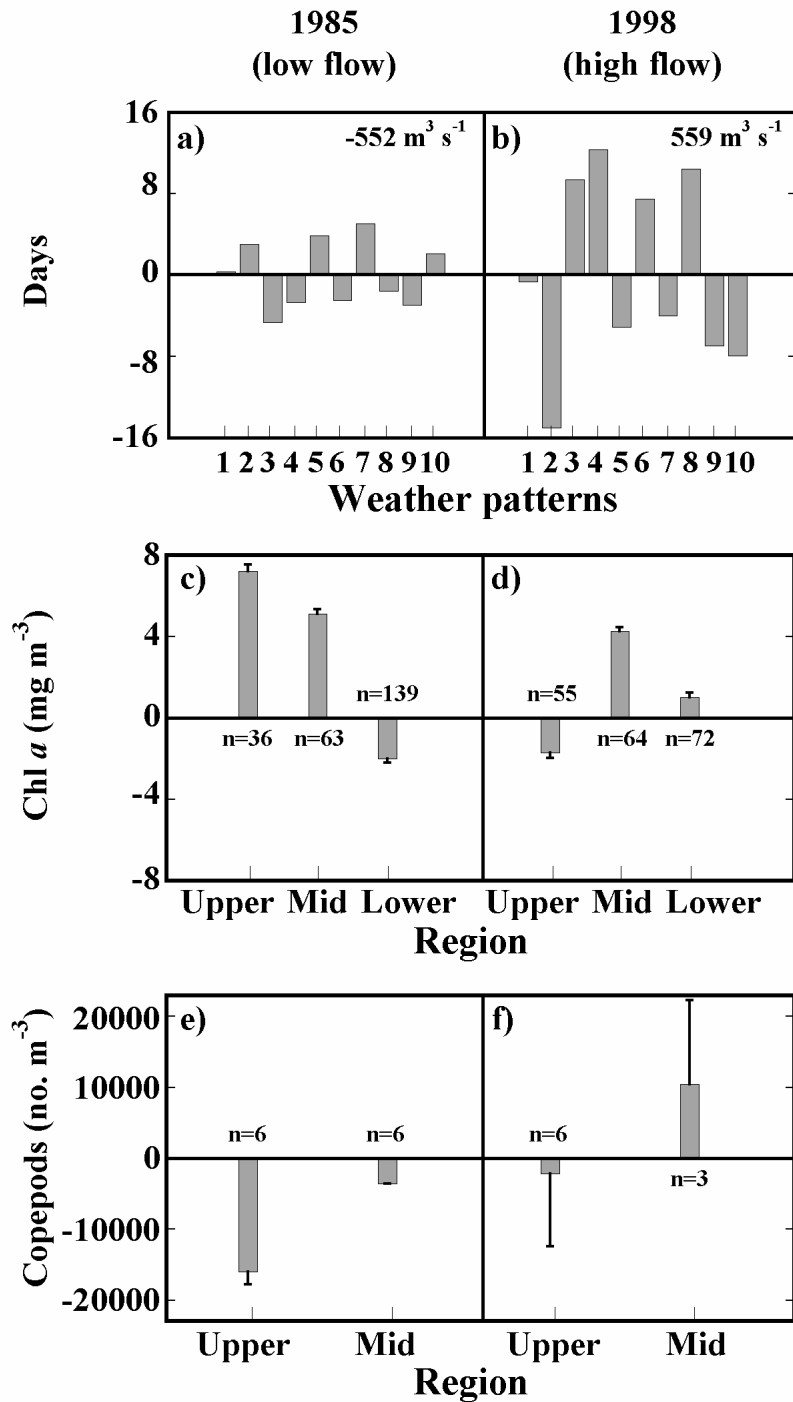


Fig. 2.11. Planktonic response in spring to years of contrasting winter weather patterns. a) weather pattern anomalies for winter 1984-5, b) weather pattern anomalies for winter 1997-8, c) phytoplankton biomass anomalies for spring 1985 in three geographical regions d) phytoplankton biomass anomalies for spring 1998 in three geographical regions, e) copepod abundance anomalies for spring 1985 in two geographical regions, f) copepod abundance anomalies for spring 1998 in two geographical regions. Error bars indicate standard error.

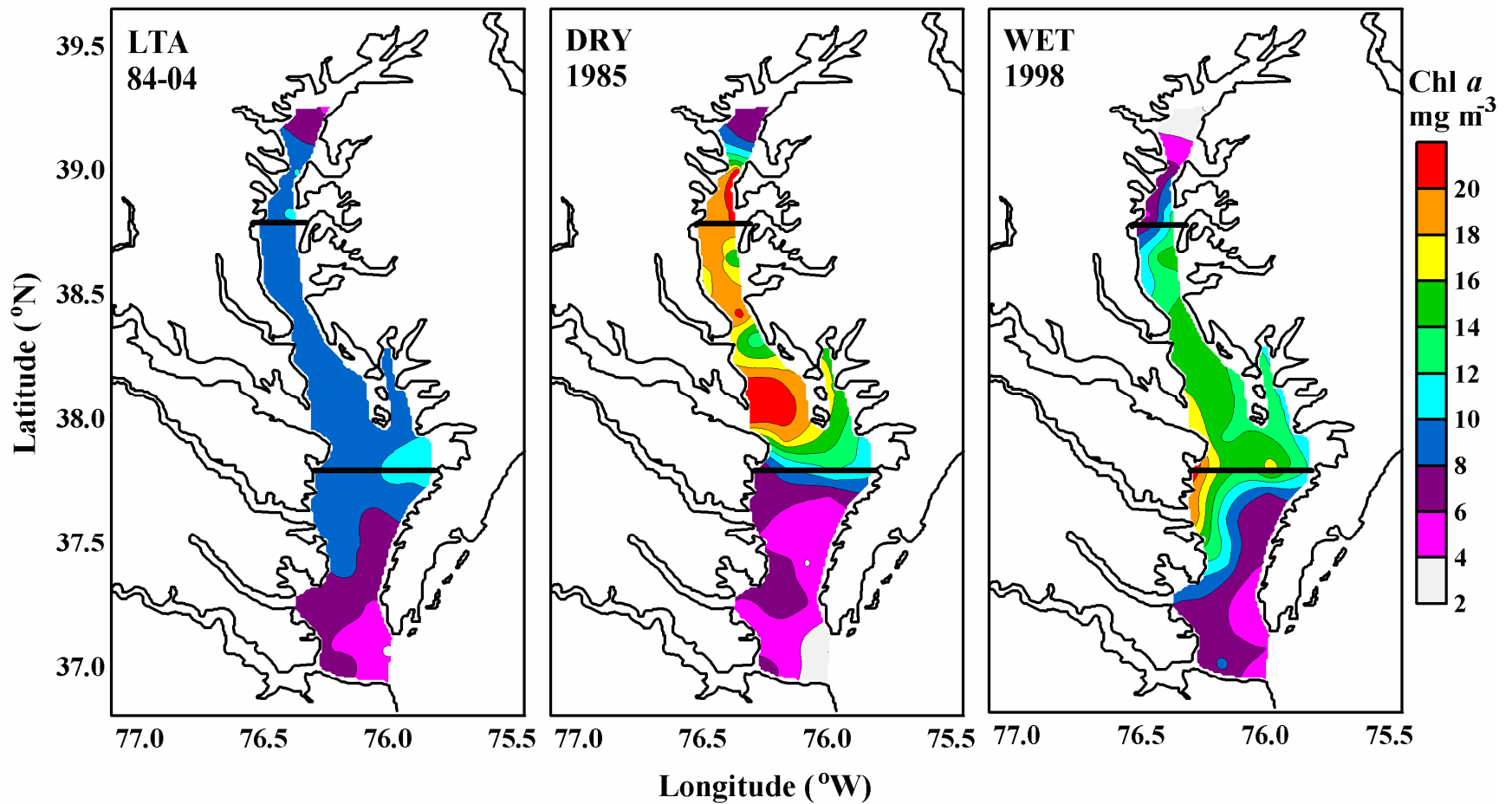


Fig. 2.12. Maps of spring phytoplankton biomass (mg m^{-3}) for long-term average condition, dry year of 1985, and wet year of 1998. Maps interpolated from Chesapeake Bay Program station data ($n=49$). Black bars demarcate upper, mid-, and lower Bay regions used in analyses.

Chapter 3

Climate Forcing of the Spring Bloom in Chesapeake Bay¹

¹Miller, W.D., and L.W. Harding, Jr. Climate forcing of the spring bloom in Chesapeake Bay. Marine Ecology Progress Series, submitted.

Abstract

Interannual variability of the spring phytoplankton bloom is strongly expressed in estuarine ecosystems such as Chesapeake Bay. Quantifying this variability is essential to resolve ecosystem responses to eutrophication from variability imposed by climate. I developed a ‘synoptic climatology’ from surface sea-level pressure (SLP) maps to categorize and quantify atmospheric circulation patterns and address climate forcing of phytoplankton dynamics in the Bay. The 10 patterns I identified had unique frequencies-of-occurrence and associated meteorological conditions (i.e., precipitation, temperature, wind speed and direction). Four measures of phytoplankton biomass, surface chlorophyll-a (B), euphotic layer chlorophyll-a (B_{eu}), water column chlorophyll-a (B_{wc}), and total biomass (B_{tot}), were obtained from remotely sensed ocean color data spanning 16 yr (1989-2004) combined with concurrent shipboard data. Years with more frequent warm/wet weather patterns had spring blooms that reached peak biomass farther seaward in the estuary, were greater in magnitude, occurred later in the spring, and covered a larger area than years with a predominance of cool/dry weather patterns. Winter weather pattern frequencies were used to forecast spring B , B_{eu} , B_{wc} , and B_{tot} , explaining between 23 and 89 % of the variance in the regional time series. Residuals from these models did not show time-trends attributable either to accelerating eutrophication or to management actions decreasing nutrient loadings. These findings extend our understanding of climatic influences on phytoplankton dynamics in the Bay by quantifying the effects of synoptic climate variability on spring bloom intensity, supporting forecasts of seasonal phytoplankton biomass based on sub-continental scale weather patterns in this mid-Atlantic estuary.

Introduction

Climate variability strongly influences marine ecosystems (McGowan et al., 1998; Stenseth et al., 2002), exemplified by basin-scale biological responses to El Niño-Southern Oscillation (ENSO; Chavez et al., 1999), and the North Atlantic Oscillation (NAO; Ottersen et al., 2001). Indices of ENSO and NAO capture the holistic nature of climate better than individual weather measurements (Ottersen et al., 2004). Global data from remotely sensed ocean color and temperature observations, coupled to climate indices, have contributed to our understanding of ocean-atmosphere interactions that drive phytoplankton dynamics (Behrenfeld et al., 2001). In some areas, however, large-scale climate indices are not strongly expressed and sub-continental processes assume greater importance in forcing local meteorological conditions (Stenseth et al., 2003). An alternative approach that derives a holistic measure of climate variability, while retaining local relevance, is to construct a regional ‘synoptic climatology’ (cf. Yarnal, 1993). In this paper, I present data and analyses to document regional climate effects on spring bloom intensity in Chesapeake Bay. This work draws on 16 yr of ocean color observations from aircraft, coincident data from shipboard measurements, and a synoptic climatology that captures seasonal to interannual variability of weather patterns linked to precipitation and freshwater flow.

Interannual variability of phytoplankton biomass and primary productivity is strongly expressed in temperate estuaries and multiple causes including freshwater flow, nutrient loading, and turbidity underlie that variability (Boynton et al., 1982). To this end, the proximal effects of freshwater flow on phytoplankton dynamics have

been documented for a number of estuarine systems, including the Hudson River (Malone, 1977), San Francisco Bay (Cloern et al., 1983), the Neuse River (Mallin et al., 1993), and the Loire River estuary (Relexans et al., 1988). These studies have shown that the magnitude of phytoplankton biomass often co-varies with flow and attendant properties, but the relationships are generally dependent on characteristics unique to individual systems (e.g. circulation, residence time, morphometry, tides, nutrient and sediment loading). While I recognize the important role that flow plays in determining spatial and temporal dynamics of phytoplankton in estuaries, indices of regional climate may provide more comprehensive measures of environmental influences. A missing element of our understanding is a quantitative description of the role of regional climate in forcing variability of phytoplankton biomass, such as has emerged for some parts of the global ocean using ENSO and NAO indices. This is an important area of research as we attempt to predict effects of climate change and nutrient enrichment on estuarine and coastal ecosystems (Cloern, 2001).

Freshwater flow into Chesapeake Bay is maximal in winter-spring, as it is in many temperate estuaries; dominated by the freshet of the Susquehanna River that largely determines gradients of light and nutrient limitation along the north-south axis of the Bay (Harding et al., 1986). The position, magnitude, timing, and extent of the winter-spring diatom bloom are determined in large part by winter-spring flow (Malone, 1992, Harding, 1994), and variability of flow during this period has recently been linked to synoptic-scale climate for winter (Miller et al., 2006). There is an abundant literature that supports the interaction of atmospheric circulation, precipitation, and freshwater flow (Cayan and Peterson, 1989; McCabe and Ayers,

1989), including findings for the Susquehanna River (Crane and Hewitson, 1998; Najjar, 1999). I suggest that a major source of interannual variability of spring bloom intensity, expressed by several measures of phytoplankton biomass, can be traced to differences in the frequency and types of winter weather patterns prevailing in the Bay's watershed in a given year.

The work described here relates winter climate variability at the synoptic scale (Yarnal, 1993) to spring phytoplankton dynamics in Chesapeake Bay through links to freshwater flow and other environmental parameters influenced by climate (Miller et al., 2006). Climate indices influence ecology through local weather patterns. Therefore a synoptic climatology that captures regional weather variability should outperform large-scale indices in explaining ecosystem variability by removing a degree of complexity between climate and ecology (Stenseth et al., 2003). I tested the hypothesis that interannual differences in the frequencies of winter weather types identified using a synoptic climatology represent the predominant source of variability for spring phytoplankton biomass in Chesapeake Bay. To address this hypothesis I: (1) classified and quantified variability of atmospheric circulation patterns in the region using a synoptic climatology; (2) quantified the position, magnitude, timing, and extent of the spring bloom using a 16 y time-series of surface chlorophyll-a (B), euphotic layer chlorophyll-a (B_{eu}), water column chlorophyll-a (B_{wc}), and total biomass (B_{tot}) from aircraft remote sensing; (3) developed multiple regression models using the frequencies of predominant weather patterns as independent variables and four biomass measures as dependent variables; (4)

examined residuals of spring phytoplankton biomass after removal of the climate signal to resolve trends.

Methods

Synoptic climatology

Regional scale climate variability was quantified using an eigenvector-based, map-pattern, synoptic climatology classification as described in Yarnal (1993) and Miller et al. (2006). I obtained 5° x 5° latitude - longitude gridded, sea-level pressure (SLP) data from the National Center for Atmospheric Research (NCAR; <http://dss.ucar.edu>) to create a 48-point (6 x 8) grid of SLP data covering the area 25° to 50° N latitude and 65° to 100° W longitude. Principal component analysis (PCA) was performed on a correlation matrix of daily SLP against time (days) to reduce spatial variability in the SLP data from the original 48 points to a smaller number (7) of new variables that explained the majority of the variability (90%) in the original data. Those seven variables were submitted to a two-stage clustering procedure to group the data into similarly occurring modes of variance that related to similar atmospheric circulation patterns. The first stage of the clustering procedure (average linkage) was used to determine the number of clusters (10) that made up a significant fraction (>2%) of the total number of days, and to determine 'seed' values for the subsequent *k*-means clustering procedure. The second clustering technique (*k*-means) regrouped the data into one of 10 dominant seed clusters I determined were important using the average linkage clustering technique. Average SLP maps for each of the 10 clusters were then produced by taking the mean value for each grid point within the

daily maps. The seasonal frequencies-of-occurrence of each weather pattern for every year were then computed for use in multiple regression models.

Remotely sensed data

B (mg chl a m^{-3}) was determined for the surface layer using aircraft ocean color measurements from light aircraft (Harding et al., 1994; 1995). Flights were conducted ~20-30 times per year (Mar - Oct) on a set of tracks covering the main stem Bay (Fig. 3.1). Geo-referenced data were collected from an altitude of 150 m at a ground speed of approximately 50 m s^{-1} using multispectral radiometers. NASA's Ocean Data Acquisition System (ODAS) consisting of three nadir-viewing radiometers (460, 490, and 520 nm) with 15 nm bandwidths and 2° field-of-view was used from 1989-95. Successive versions of the commercial Sea-viewing Wide Field-of-view Sensor (SeaWiFS) Aircraft Simulator (SAS II, III - Satlantic, Inc. Halifax, NS, Canada) with 10 nm bandwidths, 3.5° field-of-view, and seven and 13 wavelengths, respectively (SAS II 412, 443, 490, 510, 555, 670, and 683 nm; SAS III 380, 400, 412, 443, 470, 490, 510, 555, 670, 685, 700, 780, and 865 nm) were used from 1995-2004.

B was computed using a spectral curvature algorithm (Campbell and Esaias, 1983) applied to water-leaving radiances at 460, 490, and 520 nm for ODAS, and 443, 490, and 555 nm for SAS II and III. Radiometric calibrations were made at NASA for ODAS and at Satlantic, Inc. for SAS II and III. Retrievals of B relied on local algorithms developed from matchups with concurrent *in-situ* measurements from monitoring cruises of EPA Chesapeake Bay Program (CBP; <http://www.chesapeakebay.net/>) and our own cruises. I defined a match as $\pm 12 \text{ h}$ on the same day, $\pm 0.01^\circ$ latitude, and $\pm 0.005^\circ$ longitude (Harding et al., 1994; 1995;

Weiss et al., 1997). The working equation retrieved $\log_{10} B$ with an RMS error of 0.21 (log units). Flight data were interpolated onto a 1 km² grid for visualization and further analyses using a two-dimensional, inverse-distance-squared, octant search (Harding et al., 1994; 1995).

Integrated biomass (B_{eu} , B_{wc} and B_{tot})

B_{eu} (mg chla m⁻²) was computed for each grid cell as the product of B and euphotic-layer depth (Z_p), estimated as the 1% isolume from Secchi depth for the closest CBP cruise station (≤ 2 weeks). B_{wc} (mg chla m⁻²) was calculated from log-log regressions of bathymetrically-weighted integrals of chla from vertical profiles, $\langle B_{wc} \rangle$, on B developed with CBP data (cf. Harding et al., 1994). Analysis of variance showed statistically significant differences in the slopes of regression equations for different years; accordingly I used equations developed for each year to generate $\langle B_{wc} \rangle$ from remotely sensed B . Back-transformed $\langle B_{wc} \rangle$ data were combined with depth (H) for each grid cell from a digital bathymetry to give B_{wc} . All three biomass measures were log-normally distributed and were \log_{10} transformed for all analyses and back-transformed for graphical display. Total biomass, B_{tot} (metric tons chla), was calculated as the sum of all B_{wc} measurements for the entire Bay. Data from depths greater than the median Bay depth (7.7 m) were used to calculate means for regional regression models.

Data were analyzed for six regions of the main stem Bay defined by latitude (Harding, 1994; Fig. 3.1). Regional means for spring (Apr-May) were computed for B , B_{eu} , B_{wc} , and B_{tot} from flights spanning 1989-2004. Data from 5 to 15 flights were used for each spring, depending on weather and aircraft availability. Shipboard data

were substituted for aircraft data for spring 1996 due to instrument malfunctions. No statistically significant ($\tau > 0.05$, Mann-Kendall Trend Test) trends were observed in any of the regional time series.

Ancillary data

Temperature and precipitation data were obtained from the National Climate Data Center (NCDC; <http://cdo.ncdc.noaa.gov>). Divisional data from the eight climatic regions within the Susquehanna River basin (Pennsylvania divisions 4, 5, 6, 7, 8; Maryland division 6; New York divisions 1, 2) were weighted by area to produce a single estimate of temperature or precipitation. Climate division data were used to provide comprehensive measures of temperature and precipitation from all stations in a division (Guttman and Quayle, 1996). Freshwater flow ($\text{m}^3 \text{s}^{-1}$) for the Susquehanna River was obtained from the United States Geological Survey gauging station at the Conowingo Dam (USGS-01578310; <http://waterdata.usgs.gov/nwis>). Winter (Dec.-Feb.) climate indices for ENSO and NAO were obtained from the National Weather Service, Climate Prediction Center (<http://www.cpc.ncep.noaa.gov>). Data on water column properties that influence phytoplankton dynamics (Z_p , and dissolved inorganic nitrogen; DIN) were obtained from CBP water quality monitoring cruises.

Statistical analyses

Multiple linear regression models were developed to investigate the relationship between regional phytoplankton biomass in spring and the frequency-of-occurrence of winter weather patterns described by the synoptic climatology. To clarify, the regional measures of phytoplankton biomass during spring were the dependent variables and the weather pattern frequencies were the independent variables and

each year was an observation ($n = 16$). Selection of independent variables for inclusion in each model was determined by the combination of weather patterns that explained the maximum amount of variance in the dataset while producing a significant model ($p < 0.05$). Explained variance was measured as the adjusted r^2 to account for the increased variance explained with increasing numbers of explanatory (independent) variables. Multi-collinearity of the independent variables was checked with the variance inflation factor (VIF) diagnostic in SAS (Cody and Smith, 2005); no variable in the models had a $VIF > 5$ (values greater than 10 indicate serious problems with multi-collinearity). Testing for trends in the residuals of the multiple linear regression models were analyzed with the Mann-Kendall trend test. All statistics were performed in SAS version 9.1 (SAS Institute, Cary, NC).

Results

Synoptic climatology

I identified 10 predominant winter weather patterns using a synoptic climatology for the eastern United States (Fig. 3.2). The resulting maps describe average SLP patterns for all days categorized into a given cluster, showing distinct structures of high and low pressure systems. Each weather pattern corresponded to a unique combination of meteorological conditions, i.e. air temperature, precipitation, wind speed, and direction (Table 3.1). Patterns 2, 7 and 10 were common in winter, produced below-average temperature ($-2.3\text{ }^{\circ}\text{C}$) and precipitation (-0.7 mm d^{-1}), and accounted for 45% of winter days during the study period. Patterns 1, 3, 4 and 8 were warmer ($2.0\text{ }^{\circ}\text{C}$) and wetter (1.3 mm d^{-1}) than average and occurred only 21% of days, but accounted for 32% of total winter precipitation (Table 3.1).

Interannual variability in the frequencies of the 10 predominant winter weather patterns was high (Fig. 3.3). Long-term average (LTA; 1989-2004) frequencies varied among clusters from a low of 2.8 days for weather pattern 8, to 16 days for weather pattern 5 (Fig. 3.3). None of the time-series for weather patterns showed statistically significant trends in frequency-of-occurrence ($\tau > 0.05$, Mann-Kendall Trend Test). Cool/dry weather patterns (2, 7 and 10) varied in concert with one another and in opposition to the warm/wet weather patterns (1, 3, 4 and 8).

Differences in the frequencies-of-occurrence of warm/wet and cool/dry weather patterns were associated with variability in precipitation and freshwater flow. I compared years with the largest positive and negative differences in warm/wet versus cool/dry weather pattern frequencies to illustrate this point. Warm/wet years (1990, 1996, 1998, and 2003) averaged 13 days more than the LTA for weather patterns 1, 3, 4 and 8 and nine days less than the LTA for patterns 2, 7 and 10 (Fig. 3.4a). Winter-spring (January-April) flow from the Susquehanna River averaged $2060 \text{ m}^3 \text{ s}^{-1}$, 18% higher than the LTA for these years. In contrast, cool/dry years (1989, 1991, 1997, and 2001) had eight days less than the LTA for patterns 1, 3, 4 and 8, and seven days above the LTA for patterns 2, 7 and 10 (Fig. 3.4b). Winter-spring flow in cool/dry years averaged $1393 \text{ m}^3 \text{ s}^{-1}$, 20% lower than the LTA.

Contrasting weather patterns were associated with distinct distributions of light and nutrients (Z_p , DIN) that influence the spring bloom of phytoplankton in the Bay. The LTA for Z_p ranged from 2.5 to 5.4 m from region 6 to region 1, with the deepest Z_p in region 2. Z_p in cool/dry years ranged from 2.8 to 6.2 m, contrasted with warm/wet years with Z_p from 1.9 to 4.4 m. Average Z_p was 1.4 m deeper in cool/dry

than warm/wet years (Fig. 3.5a). Surface-layer DIN was highest in regions 5 and 6 closest to the Susquehanna River, and decreased rapidly toward the Bay mouth (Fig. 3.5b). The LTA for DIN in these regions was $60.1 \mu\text{moles N L}^{-1}$. DIN in warm/wet years averaged $71.9 \mu\text{moles N L}^{-1}$ compared to $55.4 \mu\text{moles N L}^{-1}$ in cool/dry years.

Spring phytoplankton dynamics

Climate affected the position of the spring phytoplankton maximum using three biomass measures (Fig. 3.6). During warm/wet years, maxima of B, B_{eu} , and B_{wc} were seaward of those for cool/dry years. B peaked at $13.1 \text{ mg chla m}^{-3}$ in region 3 for warm/wet years, contrasted with $8.2 \text{ mg chla m}^{-3}$ in region 5 in cool/dry years (Fig. 3.6a). The B_{eu} peak occurred in region 2 for both climate modes, but the magnitude of the peak was greater during warm/wet years than cool/dry years (47.7 vs. $36.8 \text{ mg chla m}^{-2}$; Fig. 3.6b). A distinct B_{wc} peak occurred in region 3 during warm/wet years, while a broad plateau was observed in regions 3-5 for cool/dry years (Fig. 3.6c). Differences between warm/wet and cool/dry years were greatest in seaward regions (1-3).

Differences in B, B_{eu} , and B_{wc} between cool/dry and warm/wet years expressed as deviations from the LTA displayed consistent responses to climate forcing (Fig. 3.7). The largest positive anomalies in these biomass measures occurred in regions 1-3 during warm/wet years (Figs. 3.7a, c, e). These regions averaged 49, 22, and 57% above the LTA for B, B_{eu} , and B_{wc} , respectively. B_{eu} in region 6 had a negative anomaly in warm/wet years. The largest negative anomalies occurred in regions 1-3 during cool/dry years. Positive anomalies during warm/wet years were greater than negative anomalies during cool/dry years for each region and biomass measure.

Climate also affected the timing of the spring phytoplankton maximum, expressed as total biomass (B_{tot}). Maximum $B_{\text{tot}} \sim 717$ metric tons occurred in late May during warm/wet years and was significantly greater ($p < 0.01$) than the LTA of 455 metric tons. B_{tot} had a broad maximum of 383-445 metric tons in April-May in cool/dry years and was less than ($p > 0.05$) than the LTA (Fig. 3.8). Spring bloom intensity using this integrated measure of biomass averaged 276 metric tons greater in warm/wet than in cool/dry years.

The spatial extent of high biomass in the Bay also differed in warm/wet and cool/dry climate regimes (Fig. 3.9). The spatially-averaged, spring mean B was $8.0 \text{ mg chla m}^{-3}$ and the area with $>8 \text{ mg chla m}^{-3}$ averaged $\sim 3800 \text{ km}^2$ (Fig. 3.9b). During warm/wet years the 8 mg chla m^{-3} isopleth extended to the Bay's mouth and expanded the area with $B > 8 \text{ mg chla m}^{-3}$ to 6836 km^2 (Fig. 3.9a). Conversely, during cool/dry years the area of $B > 8 \text{ mg chla m}^{-3}$ was reduced to 1872 km^2 (Fig. 3.9c).

Regression models

Multiple linear regression models using weather pattern frequencies for winter explained 23 to 89% of the variances of B , B_{eu} , and B_{wc} for spring (Table 3.2). These models differed in the weather patterns used to develop the models, the significance of those models, and the amount of variance explained. Model performance measured as adjusted r^2 was superior in the upper Bay, close to the source of freshwater. For B , weather patterns 3, 6 and 10 were common predictors in equations that explained an average 56% of the variance (Fig. 3.10a). Models of B_{eu} explained an average 59% of the variance for all regions and had low error ($\text{RMSE} = 6.2 \text{ mg chla m}^{-2}$) (Table 3.2; Fig. 3.10b). Models of B_{eu} had weather patterns 3, 5, 6, 7 and 9 as common

independent variables. B_{wc} models explained an average of 45% of the variance, with better results in the upper Bay (regions 5 and 6). Weather patterns 1, 2, 3 and 9 were important predictors for B_{wc} (Table 3.2; Fig. 3.10c). Weather patterns 1 and 9 explained 35% of the variance in B_{tot} summed for all regions of the Bay (Table 3.2). Overall, weather patterns 3, 6, 7 and 9 were the most common independent variables in the 19 models I developed. Winter weather patterns were superior to winter-spring flow, NAO indices, and ENSO indices as predictors of B , B_{eu} , and B_{wc} for spring (Table 3.3), with the exception of B_{wc} for region 2 where a linear regression on freshwater flow explained 36% of the variance ($p < 0.01$).

Time series of observed and predicted B , B_{eu} , and B_{wc} for regional models show good agreement of model outputs and data (Fig. 3.11). Interannual variability of these biomass measures was strongly expressed, and was captured very effectively by the models. I detected no systematic under- or overprediction in the models. Positive anomalies of warm/wet weather patterns (Fig. 3.4a) in 1990, 1996, 1998 and 2003 coincided with peaks of B , B_{eu} , and B_{wc} in most regions. Residuals were generally small and not associated with peaks or troughs in the time series for these biomass measures. I used the models to remove the climate signal and analyze trends of B , B_{eu} , and B_{wc} in the 16-y data set. Residuals showed no significant trends in any of these biomass measures ($\tau > 0.05$; Mann-Kendall Trend Test).

Discussion

Synoptic climatology provides a regional alternative to large-scale climate indices as a means to characterize climate variability in the Chesapeake Bay watershed (Stenseth et al., 2003) where NAO and ENSO have limited skill in describing weather

(Table 3.3; Miller et al., 2006). The weather patterns identified in these analyses (Fig. 3.2) agree well with literature descriptions of common weather patterns for the area in terms of map structure, seasonality in frequency-of-occurrence, and conditions associated with each pattern (Fig. 3.3, Table 3.1; Hayden, 1981; Davis et al., 1993; 1997). Of particular importance to this work were four infrequently occurring patterns (1, 3, 4 and 8; <21% of winter days) that were responsible for 32% of the precipitation in the region (Table 3.1). Weather patterns 3 and 4 represent manifestations of Atlantic Coast 'Nor-Easters' (Hayden, 1981; Davis et al., 1993; Zielinski, 2002). While relatively rare in frequency-of-occurrence these patterns have disproportionate importance because of their potential to deposit significant amounts of snow over much of the watershed. This snow often stays locked in the basin as 'storage' until warmer spring temperatures release the water as part of the spring freshet (Miller et al., 2006; Najjar, 1999).

The patterns identified with this approach integrate a number of environmental parameters that influence phytoplankton dynamics, including temperature, precipitation, wind, and irradiance (Table 3.1; Davis and Kalkstein, 1990), and provide a holistic measure of climate variability (Stenseth et al., 2003). Freshwater input to the Bay has recently been related to variability of these weather pattern frequencies (Miller et al., 2006). There was coherence in the variability of several of the weather patterns described by the synoptic climatology. The frequencies of warm/wet weather patterns (1, 3, 4 and 8) tended to vary in opposition to cool/dry patterns (2, 7 and 10; Fig. 3.4). Kimmel et al. (2006) showed how these same patterns

affect zooplankton abundance, while Austin (2002) described decadal cycles of similar cool/dry and warm/wet weather patterns that affect major fisheries in the Bay.

Climate forcing and associated variability of freshwater flow have been shown to influence phytoplankton dynamics in estuaries. Cloern et al. (2005) demonstrated that a combination of weak coastal upwelling and sustained high pressure over San Francisco Bay produced conditions that led to an exceptional dinoflagellate bloom in September of 2004. Smayda et al. (2004) suggested the inverse correlation between mean annual chlorophyll and NAO in Narragansett Bay was related to changes in temperature-dependent grazing. Freshwater flow affects light availability and density stratification in Delaware Bay (Pennock, 1985), nitrogen loading to the Neuse River estuary (Rudek et al., 1991), and flushing rate of the Hudson River (Howarth et al., 2000), thereby regulating phytoplankton dynamics in these ecosystems.

The position, magnitude, timing, and extent of the spring bloom in Chesapeake Bay were highly responsive to climate forcing (Figs. 3.6-3.9). I observed: (1) a seaward displacement of the spring bloom in years with greater-than-average frequencies of warm/wet weather patterns (Fig. 3.6); (2) higher B , B_{eu} , and B_{wc} in warm/wet years than in cool/dry years, particularly in regions 1-3 (Fig. 3.7); (3) a B_{tot} maximum later in spring and significantly higher during warm/wet years than in cool/dry years (Fig. 3.8); (4) an expanded area with greater-than-average B during warm/wet years (Fig. 3.9). The responsiveness of the spring bloom to climate is consistent with changes in light and nutrient limitation along the north-south axis of the Bay described in a conceptual view (Harding et al., 2002). In sum, warm/wet years are characterized by reduced light penetration in the upper Bay, and increased

nutrient transit to the mid- and lower Bay, while the opposite conditions prevail in cool/dry years (Fig. 3.5; Harding et al., 1986; Harding, 1994).

Models based on winter weather explained a significant fraction of the variance of B , B_{eu} , and B_{wc} for spring, supporting our hypothesis that climate forcing underlies interannual variability of the spring bloom (Figs. 3.10-11). The lagged response whereby winter weather patterns exert a subsequent influence on spring phytoplankton dynamics reflects the role of regional climate variability in controlling freshwater flow and nutrient loading (Miller et al., 2006). Application of a synoptic climatology based on a quantitative classification of observed weather patterns to derive predictive models of the spring bloom proved superior to large-scale climate indices such as NAO and ENSO (Table 3.3), and improves upon previous models based on flow forcing alone (Malone et al., 1988; Harding and Perry, 1997) by capturing the ‘holistic’ nature of climate variability (Stenseth et al., 2003). The specific weather patterns identified as significant in multiple linear regression models varied because each region and its biomass estimate were uniquely forced by climate. I found biomass measures for the lower Bay were most sensitive to climate differences (regions 1-3; Figs. 3.6-3.7), while models for the upper Bay explained more of the variance (regions 4-6; Table 3.2). This is consistent with the exacerbation of light-limitation in the upper Bay in high flow that accompanies warm/wet weather patterns, and fertilization of the lower Bay wherein nutrient limitation is alleviated (Harding and Perry, 1997; Adolf et al., 2006).

The main contributions of this work were to quantify the direct link between regional climate forcing and spring phytoplankton dynamics in the Bay, and to

forecast spring biomass from winter weather. Models I present explained a large fraction of the variance of spring biomass, however, 11 to 77% remains unexplained. The synoptic climatology used here accurately quantifies the types and frequencies of weather that transit the region, but it is not capable of quantifying the intensity of the weather patterns, and this limitation is a probable source of unexplained variance in the relationships I derived. Other sources of unexplained variance include: (1) climate variability not captured by the synoptic climatology; (2) grazing or trophic interactions not influenced by climate variability; (3) changes in nutrient and sediment loading unrelated to climate, i.e. anthropogenic impacts.

Quantifying the influence of climate variability on phytoplankton biomass with regional models allows an examination of residuals for other sources of variability, such as eutrophication. However, no statistically significant trends in the residuals were observed from any of the regional regression models of biomass measures. This suggests most of the increase in phytoplankton biomass I can attribute to increased nutrient loading (Harding, 1994) occurred prior to the period of this study (1989), and supports the conclusions of Harding and Perry (1997). Kemp et al. (2005) related this lack of trend in biomass during the last 20 years to similar patterns in nutrient loading. Additionally, these results indicate there has been no reversal in conditions due to management actions. Models of phytoplankton biomass that can account for climate variability may become increasingly valuable if predicted climate change scenarios for the mid-Atlantic are realized (Najjar et al., 2000).

I addressed the hypothesis that differences in regional climate represent the predominant source of interannual variability of spring phytoplankton biomass in

Chesapeake Bay. To that end, I have: (1) described a procedure and results for classifying and quantifying daily surface SLP to characterize regional climate; (2) quantified the position, magnitude, timing, and extent of the spring bloom for contrasting climate conditions using B , B_{eu} , B_{wc} , and B_{tot} determined from a time-series of remotely sensed chl a and products derived from it; and (3) developed multiple linear regression models using the previously described winter weather patterns to describe four measures of phytoplankton biomass for spring. These models explained between 23 and 89% of the variability in the regional estimates of phytoplankton biomass. No trends were found in the residual variability of the phytoplankton estimates after the climate signal was removed.

Acknowledgements. The authors wish to thank J. E. Adolf, D. G. Kimmel, M. E. Mallonee, R. J. Wood, and all the pilots and crew of aircraft used in the Chesapeake Bay Remote Sensing Program. Support from NASA, NOAA, EPA and Maryland Sea Grant is gratefully acknowledged. WDM was supported by NASA Headquarters under an Earth System Science Fellowship. Contribution no. 3946 of Horn Point Laboratory, University of Maryland Center for Environmental Science.

References

- Adolf, J.E., C.L. Yeager, W.D. Miller, M.E. Mallonee, and L.W. Harding Jr. 2006. Environmental forcing of phytoplankton floral composition, biomass, and primary productivity in Chesapeake Bay, USA. *Estuar. Coast. Shelf Sci.*, 67, 108-122.
- Austin, H.M. 2002. Decadal oscillations and regime shifts, a characterization of the Chesapeake Bay marine climate. *Am. Fish. Soc. Symp.*, 32, 155-170.
- Behrenfeld, M.J., J.T. Randerson, C.R. McClain, G.C. Feldman, S.O. Los, C.J. Tucker, P.G. Falkowski, C.B. Field, R. Frouin, W.E. Esaias, D.D. Kolber, and N.H. Pollack. 2001. Biospheric primary production during an ENSO transition. *Science* 291, 2594-2597.
- Boynton, W.R., W.M. Kemp, and C.W. Keefe. 1982. A comparative analysis of nutrients and other factors influencing estuarine phytoplankton production, p. 69-90. In V.S. Kennedy [ed.]. *Estuarine comparisons*. Academic Press.
- Campbell, J.W., and W.E. Esaias. 1983. Basis for spectral curvature algorithms in remote sensing of chlorophyll. *Appl. Opt.*, 22, 1084-1093.
- Cayan, D.R., and D.H. Peterson. 1989. The influence of North Pacific atmospheric circulation on riverflow in the West, p. 375-397. In D.H. Peterson [ed.]. *Aspects of climate variability in the Pacific and the Western Americas*. American Geophysics Union.
- Chavez, F.P., P.G. Strutton, G.E. Friederich, R.A. Feely, G.C. Feldman, D.G. Foley, and M.J. McPhaden. 1999. Biological and chemical response of the Equatorial Pacific Ocean to the 1997-1998 El Niño. *Science* 286, 2126-2131.
- Cloern, J.E., A.E. Alpine, B.E. Cole, R.L. Wong, J.F. Arthur, and M.D. Ball. 1983. River discharge controls phytoplankton dynamics in the northern San Francisco Bay estuary. *Est. Coast. Shelf Sci.*, 21, 711-725.
- Cloern, J.E. 2001. Our evolving conceptual model of the coastal eutrophication problem. *Mar. Ecol. Prog. Ser.*, 210, 223-253.
- Cloern, J.E., T.S. Schraga, C.B. Lopez, N. Knowles, R. Grover Labiosa, and R. Dugdale. 2005. Climate anomalies generate an exceptional dinoflagellate bloom in San Francisco Bay. *Geophys. Res. Lett.*, 32, L14608, doi:10.1029/2005GL023321.
- Cody R.P., and J.K. Smith. 2005. *Applied Statistics and the SAS programming language*. 5th ed. Pearson/Prentice Hall.

- Crane, R.G., and B.C. Hewitson. 1998. Doubled CO₂ precipitation changes for the Susquehanna basin: downscaling from the genesis general circulation model. *Int. J. Climatol.*, 18, 65-76.
- Davis, R.E., B.P. Hayden, D.A. Gay, W.L. Phillips, and G.V. Jones. 1997. The North Atlantic subtropical anticyclone. *J. Clim.*, 10, 728-744.
- Davis, R.E., R. Dolan, and G. Demme. 1993. Synoptic climatology of Atlantic coast north-easters. *Int. J. Climatol.*, 13, 171-189.
- Davis, R.E., and L.S. Kalkstein. 1990. Development of an automated spatial synoptic climatological classification. *Int. J. Climatol.*, 10, 769-794.
- Guttman, N.B., and R.G. Quayle. 1996. A historical perspective of U.S. climate divisions. *Bull. Am. Meteorol. Soc.*, 77, 293-303.
- Harding, Jr., L.W. 1994. Long-term trends in the distribution of phytoplankton in Chesapeake Bay: roles of light, nutrients, and streamflow. *Mar. Ecol. Prog. Ser.*, 104, 267-291.
- Harding, Jr., L.W., B.W. Meeson, and T.R. Fisher. 1986. Phytoplankton in two East coast estuaries: photosynthesis-light curves and patterns of carbon assimilation. *Est. Coast. Shelf Sci.*, 23, 773-806.
- Harding, Jr., L.W., and E.S. Perry. 1997. Long-term increases of phytoplankton biomass in Chesapeake Bay, 1950-1994. *Mar. Ecol. Prog. Ser.*, 157, 39-52.
- Harding, L.W., E.C. Itsweire, and W.E. Esaias. 1994. Estimates of phytoplankton biomass in the Chesapeake Bay from aircraft remote sensing of chlorophyll concentrations, 1989-92. *Remote Sen. Environ.*, 49, 41-56.
- Harding, L.W., E.C. Itsweire, and W.E. Esaias. 1995. Algorithm development for recovering chlorophyll concentrations in the Chesapeake Bay using aircraft remote sensing, 1989-91. *Photogramm. Eng. Remote Sens.*, 61, 177-185.
- Harding, Jr., L.W., M.E. Mallonee, and E.S. Perry. 2002. Toward a predictive understanding of primary productivity in a temperate, partially stratified estuary. *Est. Coast. Shelf Sci.*, 55, 437-463.
- Hayden, B.P. 1981. Secular variation in Atlantic coast extratropical cyclones. *Mon. Weather Rev.*, 109, 159-167.
- Howarth, R.W., D.P. Swaney, T.J. Butler, and R. Marino. 2000. Climatic control on eutrophication of the Hudson River estuary. *Ecosystems* 3, 210-215.

- Kemp, W.M., W.R. Boynton, J.E. Adolf, D.F. Boesch, W.C. Boicourt, G. Brush, J.C. Cornwell, T.R. Fisher, P.M. Glibert, J.D. Hagy, L.W. Harding, E.D. Houde, D.G. Kimmel, W.D. Miller, R.E.I. Newell, M.R. Roman, E.M. Smith, and J.C. Stevenson. 2005. Eutrophication of Chesapeake Bay: Historical trends and ecological interactions. *Mar. Ecol. Prog. Ser.*, 303, 1-29.
- Kimmel, D.G., W.D. Miller, and M.R. Roman. 2006. Regional scale climate forcing of mesozooplankton dynamics in Chesapeake Bay. *Estuaries* (in press).
- Mallin, M.A., H. W. Paerl, J. Rudek, and P.W. Bates. 1993. Regulation of estuarine primary production by watershed rainfall and river flow. *Mar. Ecol. Prog. Ser.*, 93, 199-203.
- Malone, T.C. 1977. Environmental regulation of phytoplankton productivity in the Lower Hudson estuary. *Est. Coast. Mar. Sci.*, 5, 157-171.
- Malone, T.C., L.H. Crocker, S.E. Pike, and B.W. Wendler. 1988. Influences of river flow on the dynamics of phytoplankton production in a partially stratified estuary. *Mar. Ecol. Prog. Ser.*, 48, 235-249.
- Malone, T.C. 1992. Effects of water column processes on dissolved oxygen, nutrients, phytoplankton and zooplankton, p. 61-112. In D.E. Smith, M. Leffler, and G. Mackiernan [eds.]. *Oxygen Dynamics in the Chesapeake Bay: A Synthesis of Recent Research*. Maryland Sea Grant Program.
- McCabe, G.J., and M.A. Ayers. 1989. Hydrologic effects of climate change in the Delaware River basin. *Water Resour. Bull.*, 25, 1231-1242.
- McGowan, J.A., D.R. Cayan, and L.M. Dorman. 1998. Climate-ocean variability and ecosystem response in the Northeast Pacific. *Science* 281, 210-217.
- Miller, W.D., D.G. Kimmel, and L.W. Harding Jr. 2006. Predicting spring discharge of the Susquehanna River from a synoptic climatology for the eastern United States. *Water Resour. Res.*, 42, W05414, [doi:10.1029/2005WR004270].
- Najjar, R.G. 1999. The water balance of the Susquehanna River Basin and its response to climate change. *J. Hydrol.*, 219, 7-19.
- Najjar, R.G., H.A. Walker, P.J. Anderson, E.J. Barron, R.J. Bord, J.R. Gibson, V.S. Kennedy, C.G. Knight, J.P. Megonigal, R.E. O'Connor, C.D. Polsky, N.P. Psuty, B.A. Richards, L.G. Sorenson, E.M. Steele, and R.S. Swanson. 2000. The potential impacts of climate change on the mid-Atlantic coastal region. *Clim. Res.*, 14, 219-233.
- Ottersen G., N.C. Stenseth, and J.W. Hurrell. 2004. Climate fluctuations and marine systems: a general introduction to the ecological effects, p. 3-14. In N.C. Stenseth,

- G. Ottersen, J.W. Hurrell, and A. Belgrano [eds]. Marine ecosystems and climate variation: the North Atlantic a comparative perspective. Oxford University Press.
- Ottersen, G., B. Planque, A. Belgrano, E. Post, P.C. Reid, and N.C. Stenseth. 2001. Ecological effects of the North Atlantic Oscillation. *Oecologia* 128, 1-14.
- Pennock, J.R. 1985. Chlorophyll distributions in the Delaware Estuary: regulation by light limitation. *Est. Coast. Shelf Sci.*, 21, 711-725.
- Relexans, J.C., M. Meybeck, G. Billen, M. Brugeaille, H. Etcheber, and M. Somville. 1988. Algal and microbial processes involved in particulate organic matter dynamics in the Loire Estuary. *Est. Coast. Shelf Sci.*, 27, 625-644.
- Rudek J., H.W. Paerl, M.A. Mallin, and P.W. Bates. 1991. Seasonal and hydrological control of phytoplankton nutrient limitation in the lower Neuse River Estuary, North Carolina. *Mar. Ecol. Prog. Ser.*, 75, 133-142.
- Smayda, T.J., D.G. Borkman, G. Beaugrand, and A. Belgrano. 2004. Responses of marine phytoplankton populations to fluctuations in marine climate, p. 49-58. In N.C. Stenseth, G. Ottersen, J.W. Hurrell, and A. Belgrano [eds]. *Marine ecosystems and climate variation: the North Atlantic a comparative perspective*. Oxford University Press.
- Stenseth, N.C., A. Mysterud, G. Ottersen, J.W. Hurrell, K.S. Chan, and M. Lima. 2002. Ecological effects of climate fluctuation. *Science* 297, 1292-1296.
- Stenseth, N.C., G. Ottersen, J.W. Hurrell, A. Mysterud, M. Lima, K.S. Chan, N.G. Yoccoz, and B. Adlandsvik. 2003. Studying climate effects on ecology through the use of climate indices: the North Atlantic Oscillation, El Niño Southern Oscillation and beyond. *Proc. R. Soc. Lond., B* 270, 2087-2096.
- Weiss, G.M., L.W. Harding, E.C. Itsweire, J.W. Campbell. 1997. Characterizing lateral variability of phytoplankton chlorophyll in Chesapeake Bay with aircraft ocean color data. *Mar. Ecol. Prog. Ser.*, 149, 183-199.
- Yarnal, B. 1993. *Synoptic Climatology in Environmental Analysis*, Belhaven Press.
- Zielinski, G.A. 2002. A classification scheme for winter storms in the eastern and central United States with emphasis on "Nor'easters". *Bull. Am. Meteorol. Soc.*, 83, 37-51.

Table 3.1. Meteorological characteristics for weather patterns during winter 1989-2004. Wind speed and direction based on data from Baltimore-Washington International airport.

Weather Pattern	%	Temperature Anomaly(\pm SE) ($^{\circ}$ C)	Precipitation Anomaly(\pm SE) (mm)	Wind Direction	Wind Speed (m s^{-1})	Conditions
1 ^a	6.8	3.4 (\pm 0.46)	1.0 (\pm 0.52)	W	3.0	warm/wet
2 ^b	17.0	-3.4 (\pm 0.32)	-0.9 (\pm 0.20)	NW	3.7	cool/dry
3 ^c	6.1	-0.3 (\pm 0.48)	0.7 (\pm 0.54)	N	3.4	seasonal/wet
4 ^c	4.5	2.3 (\pm 0.51)	2.5 (\pm 0.83)	W	3.9	warm/wet
5	17.4	2.5 (\pm 0.33)	0.4 (\pm 0.30)	W	2.7	warm/wet
6	7.7	-0.1 (\pm 0.46)	0.0 (\pm 0.43)	NE	2.3	seasonal
7	13.0	-2.1 (\pm 0.36)	-0.3 (\pm 0.23)	W	4.7	cool/dry
8	3.3	3.2 (\pm 0.72)	1.5 (\pm 0.83)	NE	2.5	warm/wet
9	9.2	2.1 (\pm 0.43)	-0.5 (\pm 0.27)	S	2.0	warm/dry
10	15.0	-1.3 (\pm 0.35)	-0.7 (\pm 0.21)	S	2.0	cool/dry

^a Bermuda High

^b Ohio Valley High

^c Nor'easter

Table 3.2. Results from multiple linear regression models of winter weather pattern frequencies on measurements of regional spring phytoplankton standing stock. Units for RMSE are mg chla m⁻³ for B, mg chla m⁻² for B_{eu} and B_{wc}, and metric tons chla for B_{tot}.

Variable	Region	Adjusted r ²	p-value	Weather patterns	RMSE
B	1	0.41	0.050	1,2,3,7,10	1.7
	2	0.41	0.043	5,6,9,10	2.1
	3	0.58	0.013	1,6,8,9,10	1.8
	4	0.58	0.035	2,3,4,5,6,9	1.6
	5	0.66	0.005	3,4,6,7,10	0.9
	6	0.74	0.007	1,2,3,4,5,7,8	0.9
B _{eu}	1	0.36	0.082	1,2,3,5,7,10	8.5
	2	0.72	0.008	3,4,5,6,7,9,10	5.8
	3	0.78	0.003	2,3,6,7,8,9,10	4.6
	4	0.54	0.020	3,5,6,8,9	7.5
	5	0.70	0.006	1,2,5,7,8,9	4.7
	6	0.41	0.026	6,7,9	5.9
B _{wc}	1	0.23	0.049	1,9	21.8
	2	0.25	0.057	1,9	39.7
	3	0.44	0.031	1,2,3,4	35.9
	4	0.25	0.040	3,6,10	33.6
	5	0.65	0.011	2,3,6,7,8,10	15.5
	6	0.89	0.002	1,2,4,5,7,8,9	6.5
B _{tot}		0.35	0.025	1,9	146

Table 3.3. Linear regression results of ENSO and NAO winter climate indices and winter-spring (Jan.-Apr.) freshwater flow from the Susquehanna River on regional spring phytoplankton biomass measures, ns indicates the model was not statistically significant ($p > 0.05$).

Variable	Region	ENSO		NAO		Winter-Spring Flow	
		r^2	p-value	r^2	p-value	r^2	p-value
B	1	0.002	ns	0.062	ns	0.091	ns
	2	0.022	ns	0.067	ns	0.082	ns
	3	0.002	ns	0.066	ns	0.139	ns
	4	0.004	ns	0.053	ns	0.006	ns
	5	0.004	ns	0.009	ns	0.022	ns
	6	0.009	ns	0.012	ns	0.001	ns
B_{eu}	1	0.005	ns	0.035	ns	0.007	ns
	2	0.011	ns	0.001	ns	0.034	ns
	3	0.002	ns	0.035	ns	0.009	ns
	4	0.058	ns	0.260	ns	0.420	0.01
	5	0.022	ns	0.016	ns	0.492	0.01
	6	0.010	ns	0.037	ns	0.469	0.01
B_{wc}	1	0.016	ns	0.130	ns	0.217	0.04
	2	0.009	ns	0.150	ns	0.359	0.01
	3	0.012	ns	0.138	ns	0.305	0.02
	4	0.004	ns	0.008	ns	0.010	ns
	5	0.011	ns	0.013	ns	0.027	ns
	6	0.031	ns	0.075	ns	0.004	ns
B_{tot}		0.001	ns	0.177	ns	0.260	0.04

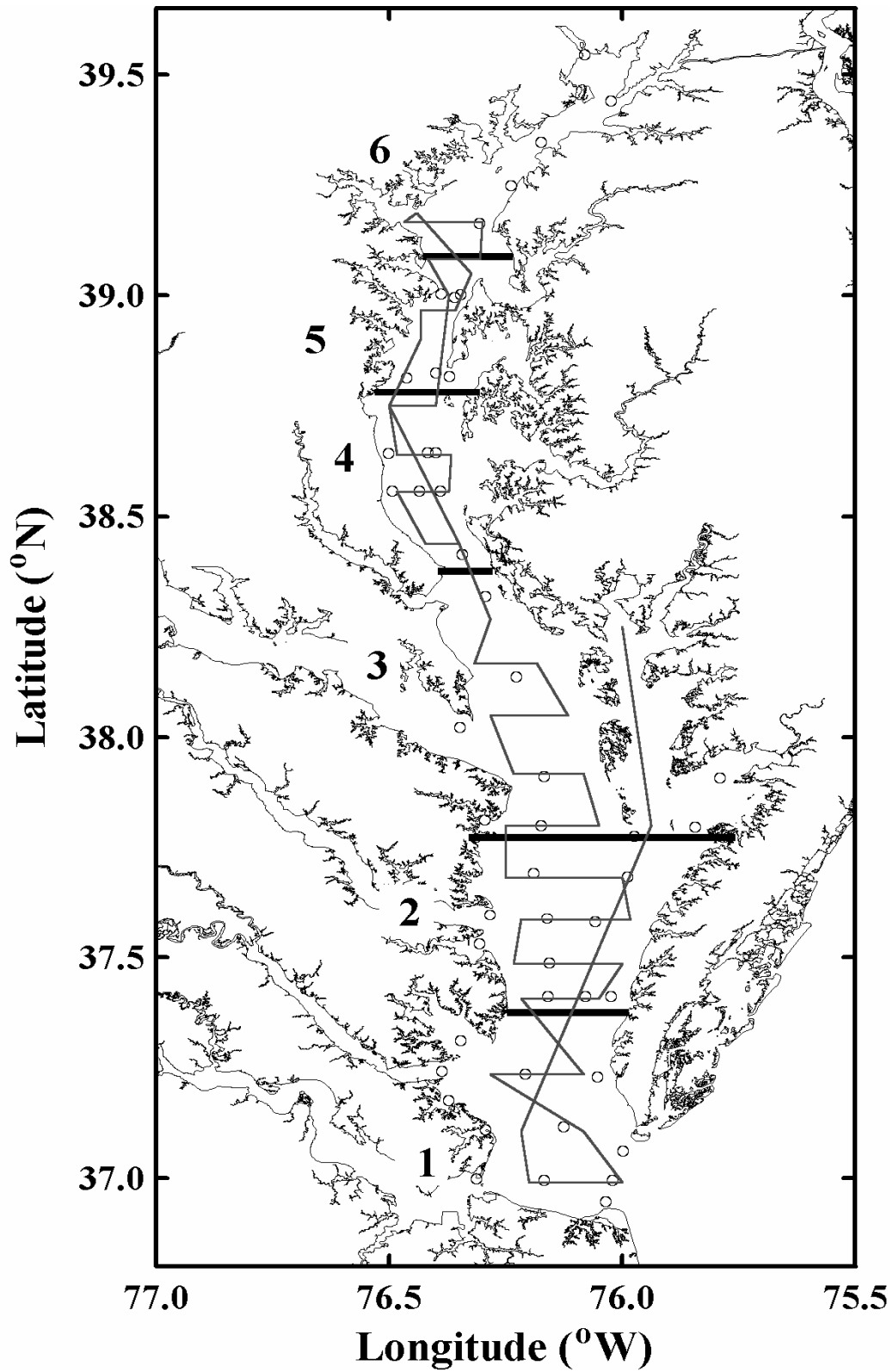


Fig. 3.1. Map of Chesapeake Bay showing flight lines from CBRSP, regions noted with heavy black lines and large numbers, and CBP stations as open circles. Regions are delineated as 1, 36.95-37.40°N; 2, 37.41-37.80°N; 3, 37.81-38.40°N; 4, 38.41-38.80°N; 5, 38.81-39.10°N; 6, 39.11-39.66°N.

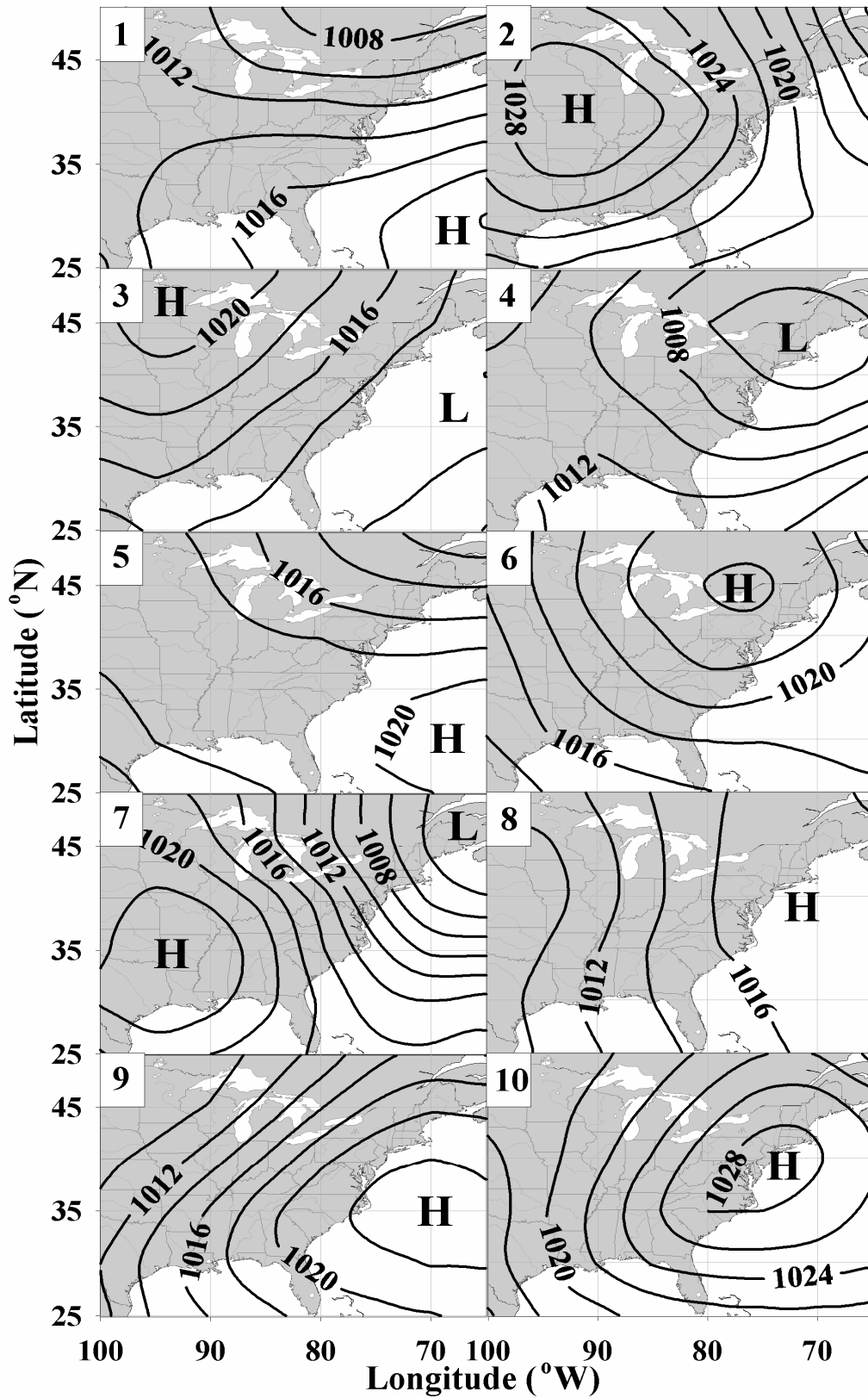


Fig. 3.2. Average sea-level pressure maps for each cluster. Weather pattern number in upper left-hand corner. H and L indicate centers of high and low pressure regions, respectively. Black lines delineate regions of constant pressure (mb).

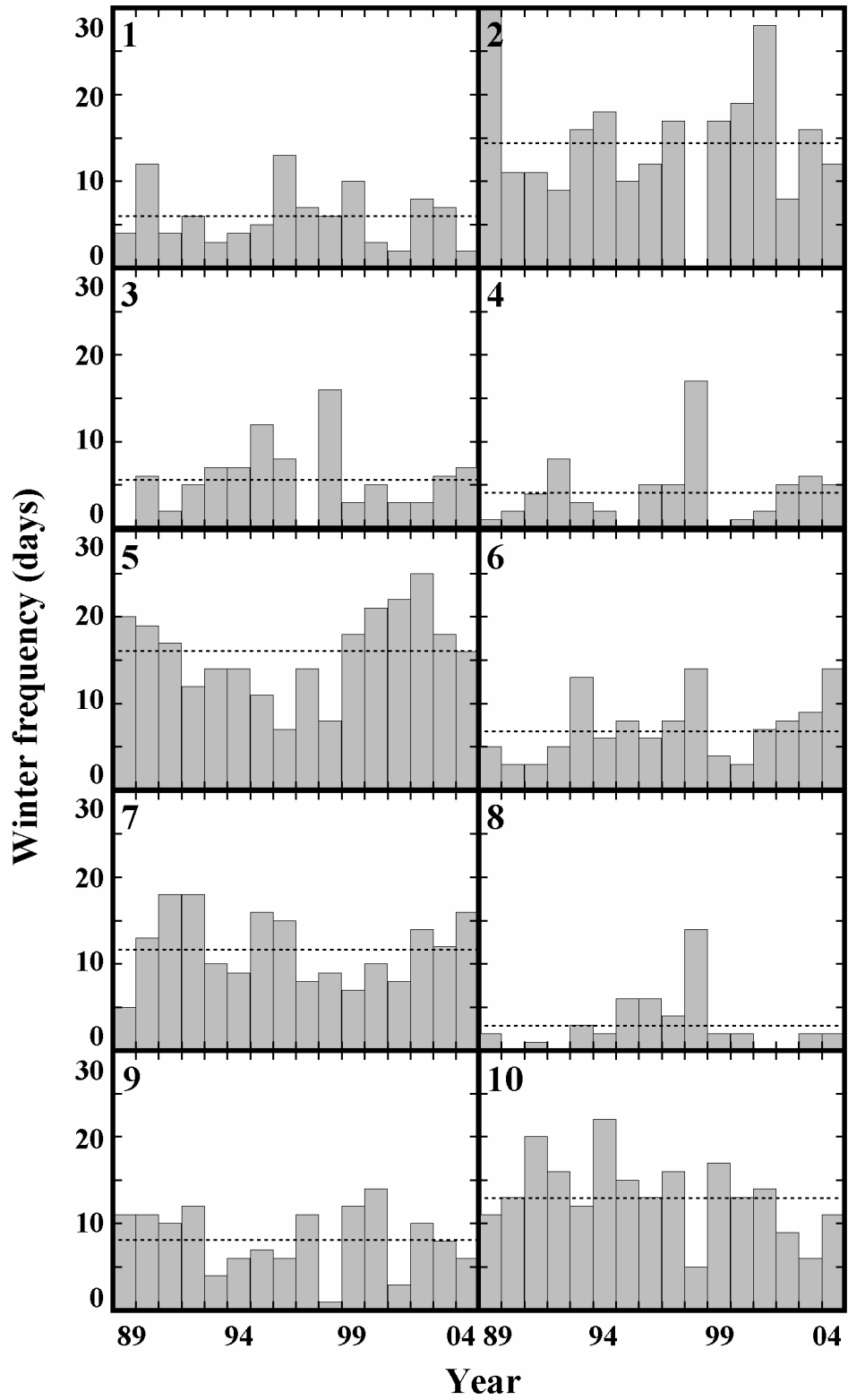


Fig. 3.3. Time series (1989-2004) of winter (December-February) frequency-of-occurrence for each cluster. Weather pattern number in upper left-hand corner. Horizontal dashed lines indicate the LTA for each weather pattern.

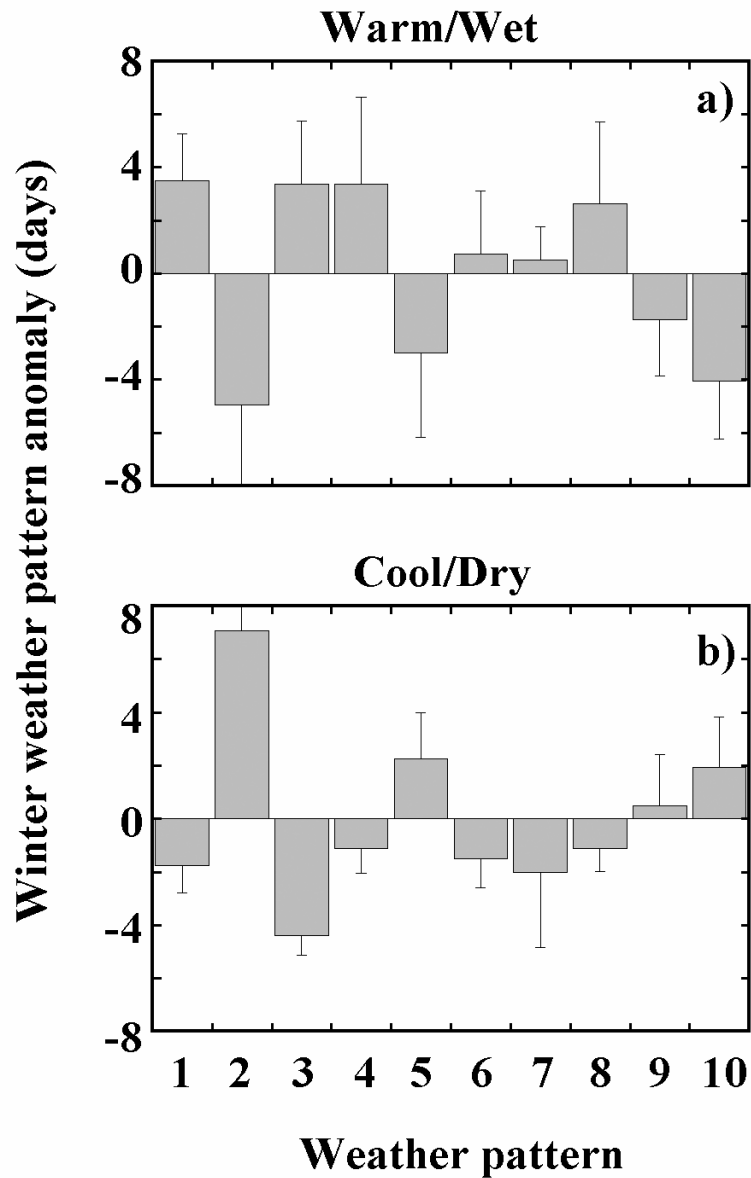


Fig. 3.4. a) Winter weather pattern deviations from LTA frequency-of-occurrence for contrasting climate extremes for years dominated by a) warm/wet weather patterns and b) cool/dry weather patterns.

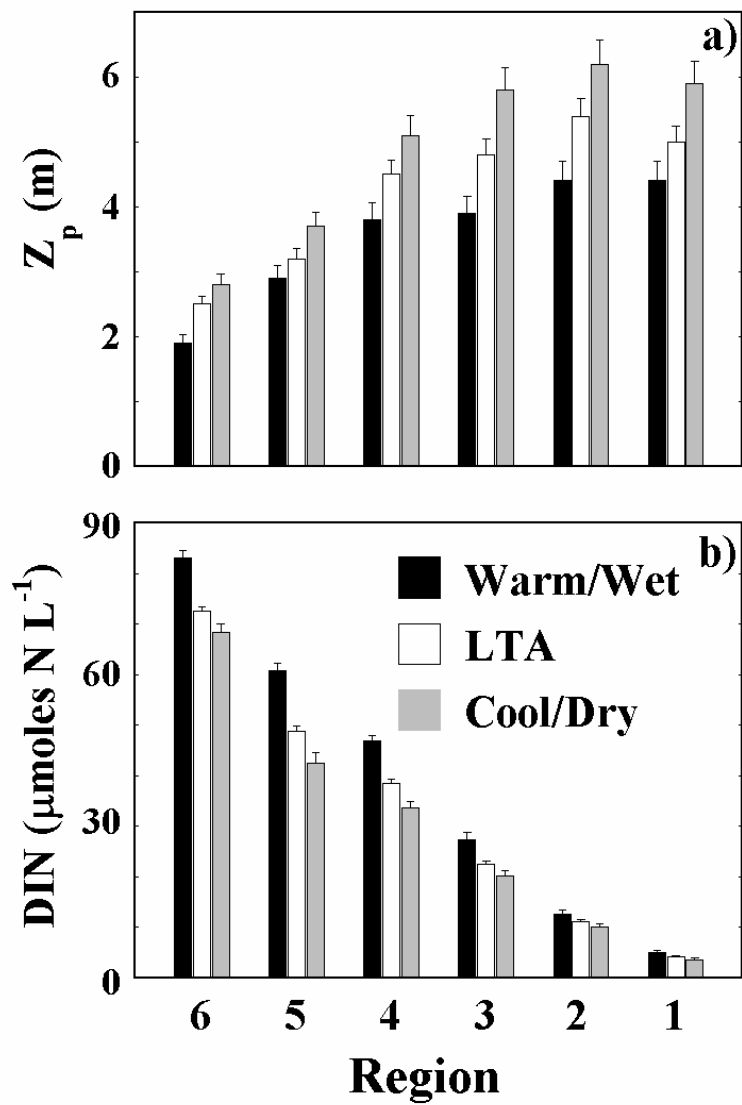


Fig. 3.5. Regional water column properties for warm/wet (black bars), LTA (open bars), and cool/dry years (gray bars) for a) Z_p and b) surface DIN. Error bars indicate standard error. Regions progress from freshwater (6) to saltwater (1).

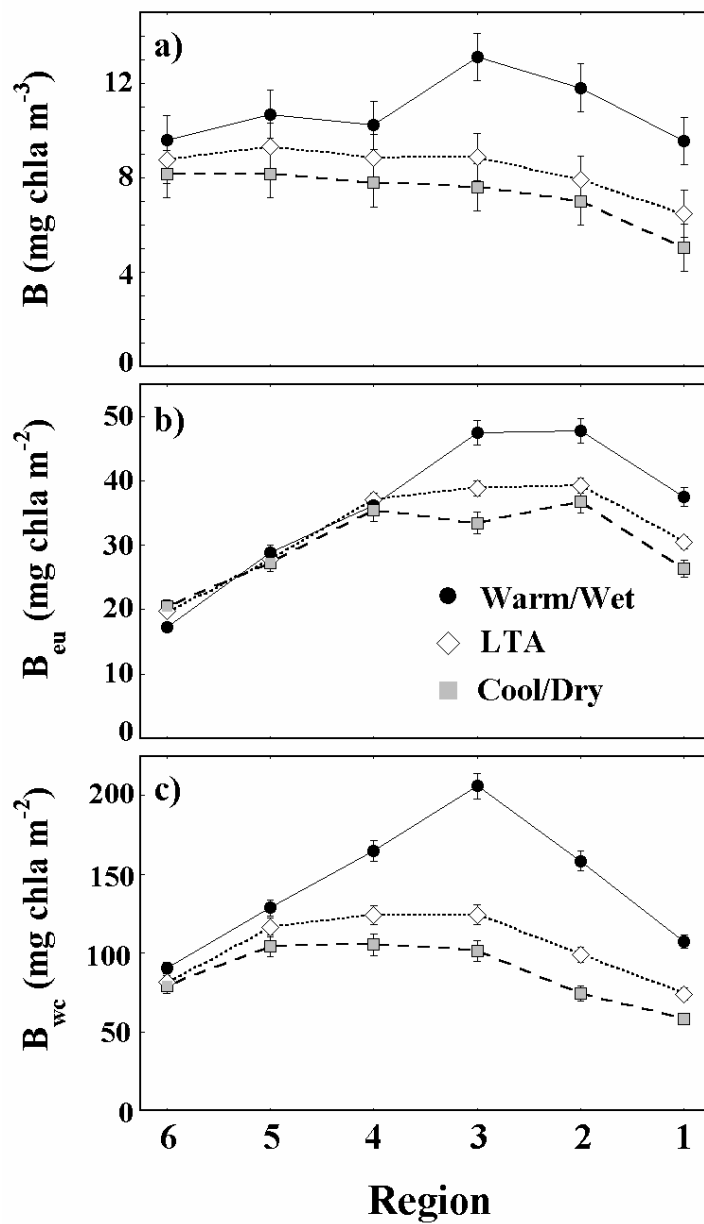


Fig. 3.6. Regional mean a) B , b) B_{eu} , and c) B_{wc} for warm/wet (black circles), LTA (open diamonds), and cool/dry (gray squares) years. Error bars indicate standard error. Regions progress from freshwater (6) to saltwater (1).

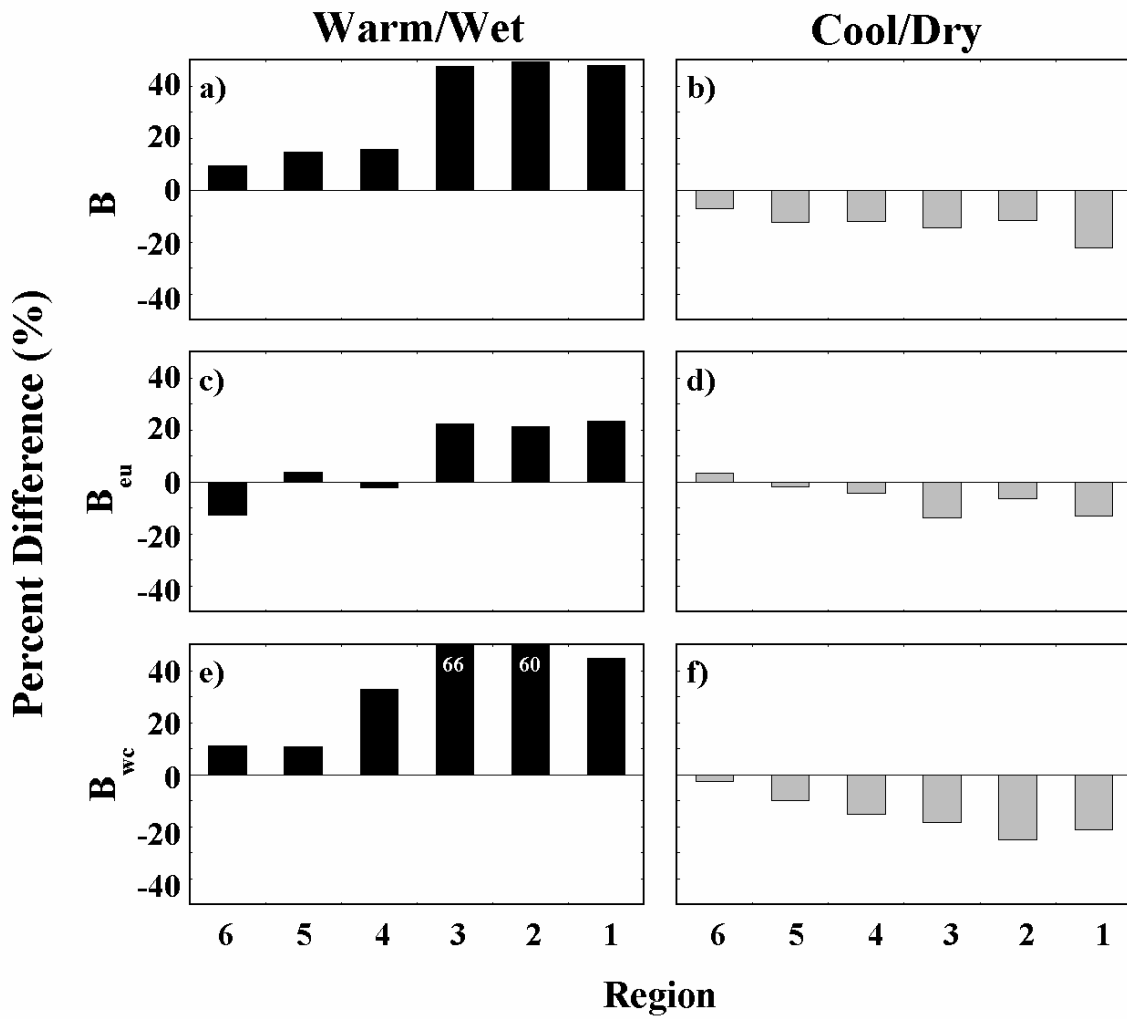


Fig. 3.7. Percent difference from LTA for 6 regions during warm/wet years a) B , c) B_{eu} , and e) B_{wc} and cool/dry years b) B , d) B_{eu} , and f) B_{wc} . Regions progress from freshwater (6) to saltwater (1).

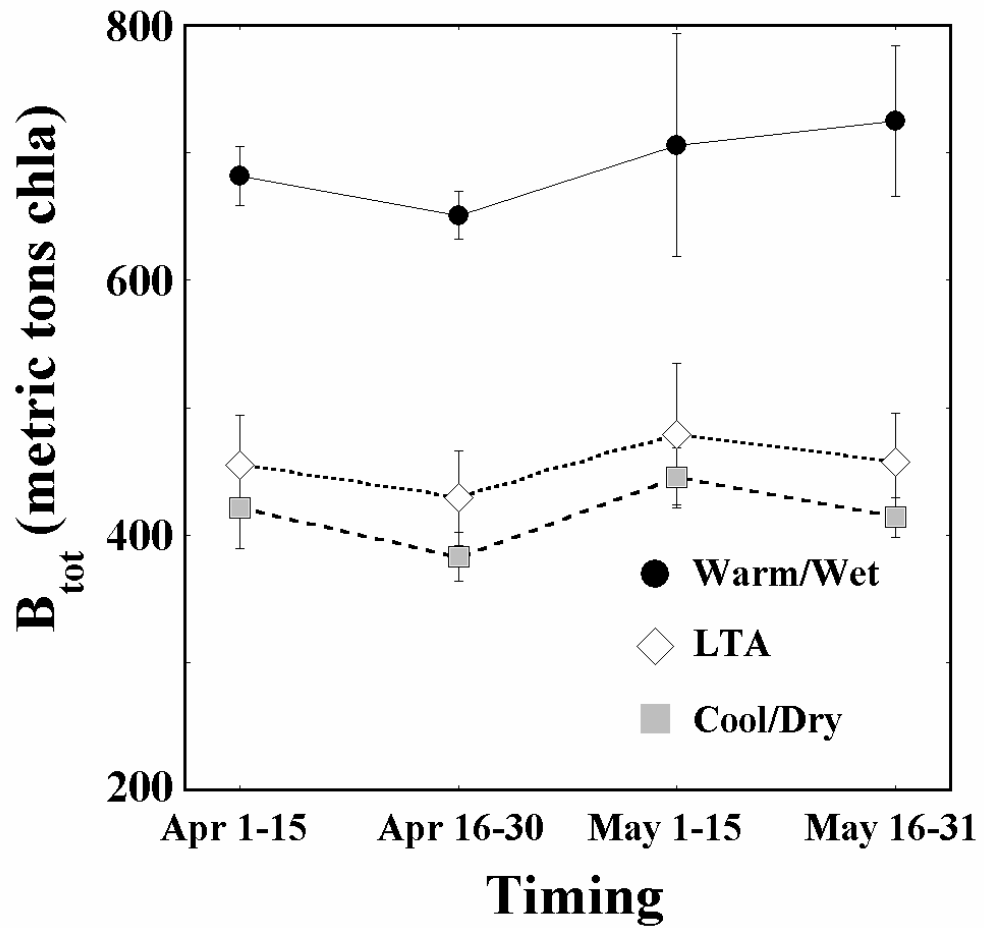


Fig. 3.8. Timing of maximum B_{tot} for warm/wet (black circles), LTA (open diamonds), and cool/dry (gray squares) years average over two week intervals.

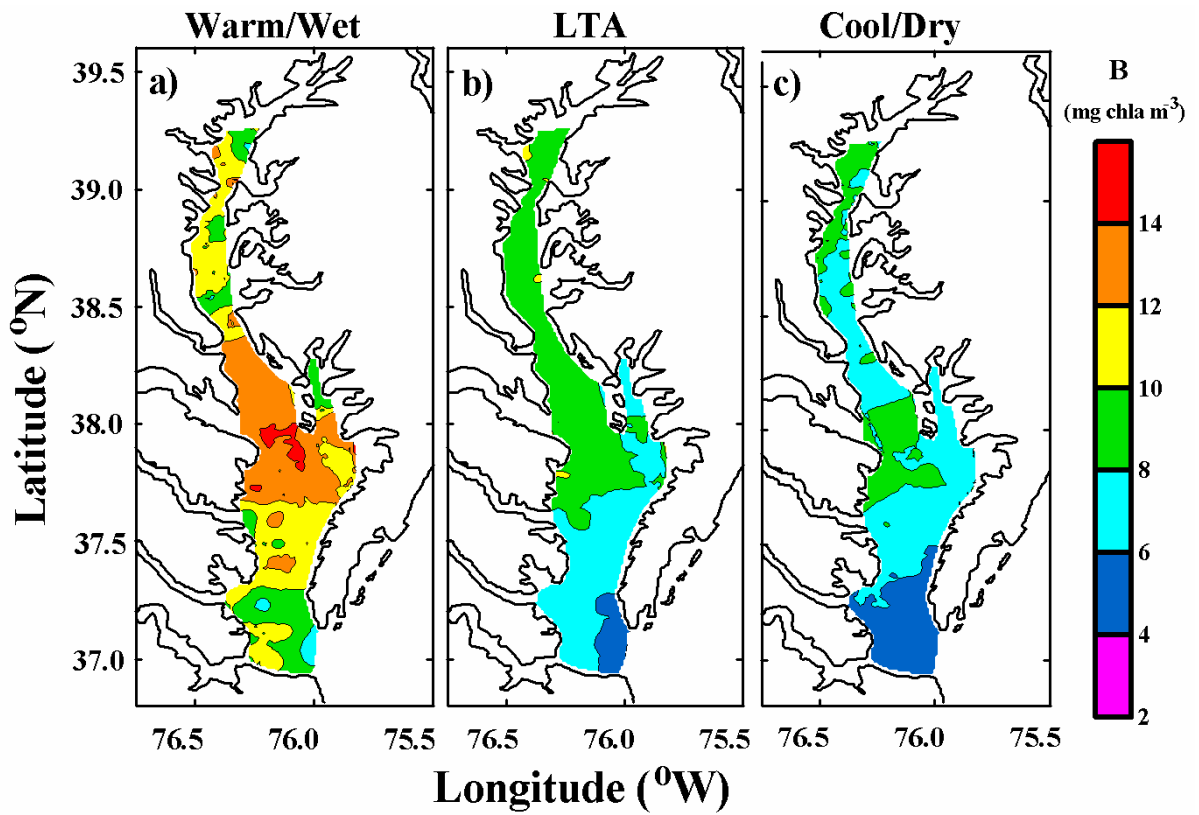


Fig. 3.9. Spatially explicit maps of B for a) warm/wet, b) LTA, and c) cool/dry years

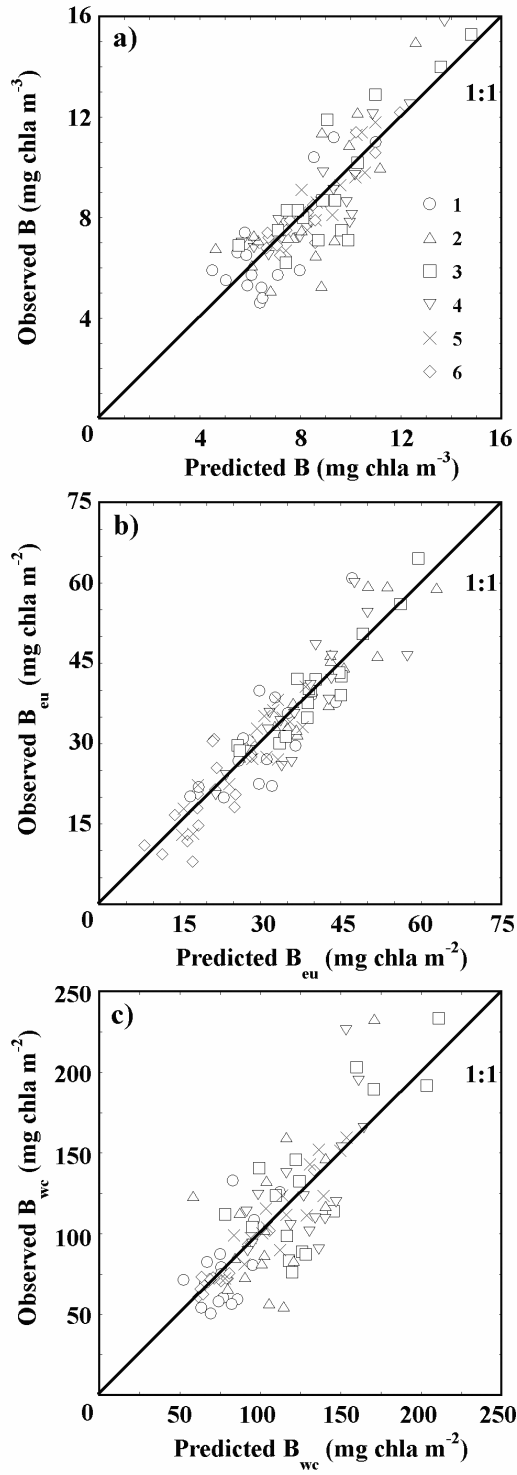


Fig. 3.10. Comparison of predicted versus observed results from regional multiple linear regression models predicting spring a) B, b) B_{eu}, c) B_{wc}.

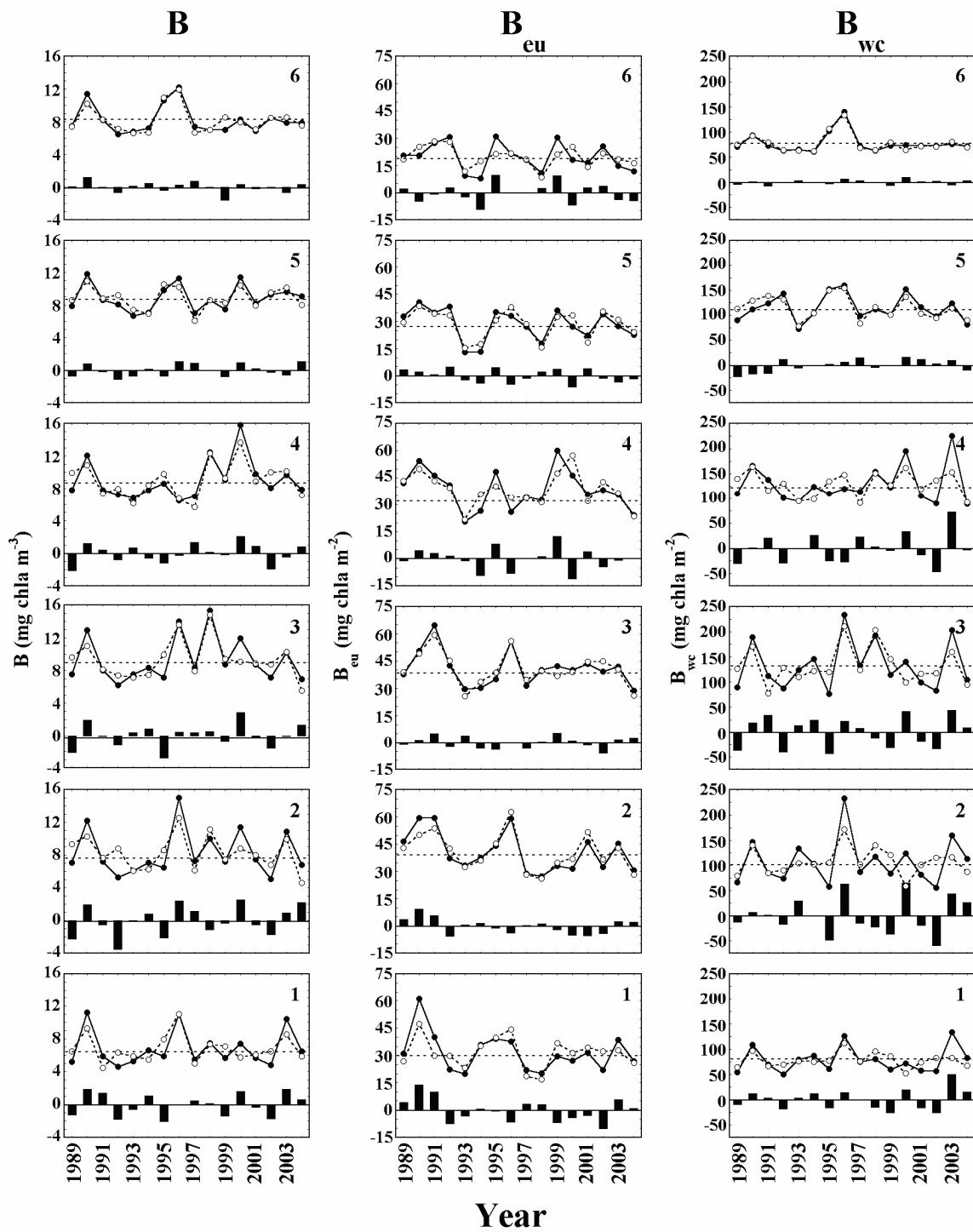


Fig. 3.11. Time series of regional predicted (open circles) and observed (black circles) results from multiple linear regression models and residuals for B, B_{eu}, B_{wc}. Horizontal dashed lines indicate the LTA for each region. Black bars indicate residuals. Region shown in upper right hand corner.

Chapter 4

Climate Forcing of Primary Productivity in Chesapeake Bay¹

¹Miller, W.D., L.W. Harding Jr., M.E. Mallonee, J.E. Adolf , and D.G. Kimmel.
Climate Forcing of Primary Productivity in Chesapeake Bay. Estuarine Coastal and
Shelf Science. To be submitted.

Abstract

I report that climate forcing drives high seasonal and interannual variability of primary productivity (PP) in Chesapeake Bay. Climate was quantified using a 'synoptic climatology' developed using frequencies of predominant weather patterns classified from daily sea-level pressure (SLP) data for the eastern United States. PP was derived using a depth-integrated model (DIM) applied to 16 yrs (1989-2004) of ocean color data from aircraft remote sensing. These data provided high spatial and temporal resolution needed to accurately compute annual and summer integral production (AIP and SIP). I found AIP and SIP were correlated, SIP was responsible for ~62% of AIP, and each integral varied approximately two-fold for a wide range of climate conditions. AIP and SIP showed strongly contrasting responses to warm/wet and cool/dry weather patterns that occurred during winter-spring. Trend analysis showed a small but significant decrease of AIP and SIP caused by decreasing photic depth, Z_p . I removed the Z_p trend prior to developing multiple linear regression models of the integrals on frequencies of winter-spring (Jan-Apr) weather patterns that explained 42-63% of the variance. These findings indicate climate early in the year sets up PP in summer, leading to predictable AIP and SIP. I suggest interannual variability of precipitation and freshwater flow as expressions of climate controls nutrient loading in spring, leading to variability of spring bloom intensity. AIP and SIP are strongly coupled to biomass generated in the spring bloom that supplies the substrate for nutrient regeneration to support summer PP. The direct link of climate to AIP and SIP gives a predictive capability with implications for forecasting key aspects of planktonic and fish dynamics in the ecosystem.

Introduction

Climate has been identified as a major source of variability for primary productivity (PP) in a variety of aquatic ecosystems, including lakes (Goldman et al., 1989), estuaries (Smayda et al., 2004), coastal waters (Lindahl et al., 1998), and the global ocean (Behrenfeld et al., 2001). High and variable PP in estuaries has been attributed to nutrient loading from watersheds associated with interannual differences in precipitation and freshwater flow (Boynton et al., 1982). Freshwater flow responds to climate variability and explains a significant amount of the variability of PP in a variety of estuaries, including the Hudson River outflow (Howarth et al., 2000), upper San Francisco Bay (Jassby et al., 2002), Neuse River (Rudek et al., 1991), and Mississippi River plume/Gulf of Mexico (Justić et al., 1997). Comprehensive measures of climate variability contain additional information that may improve these relationships, leading to a fuller understanding of the role of climate in driving interannual variability of PP.

I know that large-scale climate indices, such as the North Atlantic Oscillation (NAO) and El Niño-Southern Oscillation (ENSO) capture climate and weather variability in many parts of the world (Stenseth et al., 2002). These indices integrate the effects of multiple weather variables and provide ‘holistic’ measures of climate variability (Stenseth et al., 2003), but they are not applicable to all regions. For example, NAO does not explain variability of environmental conditions in the mid-Atlantic (Tootle et al., 2005), whereas a ‘synoptic scale’ (1,000-2,500 km) climatology has produced significant results (Miller et al., 2006; Kimmel et al., 2006). On a regional scale, synoptic climatology can be used to classify and quantify atmospheric circulation patterns and relate the frequencies-of-occurrence of those

patterns to environmental conditions (Yarnal, 1993). Miller and Harding (submitted) showed coherence of spring bloom intensity and the frequencies of ‘warm/wet’ and ‘cool/dry’ weather patterns transiting the Chesapeake Bay watershed during winter. Years dominated by warm/wet patterns had above average biomass, with maximum chlorophyll-*a* (Chl *a*) shifted down-estuary, and a spring bloom occurring in late spring. Cool/dry years showed the opposite responses, with lower Chl *a* located up-estuary.

While I have quantified climate forcing of the spring bloom, effects on another important element of the annual phytoplankton cycle in Chesapeake Bay, primary productivity (PP), have not been analyzed. The annual cycle is dominated by a winter-spring Chl *a* peak composed of large diatoms that occurs ~3 months prior to a summer PP maximum composed of small diatoms, cyanobacteria, and flagellates (Malone, 1992). The asynchrony of Chl *a* and PP maxima is related to the timing of high nutrient loading in the spring freshet, estuarine circulation, and regeneration/retention of nutrients within the Bay (Malone et al., 1988). During spring, Chl *a* increases in the presence of saturating nutrient concentrations as temperature limits both phytoplankton growth rates and zooplankton grazing pressure. In contrast, high phytoplankton growth rates in summer occur in the absence of high Chl *a* at lower nutrient concentration and higher grazing pressure (Malone et al., 1996). The accepted paradigm is that nutrients sequestered in phytoplankton biomass during spring are retained in the system via estuarine circulation and microbial remineralization and support high PP I observe during summer (Kemp and Boynton, 1984). Transient interruptions of the pycnocline during summer permit

regenerated nutrients to be re-introduced into the photic zone to support high summer PP as nutrient inputs associated with freshwater flow are low (Malone, 1992). Large interannual differences in the magnitude of Chl *a* and PP peaks have been attributed to climate variability through its effects on freshwater flow and attendant nutrient loading during spring, and wind mixing of the water column during summer (Malone et al., 1988).

Harding et al. (2002) addressed variability of PP in Chesapeake Bay using a large (n=575) dataset of PP measurements spanning a broad range of environmental conditions (1982-2000), and developed depth-integrated models (DIM) of PP. These data were also used to calculate annual integral production (AIP), but sampling was too infrequent for accurate retrievals in many years, limiting the resolution of interannual variability of this important parameter. The models used relatively simple input variables (Chl *a*, sea-surface temperature (SST), photic depth (Z_p), daylength (D_{irr}), and incident irradiance (E_o) to estimate PP. These input terms make the models amenable to use of remotely sensed data collected at high spatial and temporal resolution to support improved estimates of AIP.

In this paper, I build on earlier work that addressed regional climate forcing of precipitation and freshwater flow (Miller et al., 2006), and spring bloom intensity in Chesapeake Bay (Miller and Harding, submitted) using PP models for the Bay (Harding et al., 2002) applied to a 16 yr time series of remotely sensed Chl *a* and SST. I addressed the hypothesis that regional climate forcing drives interannual variability of AIP in Chesapeake Bay. To achieve this goal I: (1) quantified the spatial and temporal variability of PP with locally calibrated and validated models of PP

using remotely sensed data combined with land and shipboard measurements to determine AIP; (2) described consistent responses of Chl *a* and PP in summer to contrasting warm/wet and cool/dry climate regimes, quantified with a synoptic climatology; (3) assessed the predictive skill of multiple linear regression models used to quantify the variance of PP explained by frequencies of weather patterns occurring during winter-spring. By addressing these goals I show that regional-scale climate variability is an important driver of PP dynamics in Chesapeake Bay.

Methods

Model application

Gross PP was estimated using the Chesapeake Bay Productivity Model (CBPM-2) (Harding et al., 2002). This DIM (eq. 1) is a modification of the Vertically Generalized Productivity Model (VGPM; Behrenfeld and Falkowski, 1997) that was log-transformed to allow incorporation of locally calibrated coefficients for each independent variable. It contains a model of the ‘phytoplankton physiology’ term, P_{opt}^B , that shares independent variables with the core model and makes it useful for remotely sensed data. CBPM-2 was calibrated with data collected over 17 yrs (1982-1998), and produced estimates of PP with a root mean square error (RMSE) of 49.7%. Validation with data from 1999-2000 not used in model calibration produced estimates with RMSE of 47.6%. The independent variables include: surface Chl *a* (mg m^{-3}), incident irradiance, E_o ($\text{E m}^{-2} \text{d}^{-1}$), used as $tE_o = (E_o/(E_o + 4.1))$ to describe the saturating effect of incident irradiance (Behrenfeld and Falkowski, 1997), photic depth, Z_p (m) estimated as the 1 % isolume, daylength, D_{irr} (h), sea-surface temperature, SST ($^{\circ}\text{C}$).

$$\log PP_{\text{gross}} = 0.1619 + 0.7721 \cdot \log \text{Chl } a + 2.0344 \cdot \log tE_o + 0.8115 \cdot \log Z_p + 0.0342 \cdot \log D_{\text{irr}} + 1.2817 \cdot \log \text{SST} \quad (1)$$

Data sources for independent variables were: (1) Chl *a* and SST from aircraft remote sensing; (2) Z_p from bi-weekly to monthly monitoring cruises of EPA Chesapeake Bay Program (CBP; <http://www.chesapeakebay.net/>); (3) E_o from a LiCor model 192 2π sensor at Smithsonian Environmental Research Lab (SERC, Edgewater, MD); (4) D_{irr} calculated from latitude and day-of-year. All data were mapped onto a common 1 km² grid, producing approximately 7000 grid cells for each flight/cruise. Data from 18-37 flights and cruises per year were combined to produce annual coverage of the Bay. The number of flights for each year varied depending on weather and aircraft availability. Shipboard data were substituted for aircraft data for 1996 due to instrument malfunctions. Data were analyzed for three regions of the mainstem Bay defined by latitude and average salinity location (Harding et al., 1997; Fig. 4.1). Summer was defined as June through September for determination of SIP.

Remotely sensed data

Chl *a* (mg m⁻³) was determined using ocean color measurements from light aircraft as part of the Chesapeake Bay Remote Sensing Program (CBRSP; <http://www.cbrsp.org>; Harding et al., 1994, 1995). Geo-referenced data were collected from an altitude of 150 m and a ground speed of approximately 50 m s⁻¹ using nadir-viewing multispectral radiometers (ODAS, SAS II, and SAS III; Harding et al., 2001). Chl *a* was computed using a spectral curvature algorithm (Campbell and Esaias, 1983) applied to water-leaving radiances in the blue-green region of the visible spectrum. Radiometric calibrations were made annually for all instruments.

Retrievals of Chl *a* relied on regional algorithms calibrated with matches to *in-situ* measurements from CBP and our own cruises. I defined a match as ± 12 h on the same day, $\pm 0.01^\circ$ latitude, and $\pm 0.005^\circ$ longitude (Harding et al., 1994; 1995). The working equation retrieved \log_{10} Chl *a* with an RMSE of 0.21 (log units). Flight data were interpolated onto a 1 km^2 grid for visualization and further analyses using a two-dimensional, inverse-distance-squared, octant search (Harding et al., 1994; 1995). SST was determined with an infrared (IR) temperature sensor (Heimann Instruments Inc.).

Synoptic climatology

Methods to quantify regional scale climate variability using a synoptic climatology followed Yarnal (1993), Miller et al. (2006), and Kimmel et al. (2006). Briefly, I used gridded, daily surface sea-level pressure (SLP) data from the National Center for Atmospheric Research (NCAR; <http://dss.ucar.edu>) to create a 48-point (6×8) grid of SLP data covering the eastern United States (25° - 50° N x 65° - 100° W). Principal component analysis (PCA) was used as a data-reduction step to decrease the number of variables submitted to two-stages of clustering (average linkage and *k*-means). The cluster analyses grouped the data into similarly occurring modes of variance that related to similar atmospheric circulation patterns. Average SLP maps for each of the ten dominant clusters were then determined by taking the mean value for each grid point within the daily maps. The seasonal frequencies-of-occurrence of each weather pattern were then computed for every year and used in multiple linear regression models. Temperature and precipitation data were obtained from the National Climate Data Center (NCDC; <http://cdo.ncdc.noaa.gov>).

Statistical analyses

I used multiple linear regression models to quantify relationships of AIP and SIP to frequencies-of-occurrence of weather patterns for a range of time windows. Regional and whole Bay measures of AIP and SIP were the dependent variables, weather pattern frequencies for various time periods were the independent variables, and each year was an observation ($n = 16$). Selection of independent variables for inclusion in each model was determined by the combination of weather patterns that explained the maximum amount of variance in the dataset while producing a significant ($p < 0.05$) model. Explained variance was measured as the adjusted r^2 to account for the increased variance explained with increasing numbers of explanatory (independent) variables. Multi-collinearity of the independent variables was checked with the variance inflation factor (VIF) diagnostic in SAS (Cody and Smith, 2005); no variable in the models had a $VIF > 5$ (values greater than 10 indicate serious problems with multi-collinearity). Mann-Kendall trend tests were used to investigate the relationships between dependent variables and time. All statistics were performed in SAS version 9.1 (SAS Institute, Cary, NC).

Results

Interannual variability of PP

Time series of monthly, average PP for the 16 yr study showed high interannual variability, dominated by summer (June-September) (Fig. 4.2). Annual averages showed highest values in the meso- and polyhaline regions at 840 and 828 $\text{mg C m}^{-2} \text{d}^{-1}$, respectively, and the oligohaline was significantly lower (698 $\text{mg C m}^{-2} \text{d}^{-1}$). Summer maxima showed 2- to 3-fold differences among years and averaged 1653 $\text{mg C m}^{-2} \text{d}^{-1}$.

$\text{C m}^{-2} \text{ d}^{-1}$ for the oligohaline, $1957 \text{ mg C m}^{-2} \text{ d}^{-1}$ for the mesohaline, and $1860 \text{ mg C m}^{-2} \text{ d}^{-1}$ polyhaline regions. Secondary PP peaks were observed for a number of years in spring.

AIP and SIP showed two-fold variability with the greatest range in the polyhaline (range = $226 \text{ g C m}^{-2} \text{ yr}^{-1}$) and lowest in the oligohaline (range = $96 \text{ g C m}^{-2} \text{ yr}^{-1}$) (Fig. 4.3). Average Bay-wide AIP for the 16-yr time series was $301 \text{ g C m}^{-2} \text{ yr}^{-1}$. AIP was highest in the mesohaline ($306 \text{ g C m}^{-2} \text{ yr}^{-1}$) and lowest ($256 \text{ g C m}^{-2} \text{ yr}^{-1}$) in the oligohaline. Bay-wide SIP averaged $189 \text{ g C m}^{-2} \text{ summer}^{-1}$, whereas regional values ranged from a low of $164 \text{ g C m}^{-2} \text{ summer}^{-1}$ in the oligohaline to $193 \text{ g C m}^{-2} \text{ summer}^{-1}$ in the mesohaline. For the whole Bay, the polyhaline was responsible for 52.6% of AIP, the mesohaline 42.5%, and the oligohaline only 4.8%. There were differences in production between regions, but the proportion of Bay-wide production associated with each region was primarily a function of the area encompassed. SIP constituted a large and consistent fraction of AIP, ranging from 55 to 79% with an average of 62%. Simple linear regression of AIP on SIP for all regions produced a highly significant relationship ($p < 0.001$) that explained 92% of the variance of AIP (Fig. 4.4). When examined regionally, summer production only explains 75% of the variance of AIP in the oligohaline, while 94-95% of the variance of AIP is explained by SIP for the meso- and polyhaline, respectively.

Trends of AIP and SIP

Mann-Kendall trend tests of monthly average PP showed negative trends for most months, with significant slopes ($p < 0.05$) in summer (Fig. 4.5). The magnitudes of the trends were greatest in the meso- and polyhaline Bay (Fig. 4.5). As AIP and SIP are

tightly coupled (Fig. 4.4), and the observed monthly trends were most significant in summer (Fig. 4.5), further analyses focused on SIP. I found decreasing trends of SIP were significant ($p < 0.05$) for all regions except the oligohaline ($p > 0.10$) with slopes ranging from -2 to $-6 \text{ g C m}^{-2} \text{ summer}^{-1}$ (Fig. 4.6). The trend explained 26 to 30% of the variance in the SIP dataset. Residuals from trend lines were used in further analyses of climate forcing on SIP as they showed no trends. Similar patterns were observed for AIP with the time trend explaining 19 to 34% of the variance in the time series and slopes ranging from -3.6 to $-9.0 \text{ g C m}^{-2} \text{ yr}^{-1}$.

The five input terms to the PP model were analyzed for trends to determine the source of the observed PP trend. No statistically significant relationships were found for D_{irr} , E_o , SST, or Chl a , whereas Z_p showed significant ($p < 0.05$) decreasing trends for all regions, explaining 31% of the variance in the time series (Fig. 4.7). Z_p decreases ranged from 4 cm summer^{-1} in the polyhaline to 8 cm summer^{-1} in the oligohaline. No trends were observed in any of the bio-optical properties that could explain the observed declines of Z_p (i.e., Chl a , total suspended sediments, TSS, or chromophoric dissolved organic matter (CDOM)). While no sufficiently resolved CDOM dataset was available, CDOM is known to vary with salinity and no significant trends of salinity were observed.

Winter-spring weather pattern characteristics

The frequencies-of-occurrence of regional weather patterns (Fig. 4.8) over 17 separate time periods, from winter through summer, were examined to determine their influence on SIP residuals (Z_p trend removed). The frequencies of winter-spring (January-April) patterns explained the largest amount of variance and produced

significant models. Comparisons using other combinations of months, including summer, did not produce significant models. Frequencies-of-occurrence of the ten weather patterns during winter-spring showed considerable variability over the 16-yr time series, but I observed no significant trends in any of the frequencies (Fig. 4.9). Weather pattern frequencies over the four-month period averaged 8.9 (pattern 4) to 15.9 days (pattern 5) and varied between 1 and 30 days. A more comprehensive description of the weather patterns and their characteristics can be found in Miller et al. (2006).

Weather patterns were stratified by similar temperature and precipitation anomalies (i.e., warm/wet vs. cool/dry). Warm/wet weather patterns (1, 3, 4 and 8; Table 4.1) had temperatures and precipitation that averaged 2.7°C and 1.0 mm d^{-1} above the long-term averages (LTAs) for this time period (1989-2004). Cool/dry weather patterns (2, 7, and 10; Table 4.1) had temperatures 4.3°C and precipitation 0.8 mm d^{-1} below the LTA. Years with above-average frequencies of warm/wet weather patterns (1991, 1996, 1998, and 2003) had higher precipitation (2.94 vs. 2.20 mm d^{-1}) and slightly higher temperatures (1.44 vs. 1.39°C) than years dominated by cool/dry weather patterns (1989, 1997, 2001, and 2002) (Fig. 4.10). I also observed considerable differences of freshwater flow (3819 vs. $1882\text{ m}^3\text{ s}^{-1}$) and nitrogen loading (67.5 vs. $29.9 \times 10^6\text{ kg N}$) into Chesapeake Bay in years with warm/wet or cool/dry winter-springs.

Phytoplankton dynamics during contrasting years

Phytoplankton responses during summers following either warm/wet or cool/dry winter-springs were consistent for all regions of the Bay as measured by Chl *a* and

SIP anomalies (Fig. 4.11). SIP and Chl *a* were 9 and 17% above average, respectively, during warm/wet years and 10 and 12% below average during cool/dry years. AIP and photic-layer Chl *a* also showed positive anomalies (7 and 11% respectively) for warm/wet years and negative anomalies (6 and 8%) in cool/dry years. I did not observe consistent patterns in summer conditions for any variables known to influence phytoplankton dynamics, including dissolved inorganic nitrogen (DIN), Z_p , SST, or E_o (data not shown). The consistent response between Chl *a* and SIP was expected because Chl *a* is a term in the productivity model used to calculate SIP, and 47 to 74% of the variance of SIP is explained by Chl *a* alone.

The progression of Chl *a* expressed as the moving average from winter through summer showed consistent deviations from the LTA for warm/wet and cool/dry years (Fig. 4.12). These deviations were most pronounced for the meso- and polyhaline regions of the Bay. During warm/wet years, Chl *a* averaged $\sim 1.3 \text{ mg m}^{-3}$ (16%) above the LTA in winter-spring and remained above average for the balance of spring and summer. Conversely, during cool/dry winter-springs, Chl *a* averaged $\sim 1.0 \text{ mg m}^{-3}$ (11%) below the LTA and remained below-average through summer. Similar patterns were detected for photic-layer Chl *a*, but not for DIN, Z_p , SST, or E_o . Differences were less pronounced in the oligohaline region where Chl *a* was below the LTA for warm/wet years in winter-spring but gradually increased through summer.

SIP predictions from weather pattern variability

I developed multiple linear regressions of SIP on frequencies-of-occurrence of weather patterns as AIP and SIP were strongly correlated. Regressions of SIP on frequencies-of-occurrence for winter-spring produced significant models ($p < 0.05$)

for all regions, explaining 42 to 63% of the remaining variance of SIP after the Z_p trend was removed (Table 4.2; Fig. 4.13). Time series showed good agreement for all years, including the observed 1994 peak in production. Model predictions were weakest for 2003 in all regions. Exclusion of data from this year resulted in models that explained 10 to 35% more of the variance. Weather patterns 2, 4, 5, and 10 were the most common independent variables in the multiple linear regression models (Table 4.2). Scatter plots of SIP predicted from weather patterns versus observed SIP residuals showed the skill of model predictions was strong for the entire range of observed values (Fig. 4.13). Models using summer Chl *a* or AIP as the dependent variable were significant and explained comparable amounts of the variance (Table 4.2). However, models based on frequencies of spring or summer weather patterns as the independent variables were not consistently significant and explained less of the variance. With ~30% of the variance in SIP explained by the Z_p trend and 42 to 63% of the remaining variance explained by winter-spring climate, only ~20 to 30% remains unexplained and showed no trends or relationships to summer environmental conditions.

Discussion

PP dynamics

PP time series determined from recently developed models applied to remotely sensed ocean color data were in good agreement with earlier reports (Fig. 4.2; Harding et al., 1986; Marshall and Nesius, 1996). The estimates provided sufficient spatial and temporal resolution to resolve interannual differences of AIP and SIP to quantify climate forcing (Harding et al., 2002). Interannual variability of AIP was

about a factor of two (Fig. 4.3), a range not uncommon for estuaries dominated by hydrologic forcing (Jassby et al., 2002). Estimates of AIP from the time series I developed were lower than shipboard values (Harding et al., 2002), probably due to differences in samples sizes, station coverage, and temporal resolution underlying the integrals. The regional distribution of production in the Bay provides insight into why Bay-wide PP is so responsive to climate forcing. The polyhaline is responsible for over half (52.4%) of whole Bay AIP and is also the region of the Bay most sensitive to climate forcing (Harding and Perry, 1997; Miller and Harding, submitted).

Estimating AIP from SIP has ramifications for fisheries production models and other ecosystem-scale analyses by reducing the information that is required to accurately determine AIP. The shape of the annual PP cycle is very consistent (Fig. 4.2), dominated by a summer maximum that contributes significantly to the annual integral. Malone (1992) determined that summer production (June-August) contributed an average of 45% to annual production for 1984-1988, similar to our estimate (~62%) when September production is included in the calculation. The strong ($r^2 = 0.92$) and significant ($p < 0.001$) relationship between these two parameters (Fig. 4.4) suggests that interannual variations of PP that are relevant to AIP occur during the summer. This allows us to focus our resources more narrowly on factors that influence summer PP.

Trends of SIP

The decreasing trend in SIP was related to Z_p . The negative trend of ~ 2 to $6 \text{ g C m}^{-2} \text{ summer}^{-1}$ was not expected but explained $\sim 30\%$ of the variance of SIP (Fig. 4.6). Rates of decline were greatest in the meso- to polyhaline regions where most

production occurred. The cause of the decreasing trend of Z_p (Fig. 4.7) is unclear because the three properties that control light attenuation (Chl *a*, TSS, and CDOM) showed no significant trends. However, Fisher et al. (2006) showed similar decreases of Z_p over the same time period at stations in the Choptank and Patuxent Rivers, subestuaries of Chesapeake Bay, related to changes in Chl *a* and TSS.

Phytoplankton responses to weather pattern variability

Previous studies have related regional climate variability, quantified using a synoptic climatology (Fig. 4.8), to a variety of ecosystem responses in Chesapeake Bay including: the spring freshet from the Susquehanna River (Miller et al., 2006); zooplankton abundance in the oligo- and mesohaline Bay (Kimmel et al., 2006); and timing, position, and magnitude of the spring bloom (Miller and Harding, submitted). Here, I described climate forcing of PP quantified by the frequencies of winter-spring weather patterns (Fig. 4.9). Chl *a* and SIP showed consistent responses for contrasting years of warm/wet or cool/dry winter-spring weather in all regions of the Bay (Fig. 4.11). Summer water column conditions (i.e., DIN, Z_p , SST) did not show similar responses, suggesting that the winter-spring climate was not influencing summer phytoplankton dynamics through changes in summer environmental conditions. However, the progression of Chl *a* from winter to summer in the meso- and polyhaline Bay (Fig. 4.12) suggested Chl *a* may integrate climate forcing and link winter-spring weather to SIP. During years with warm/wet winter-springs, above-average Chl *a* was observed in winter-spring, and during years with cool/dry winter-springs below average Chl *a* was observed, findings consistent with Miller and Harding (submitted). As the year progressed, Chl *a* associated with prevailing climate

conditions maintained its position relative to the LTA (Fig. 4.12), whereas other environmental variables that force phytoplankton dynamics did not show similar patterns. These observations are consistent with the paradigm of ‘biomass compensation’ (Malone, 1992), representing a mechanism to retain winter-spring nutrient inputs, support the summer PP maximum, and explain the observed variability of SIP in contrasting climate conditions.

Predicting SIP from winter-spring weather patterns

Multiple linear regression models of SIP on winter-spring climate explained ~42 to 63% of the residual variance of regional SIP after the Z_p trend was removed (Fig. 4.13). Combined, these two sources of variability explain 60 to 71% of the variance of SIP. Several processes take place during the time lag between winter-spring and the summer PP maximum that explain high interannual variability of AIP and SIP documented in this paper and elsewhere (Harding et al., 2002). Synoptic-scale weather patterns influence freshwater flow to the estuary through interannual differences in winter precipitation stored in the watershed over winter as snow and ice (Miller et al., 2006; Najjar, 1999). Flow in winter-spring delivers over 50% of the annual nitrogen (N) load to the estuary (Malone, 1992). Phytoplankton compensate for temperature-limited uptake of nutrients during spring by increasing biomass that sequesters the nutrients in particulate organic matter (Malone et al., 1996). As the spring bloom subsides, particulate organic matter sinks below the seasonal pycnocline and is transported up-estuary via two-layer circulation. The nutrients contained in the organic matter are recycled by an active microbial community as temperatures increase during summer (Kemp and Boynton, 1992). Summer PP is then fueled by

introduction of these regenerated nutrients from below the pycnocline (Malone et al., 1988). Interannual variability of the frequencies of winter-spring weather patterns controls the timing, magnitude, and position of the spring bloom (Miller and Harding, submitted), and therefore the amount of N sequestered in particulate organic matter available to support summer PP. These results suggest winter-spring climate forcing of nutrient loading in the spring freshet drives seasonal and interannual variability of PP in Chesapeake Bay, explicitly linking regional scale weather patterns as the root cause of the observed interannual variability.

No other time window of weather pattern frequencies showed strong or consistent effects on AIP or SIP. Water-column stability during summer has been identified as a variable responsible for interannual differences of SIP (Malone, 1992). Differences in intensity of stratification provided a proxy for the magnitude/frequency of vertical flux of regenerated N from below the pycnocline to support PP. Climate variability could influence the vertical density gradient through the frequencies of storm passage and wind events. However, weather patterns for spring and summer intervals did not show consistently strong or significant relationships to summer production. A variety of reasons may explain this lack of connection: (1) the synoptic climatology may not have been the proper tool to quantify summer weather conditions; (2) the time and space scales used here may have been too coarse to resolve phytoplankton responses to event-scale climatic perturbations; or (3) this process may be less important relative to large interannual differences in nutrient loading.

PP is a highly dynamic property of estuarine ecosystems in part due to the forcing of environmental variables controlled by climate. In Chesapeake Bay, climate

influences PP through changes in regional light and nutrient dynamics on several spatial and temporal scales. In addition to PP, floral composition and Chl *a* also respond to environmental forcing in a consistent manner and interactions of these properties should be considered. Adolf et al. (2006) showed that floral composition responded in predictable ways to differences in freshwater flow, and that these responses might influence biomass-specific photosynthetic rates and therefore PP dynamics. Quantifying these environmentally forced changes in community composition with a synoptic climatology should improve our conceptual understanding of climate forcing of phytoplankton dynamics in Chesapeake Bay. In order to predict and manage ecosystem response to both anthropogenic impacts and potential climate change it is critical to understand how the several expressions of phytoplankton dynamics respond to climate variability.

Conclusions

I have shown that regional-scale climate variability quantified using a synoptic climatology explained much of the two-fold interannual variability of AIP and SIP. The frequencies of winter-spring weather patterns expressed as differences of precipitation, freshwater flow, and nutrient loading, underlie the magnitude of the summer PP maximum that leads to this variability. Other representations of climate that capture variability in summer may explain additional variance of AIP and SIP. Sustained, high resolution datasets such as the ones used in these analyses (CBRSP, CBP, NCAR, and NCDC) are critical to identify the patterns and relationships I observed. Integrating this work with other recent studies (Adolf et al., 2006; Miller and Harding, submitted) will help us better understand how floral composition,

biomass and productivity of phytoplankton respond predictably to climate variability, influencing ecosystem dynamics on a variety of time and space scales.

Acknowledgements I wish to thank Ming Li, Tom Malone, and all the pilots and crew of aircraft used in the Chesapeake Bay Remote Sensing Program. Support from NASA, NOAA, EPA and Maryland Sea Grant is gratefully acknowledged. WDM was supported by NASA Headquarters under an Earth System Science Fellowship. Contribution no. 3974 of Horn Point Laboratory, University of Maryland Center for Environmental Science.

References

- Adolf, J.E., C.L. Yeager, W.D. Miller, M.E. Mallonee, and L.W. Harding Jr. 2006. Environmental forcing of phytoplankton floral composition, biomass, and primary productivity in Chesapeake Bay, USA. *Estuar. Coast. Shelf Sci.*, 67, 108-122.
- Behrenfeld, M.J., J.T. Randerson, C.R. McClain, G.C. Feldman, S.O. Los, C.J. Tucker, P.G. Falkowski, C.B. Field, R. Frouin, W.E. Esaias, D.D. Kolber, and N.H. Pollack. 2001. Biospheric primary production during an ENSO transition. *Science* 291, 2594-2597.
- Behrenfeld, M.J., and P.G. Falkowski. 1997. Photosynthetic rates derived from satellite-based chlorophyll concentration. *Limnol. Oceanogr.*, 42, 1-20.
- Boynton, W.R., W.M. Kemp, and C.W. Keefe. 1982. A comparative analysis of nutrients and other factors influencing estuarine phytoplankton production, p. 69-90. In V.S. Kennedy [ed.]. *Estuarine comparisons*. Academic Press.
- Campbell, J.W., and W.E. Esaias. 1983. Basis for spectral curvature algorithms in remote sensing of chlorophyll. *Appl. Opt.*, 22, 1084-1093.
- Cody R.P., and J.K. Smith. 2005. *Applied Statistics and the SAS programming language*. 5th ed. Pearson/Prentice Hall.
- Fisher, T.R., J.D. Hagy, III, W.R. Boynton, and M.R. Williams. 2006. Cultural eutrophication in the Choptank and Patuxent estuaries of Chesapeake Bay. *Limnol. Oceanogr.*, 51, 435-447.
- Goldman, C.R., A.D. Jassby, and T. Powell. 1989. Interannual fluctuations in primary production: Meteorological forcing at two subalpine lakes. *Limnol. Oceanogr.*, 34, 310-323.
- Harding, Jr., L.W., B.W. Meeson, and T.R. Fisher. 1986. Phytoplankton in two East coast estuaries: photosynthesis-light curves and patterns of carbon assimilation. *Est. Coast. Shelf Sci.*, 23, 773-806.
- Harding, L.W., E.C. Itsweire, and W.E. Esaias. 1994. Estimates of phytoplankton biomass in the Chesapeake Bay from aircraft remote sensing of chlorophyll concentrations, 1989-92. *Remote Sen. Environ.*, 49, 41-56.
- Harding, L.W., E.C. Itsweire, and W.E. Esaias. 1995. Algorithm development for recovering chlorophyll concentrations in the Chesapeake Bay using aircraft remote sensing, 1989-91. *Photogramm. Eng. Remote Sens.*, 61, 177-185.
- Harding, Jr., L.W., and E.S. Perry. 1997. Long-term increases of phytoplankton biomass in Chesapeake Bay, 1950-1994. *Mar. Ecol. Prog. Ser.*, 157, 39-52.

- Harding, Jr., L.W., W.D. Miller, R.N. Swift, and C.N. Wright. 2001. Aircraft remote sensing, p. 113-122. In J.H. Steele, S.A. Thorpe, K.K. Turekian [eds.]. *Encyclopedia of Ocean Sciences*. Academic Press.
- Harding, Jr., L.W., M.E. Mallonee, and E.S. Perry. 2002. Toward a predictive understanding of primary productivity in a temperate, partially stratified estuary. *Est. Coast. Shelf Sci.*, 55, 437-463.
- Howarth, R.W., D.P. Swaney, T.J. Butler, and R. Marino. 2000. Climatic control on eutrophication of the Hudson River estuary. *Ecosystems* 3, 210-215.
- Jassby, A.D., J.E. Cloern, and B.E. Cole. 2002. Annual primary production: patterns and mechanisms of change in a nutrient-rich tidal ecosystem. *Limnol. Oceanogr.*, 47, 698-712.
- Justić, D., N.N. Rabalais, and R.E. Turner. 1997. Impacts of climate change on net productivity of coastal waters: Implications for carbon budget and hypoxia. *Clim. Res.*, 8, 225-237.
- Kemp, W.M., and W.R. Boynton. 1984. Spatial and temporal coupling of nutrient inputs to estuarine production: the role of particulate transport and decomposition. *Bull. Mar. Sci.*, 3, 242-247.
- Kemp, W.M., and W.R. Boynton. 1992. Benthic-pelagic interactions: Nutrient and oxygen dynamics, p. 149-221. In D.E. Smith, M. Leffler, and G. Mackiernan [eds.]. *Oxygen Dynamics in the Chesapeake Bay: A Synthesis of Recent Research*. Maryland Sea Grant Program.
- Kimmel, D.G., W.D. Miller, and M.R. Roman. 2006. Regional scale climate forcing of mesozooplankton dynamics in Chesapeake Bay. *Estuaries* (in press).
- Lindahl, O., A. Belgrano, L. Davidsson, and B. Hernroth. 1998. Primary production, climatic oscillations, and physico-chemical processes: the Gullmar Fjord time-series data set (1985-1996). *ICES J. Mar. Sci.*, 55, 723-729.
- Malone, T.C., L.H. Crocker, S.E. Pike, and B.W. Wendler. 1988. Influences of river flow on the dynamics of phytoplankton production in a partially stratified estuary. *Mar. Ecol. Prog. Ser.*, 48, 235-249.
- Malone, T.C. 1992. Effects of water column processes on dissolved oxygen, nutrients, phytoplankton and zooplankton, p. 61-112. In D.E. Smith, M. Leffler, and G. Mackiernan [eds.]. *Oxygen Dynamics in the Chesapeake Bay: A Synthesis of Recent Research*. Maryland Sea Grant Program.

- Malone, T.C., D.J. Conley, T.R. Fisher, P.M. Glibert, L.W. Harding, Jr., and K.G. Sellner. 1996. Scales of nutrient-limited phytoplankton productivity in Chesapeake Bay. *Estuaries* 19, 371-385.
- Marshall, H.G., and K.K. Nesius. 1996. Phytoplankton composition in relation to primary production in Chesapeake Bay. *Mar. Bio.*, 125, 611-617.
- Miller, W.D., and L.W. Harding, Jr. 2006. Climate forcing of the spring bloom in Chesapeake Bay. *Mar. Ecol. Prog. Ser.*, (submitted).
- Miller, W.D., D.G. Kimmel, and L.W. Harding, Jr. 2006. Predicting spring discharge of the Susquehanna River from a synoptic climatology for the eastern United States. *Water Resour. Res.*, 42, W05414, [doi:10.1029/2005WR004270].
- Najjar, R.G. 1999. The water balance of the Susquehanna River Basin and its response to climate change. *J. Hydrol.*, 219, 7-19.
- Rudek J., H.W. Paerl, M.A. Mallin, and P.W. Bates. 1991. Seasonal and hydrological control of phytoplankton nutrient limitation in the lower Neuse River Estuary, North Carolina. *Mar. Ecol. Prog. Ser.*, 75, 133-142.
- Smayda, T.J., D.G. Borkman, G. Beaugrand, and A. Belgrano. 2004. Responses of marine phytoplankton populations to fluctuations in marine climate, p. 49-58. In N.C. Stenseth, G. Ottersen, J.W. Hurrell, and A. Belgrano [eds]. *Marine ecosystems and climate variation: the North Atlantic a comparative perspective*. Oxford University Press.
- Stenseth, N.C., A. Mysterud, G. Ottersen, J.W. Hurrell, K.S. Chan, and M. Lima. 2002. Ecological effects of climate fluctuation. *Science* 297, 1292-1296.
- Stenseth, N.C., G. Ottersen, J.W. Hurrell, A. Mysterud, M. Lima, K.S. Chan, N.G. Yoccoz, and B. Adlandsvik. 2003. Studying climate effects on ecology through the use of climate indices: the North Atlantic Oscillation, El Niño Southern Oscillation and beyond. *Proc. R. Soc. Lond.*, B 270, 2087-2096.
- Tootle, G.A., T.C. Piechota, and A. Singh. 2005. Couple oceanic-atmospheric variability and U.S. streamflow. *Water Resour. Res.* 41, W12408, doi:10.1029/2005WR004381.
- Yarnal, B. 1993. *Synoptic Climatology in Environmental Analysis*, Belhaven Press.

Table 4.1. Meteorological characteristics for weather patterns during winter-spring 1989-2004. Wind speed and direction based on data from Baltimore-Washington International airport.

Weather Pattern	%	Temperature Anomaly(\pm SE) ($^{\circ}$ C)	Precipitation Anomaly(\pm SE) (mm)	Wind Direction	Wind Speed ($m s^{-1}$)	Conditions
1 ^a	9.1	3.8 (\pm 0.25)	1.1 (\pm 0.20)	SW	3.2	warm/wet
2 ^b	10.8	-6.2 (\pm 0.21)	-1.1 (\pm 0.12)	NW	4.0	cool/dry
3 ^c	10.6	-0.1 (\pm 0.24)	0.7 (\pm 0.20)	N	3.5	seasonal/wet
4 ^c	8.7	2.2 (\pm 0.22)	1.9 (\pm 0.26)	NW	3.8	warm/wet
5	12.4	0.9 (\pm 0.22)	0.1 (\pm 0.14)	W	2.8	warm/seasonal
6	8.6	-0.4 (\pm 0.27)	-0.7 (\pm 0.16)	NE	2.6	cool/dry
7	10.5	-4.5 (\pm 0.21)	-0.2 (\pm 0.16)	W	4.8	cool/dry
8	8.4	4.8 (\pm 0.26)	0.2 (\pm 0.18)	SE	2.7	warm/wet
9	9.9	3.7 (\pm 0.25)	-0.3 (\pm 0.15)	S	2.3	warm/dry
10	11.1	-2.2 (\pm 0.26)	-1.1 (\pm 0.10)	S	2.4	cool/dry

^a Bermuda High

^b Ohio Valley High

^c Nor'easter

Table 4.2. Results from multiple linear regression models of winter-spring weather pattern frequencies on measurements of regional SIP and summer Chl *a*. Units for RMSE are g C m⁻² summer⁻¹ for SIP, mg chla m⁻³ for Chl *a*, and g C m⁻² yr⁻¹ for AIP.

Variable	Region	Adjusted r ²	p-value	Weather patterns	RMSE
SIP	Whole Bay	0.42	0.037	4,5,9,10	44.3
	Oligohaline	0.63	0.025	2,4,5,6,7	17.0
	Mesohaline	0.54	0.012	4,5,9,10	31.4
	Polyhaline	0.60	0.008	2,4,5,6,7	18.1
Chl <i>a</i>	Whole Bay	0.51	0.026	1,2,4,8,10	1.4
	Oligohaline	0.63	0.004	1,2,3,10	1.6
	Mesohaline	0.60	0.011	1,2,4,8,10	1.3
	Polyhaline	0.46	0.041	1,2,4,8,10	1.8
AIP	Whole Bay	0.56	0.009	4,5,9,10	30.2
	Oligohaline	0.64	0.012	1,2,3,4,5,10	25.7
	Mesohaline	0.54	0.012	4,5,9,10	25.3
	Polyhaline	0.52	0.037	1,2,3,4,5,10	25.8

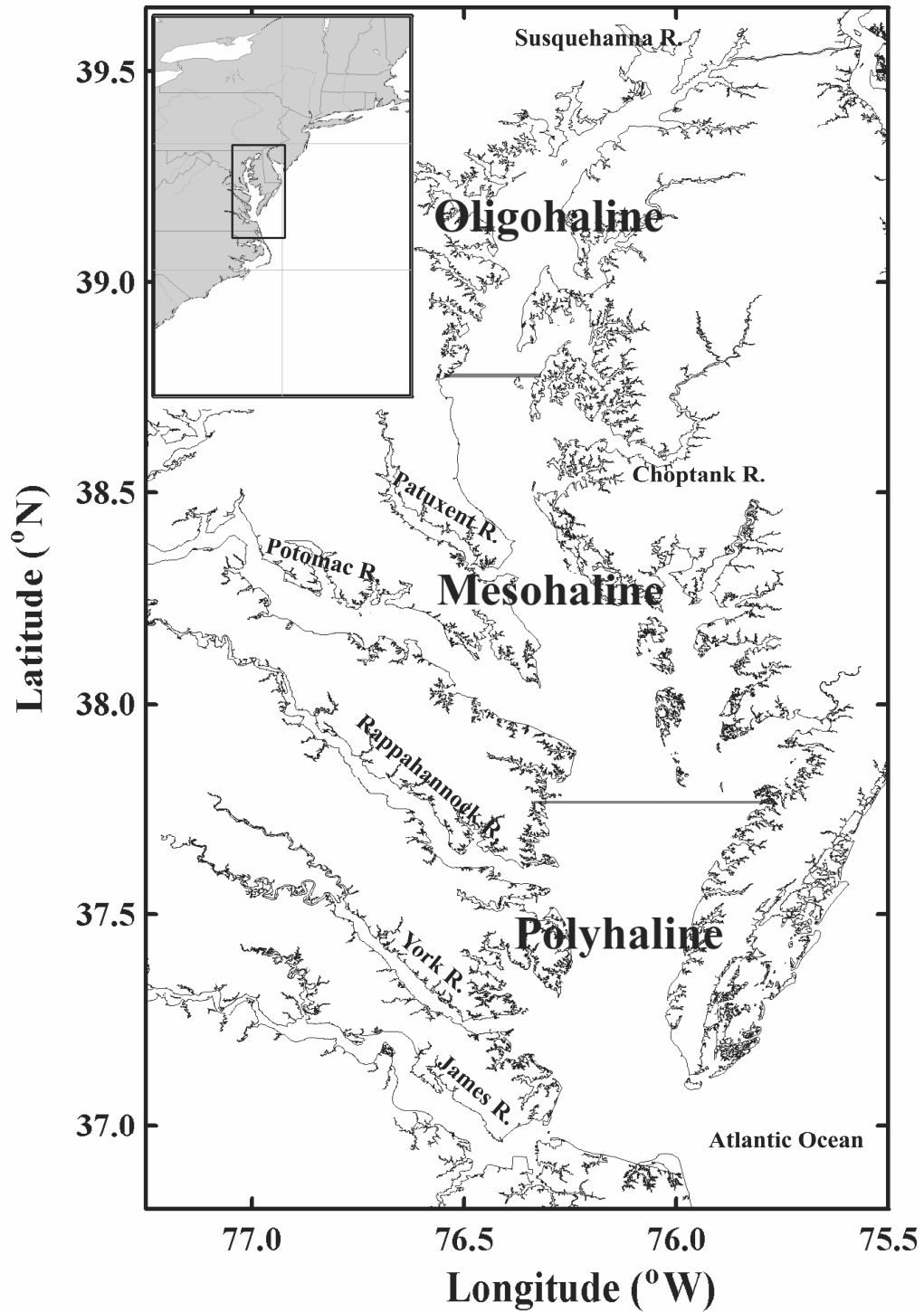


Fig. 4.1. Map of Chesapeake Bay showing regions used in analyses. Regions are delineated as polyhaline, 36.95° - 37.80° N; mesohaline, 37.81° - 38.80° N; oligohaline, 38.81° - 39.66° N.

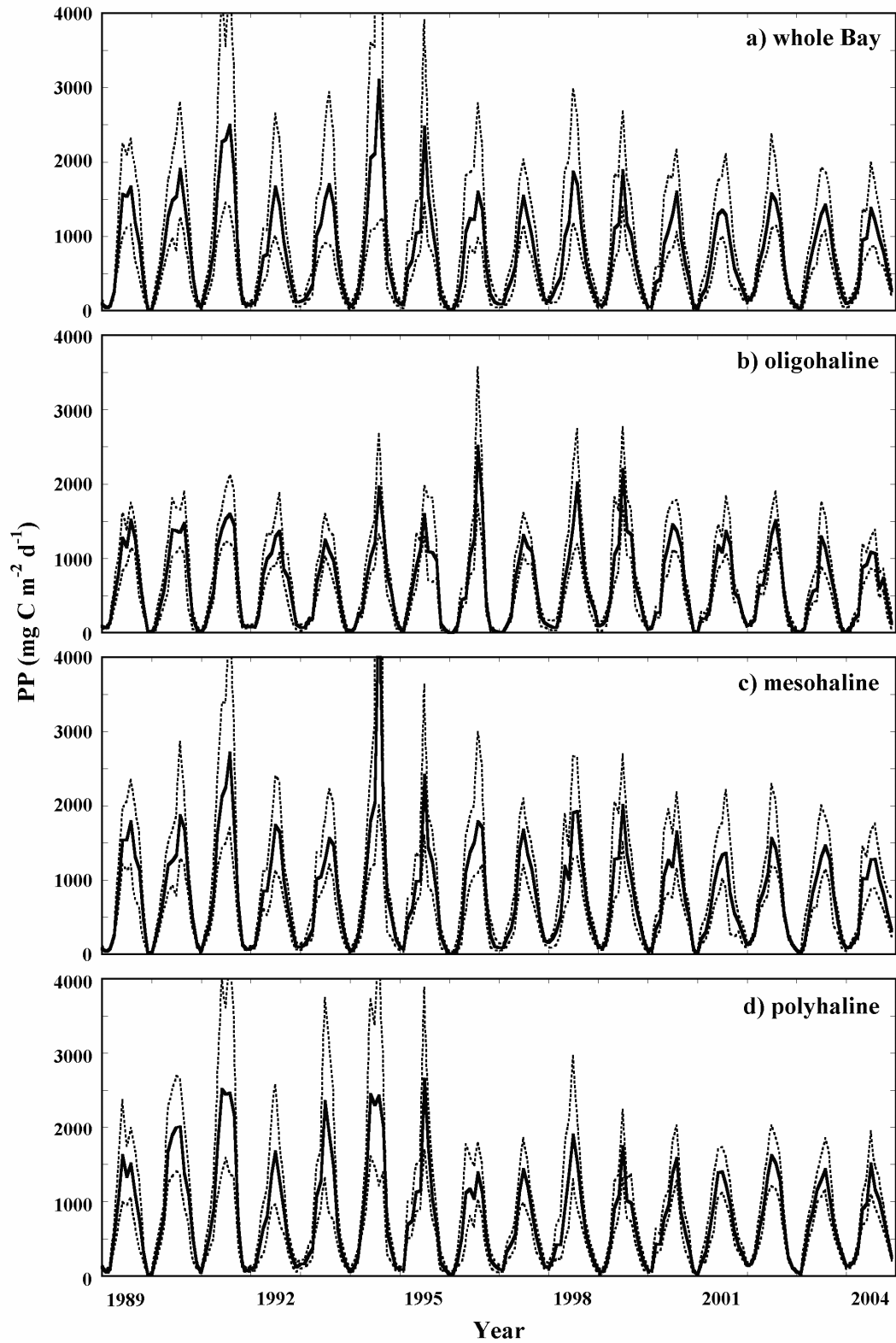


Fig. 4.2 (a-d). Time series (1989-2004) of monthly PP estimated from CBPM for 3 regions and whole Bay. Dashed lines indicate 5 and 95% confidence intervals.

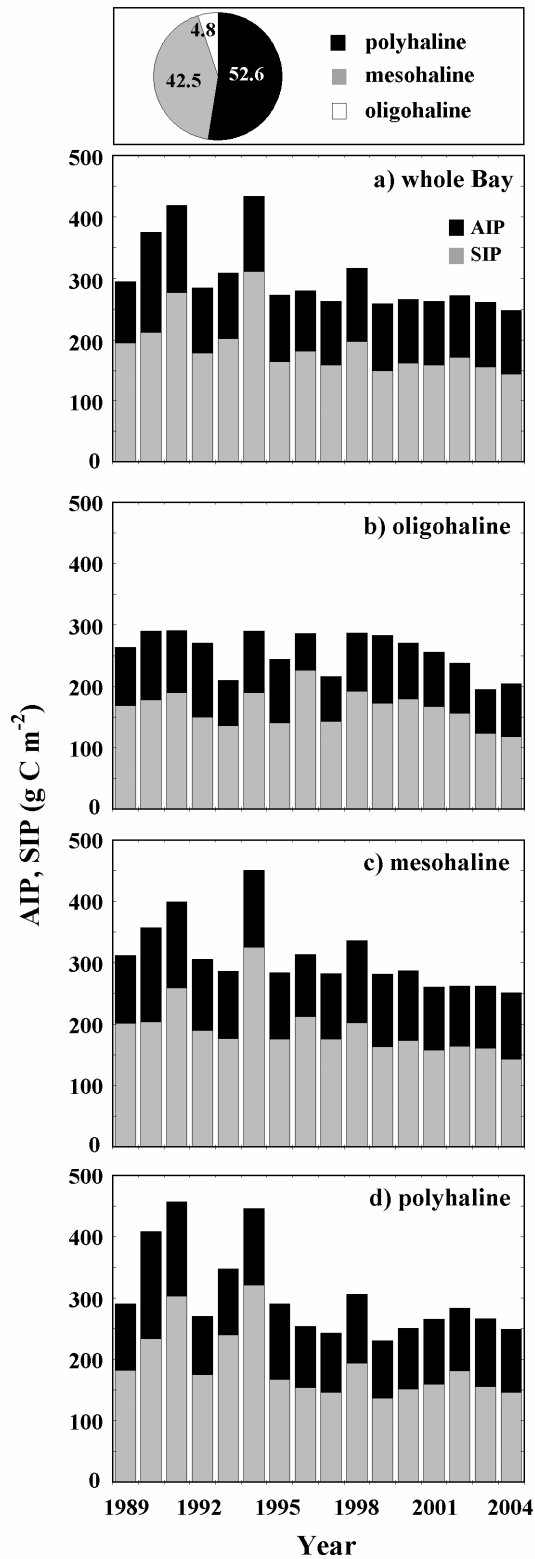


Fig. 4.3 (a-d). Time series (1989-2004) of AIP and SIP for 3 regions and whole Bay. Pie chart shows the fraction of total production accounted for by each region.

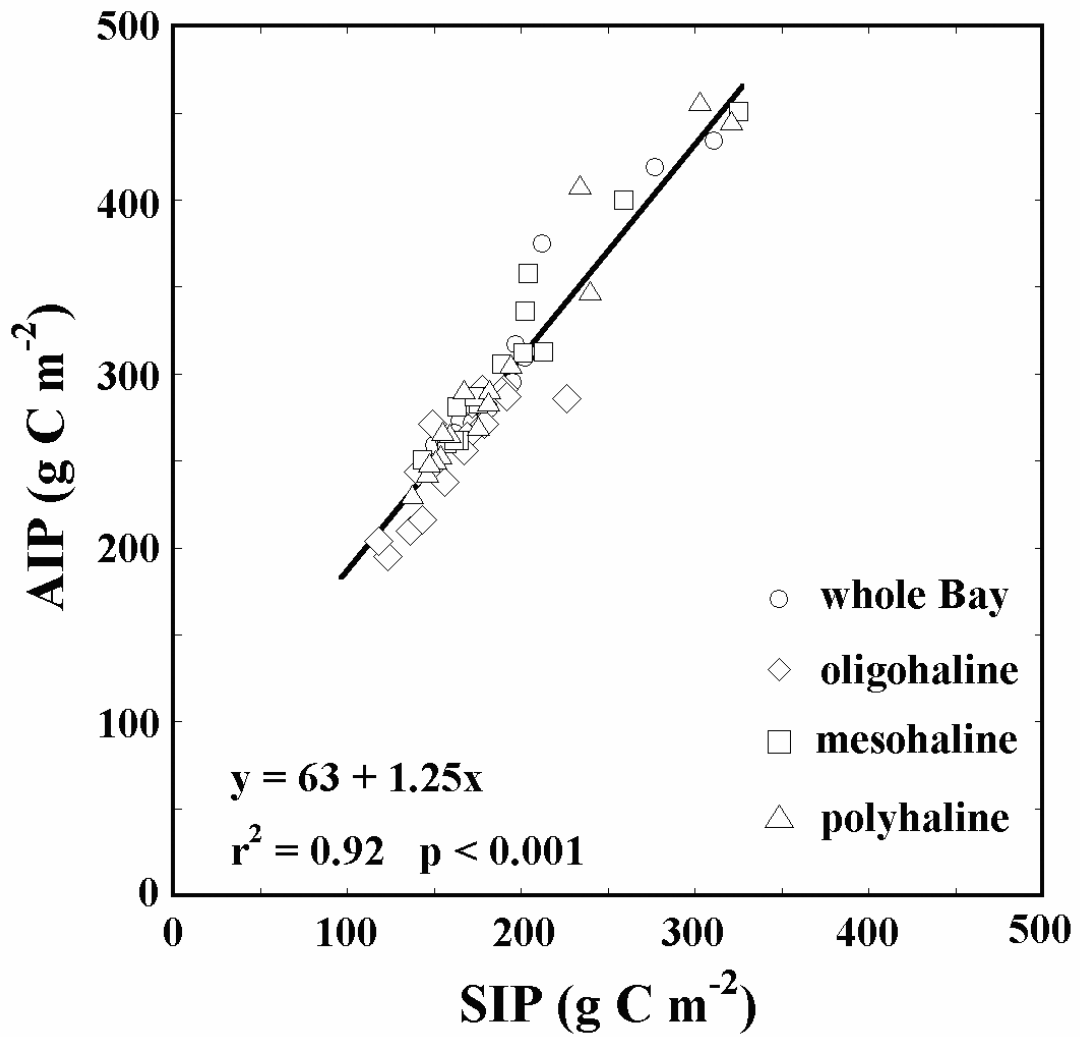


Fig. 4.4. Linear regression of AIP on SIP.

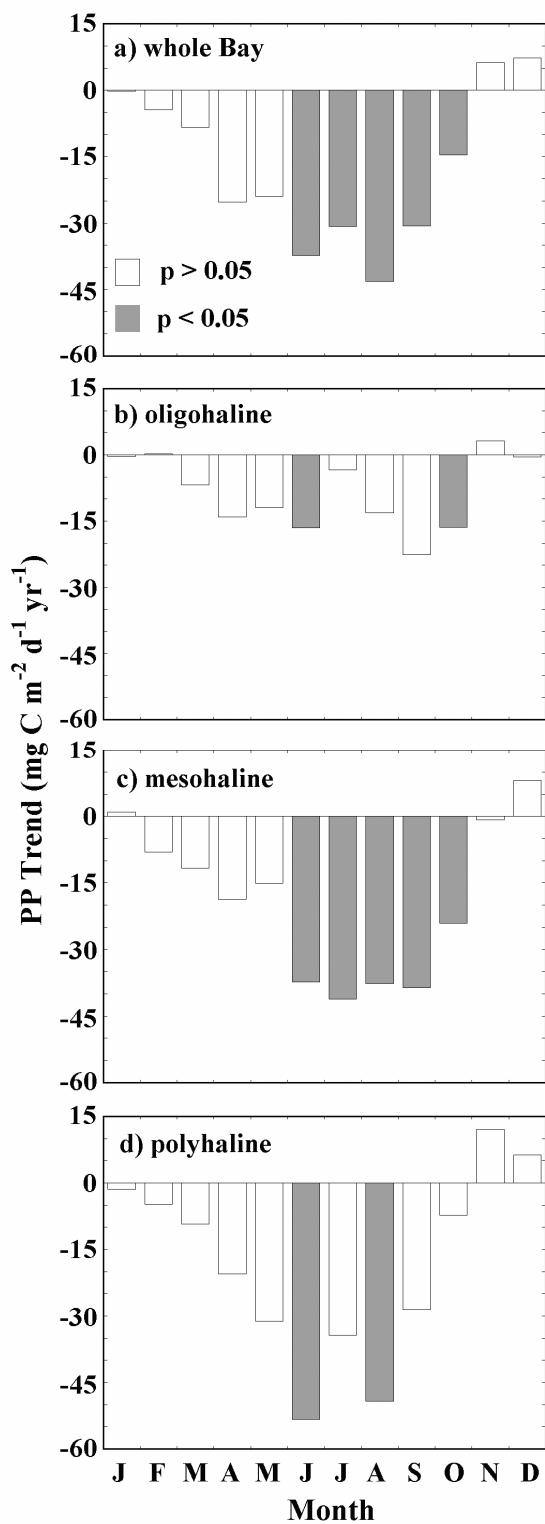


Fig. 4.5 (a-d). Results of monthly Mann-Kendall trend test for 3 regions and whole Bay. Bars indicate the direction and magnitude of relationship between monthly PP estimate and year. Shading of the bars indicates the significance of the relationship.

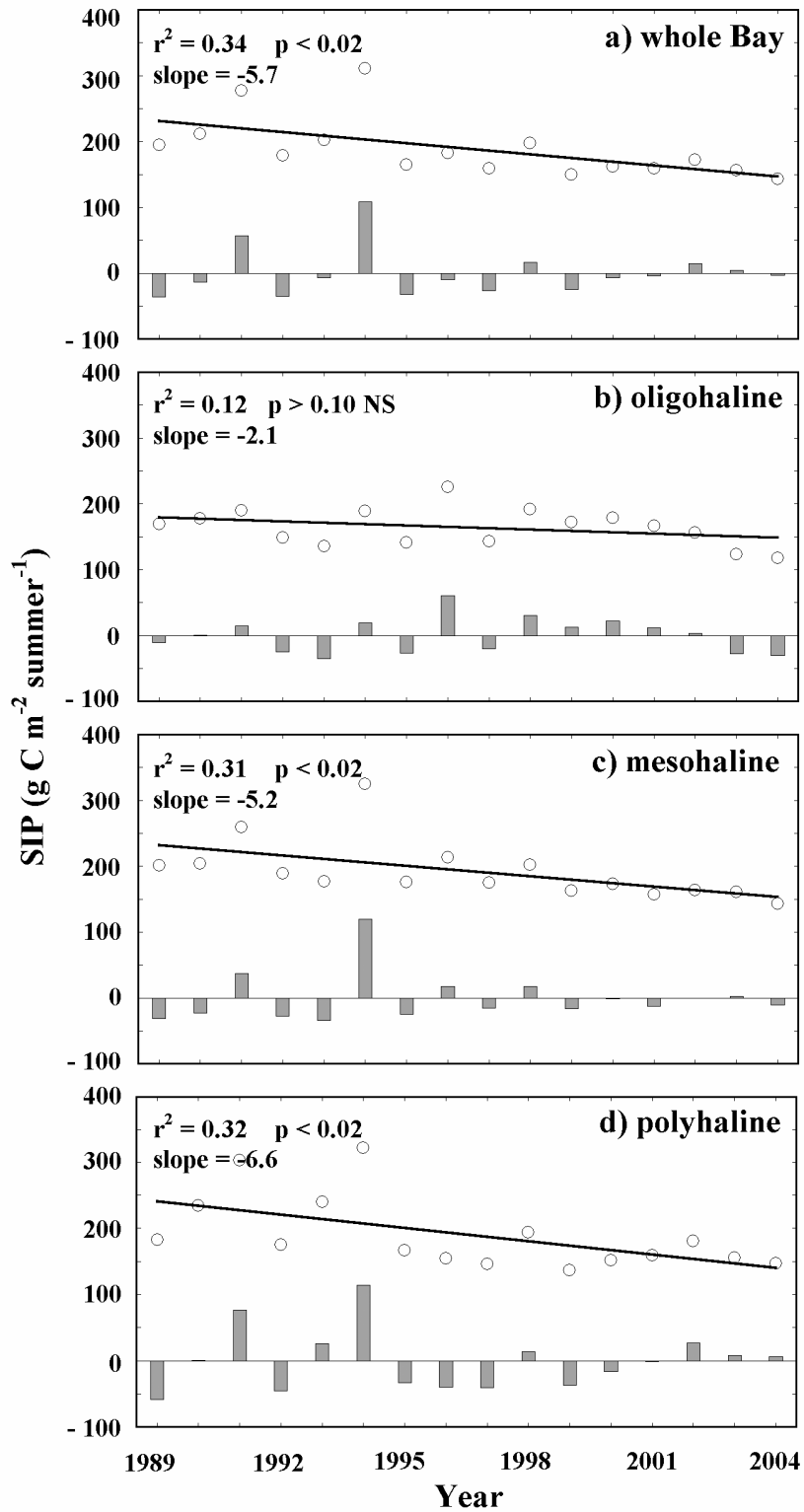


Fig. 4.6 (a-d). Time series (1989-2004) of SIP for 3 regions and whole Bay showing linear downward trend line. Grey bars represent residuals from that regression line.

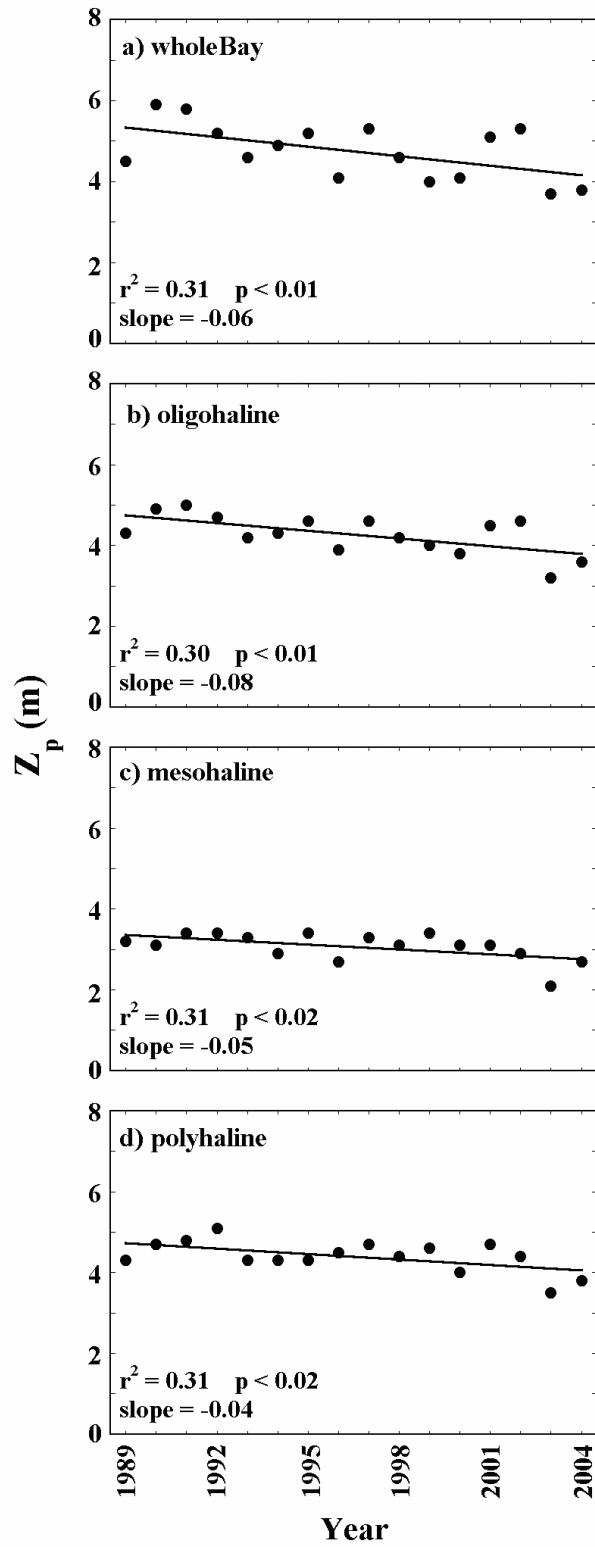


Fig. 4.7 (a-d). Time series (1989-2004) of summer Z_p for 3 regions and whole Bay showing linear downward trend line.

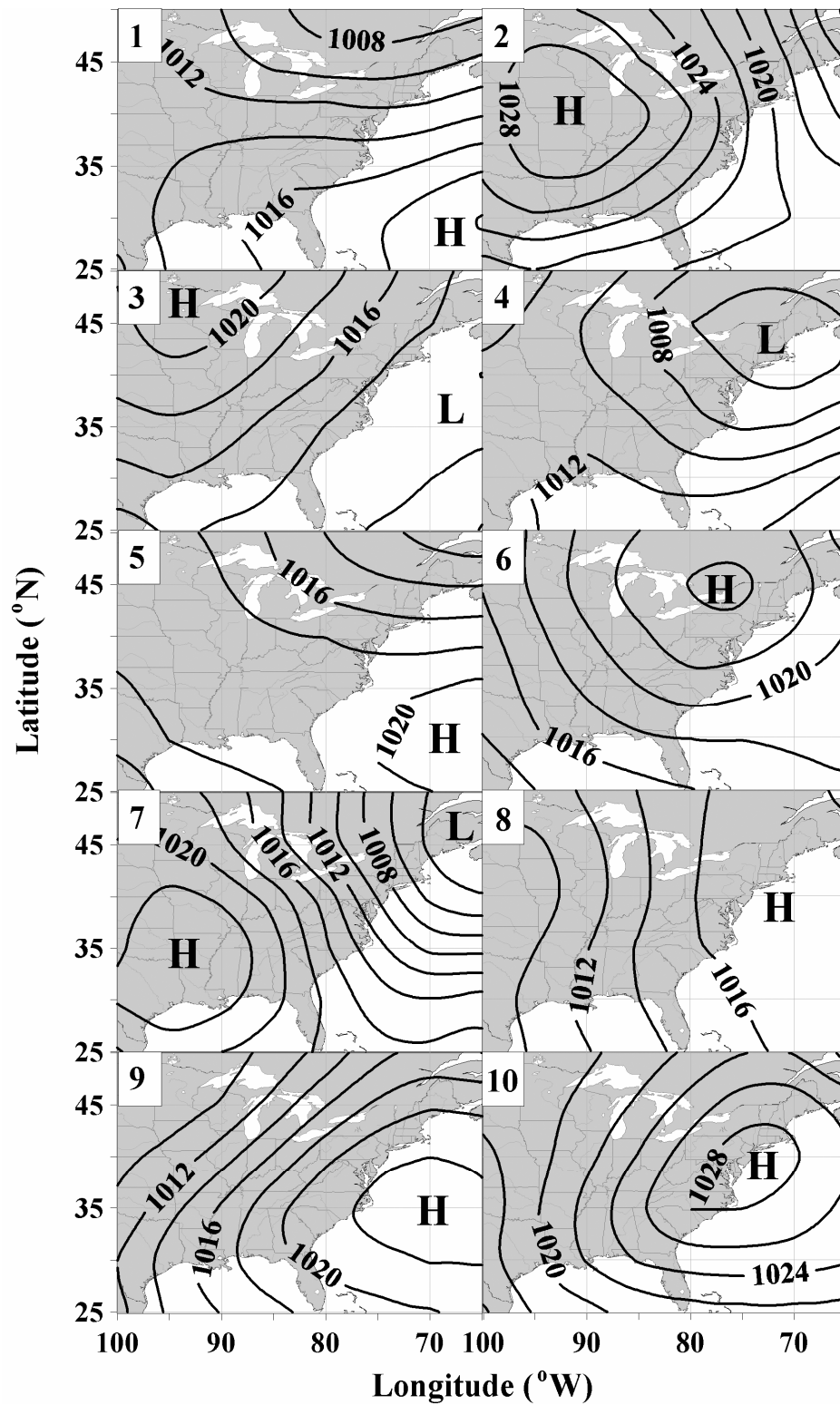


Fig. 4.8. Average sea-level pressure maps for 10 dominant weather patterns. Weather pattern number in upper left-hand corner. H and L indicate centers of high and low pressure regions, respectively. Black lines delineate regions of constant pressure (mb).

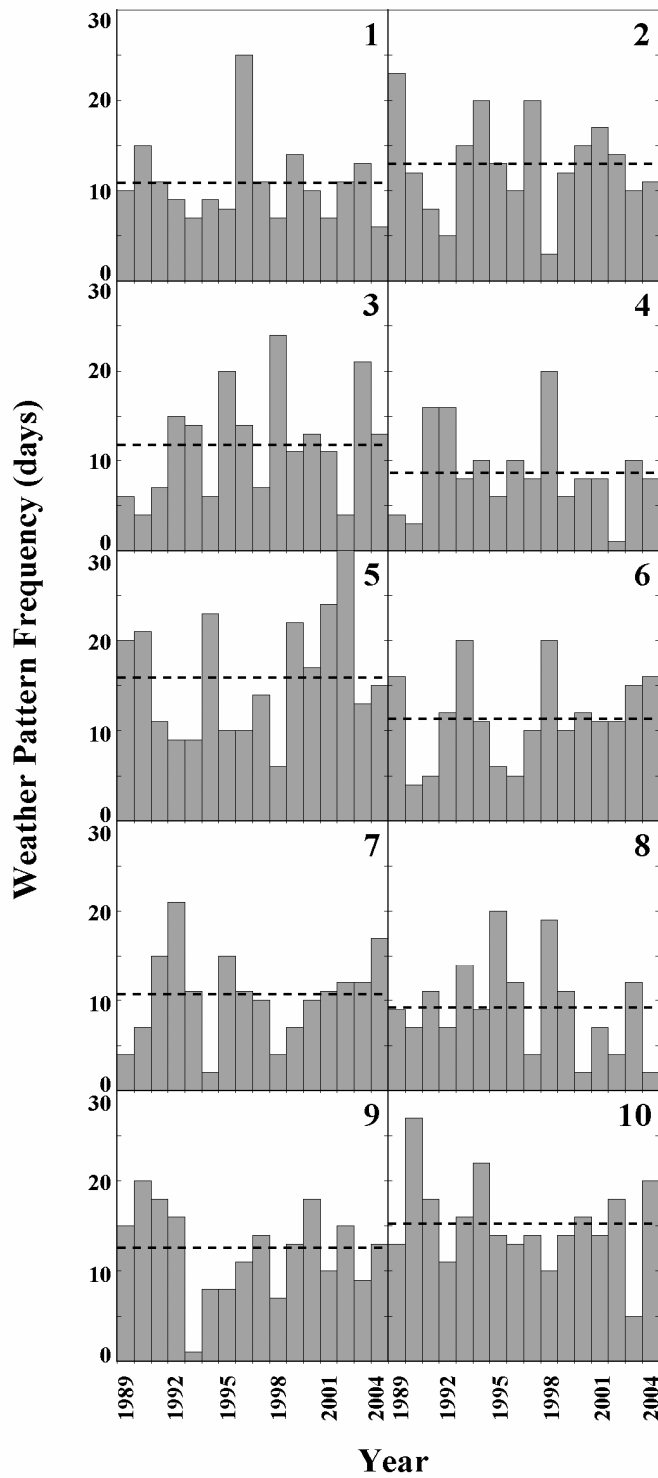


Fig. 4.9. Time series (1989-2004) of winter-spring (January-April) weather pattern frequencies-of-occurrence. Weather pattern number in upper left-hand corner. Horizontal dashed lines indicate the LTA for each weather pattern.

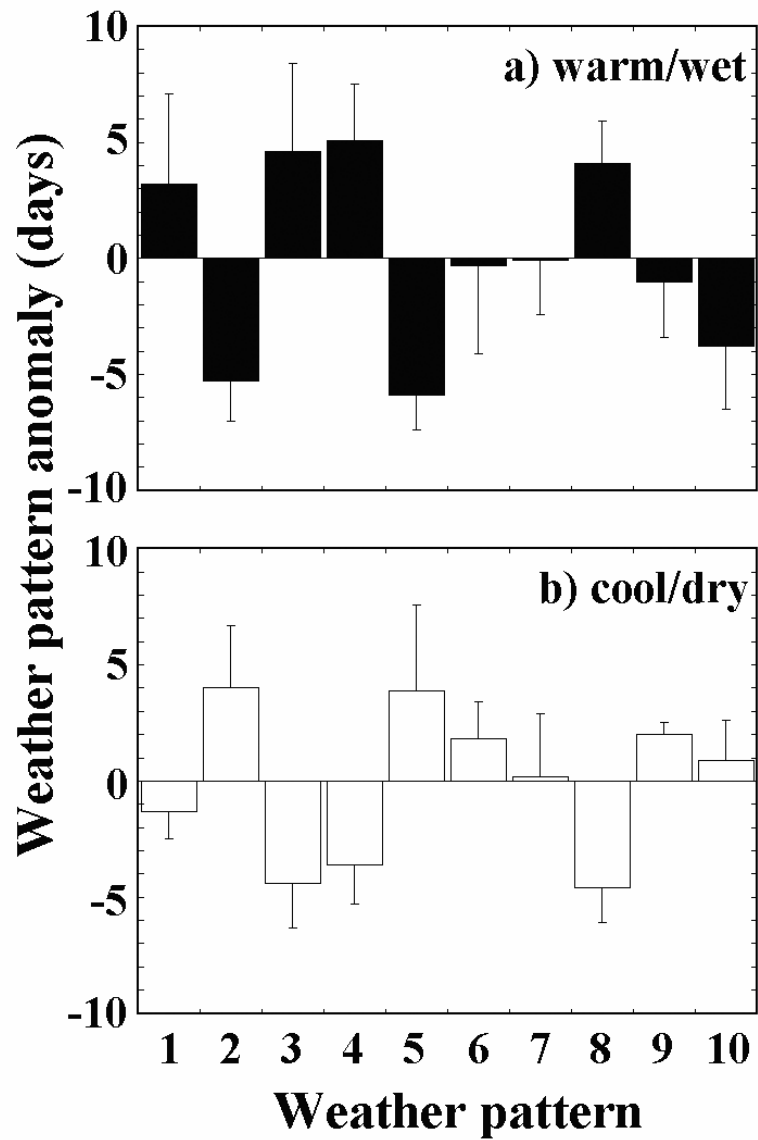


Fig. 4.10 (a-b). Winter-spring weather pattern deviations from LTA frequency-of-occurrence for contrasting climate extremes for years dominated by a) warm/wet weather patterns and b) cool/dry weather patterns. Error bars indicate (± 1 SD).

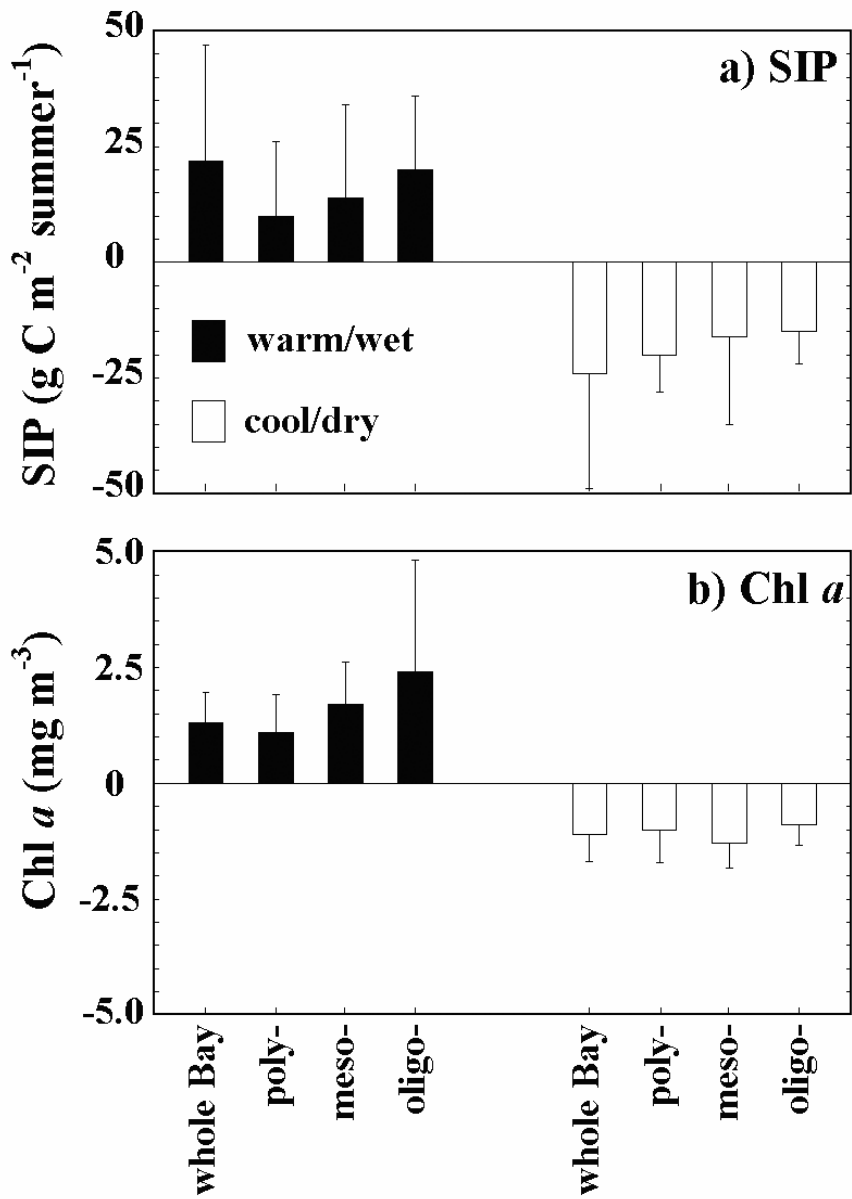


Fig. 4.11 (a-b). Phytoplankton response in summer of a) SIP and b) Chl *a* for contrasting warm/wet (black bars) and cool/dry (open bars) winter-springs. Error bars indicate (± 1 SD).

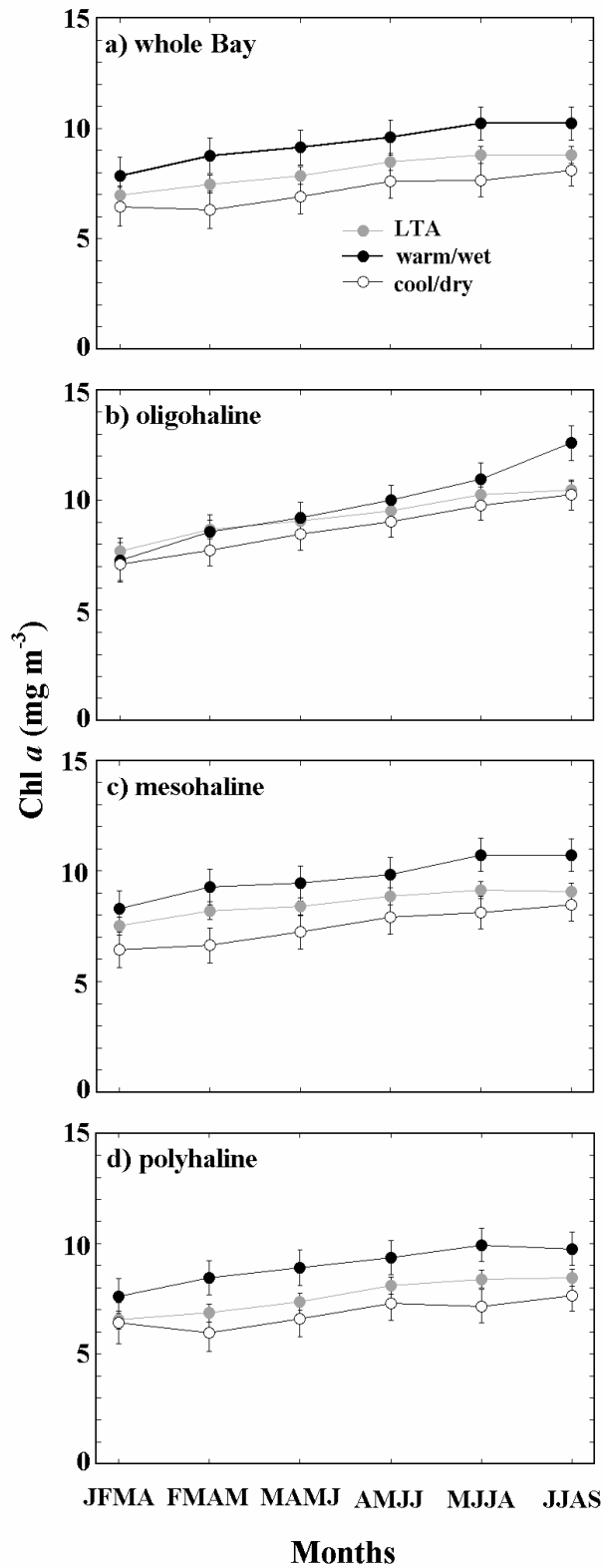


Fig. 4.12 (a-d). Moving average of Chl *a* for 3 regions and whole Bay showing Chl *a* during warm/wet years (black circles), LTA (grey circles), and cool/dry years (open circles). Error bars indicate (± 1 SD).

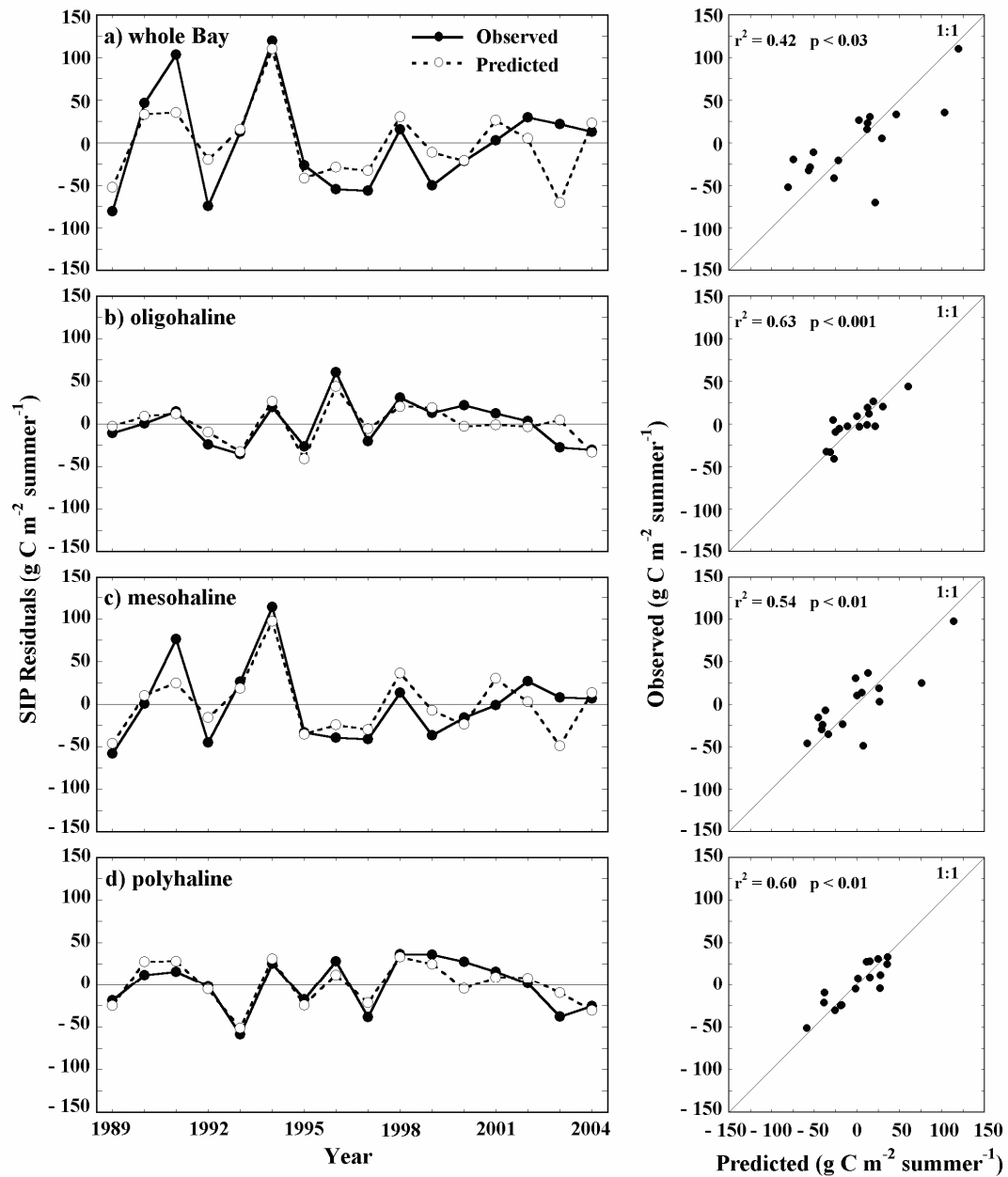


Fig. 4.13 (a-d). Time series of regional predicted (open circles) and observed (black circles) results from multiple linear regression models of winter-spring weather pattern frequencies on residual SIP for 3 regions and whole Bay. Graphs on the right side show scatter plots of observed versus predicted against the 1:1 line.

Chapter 5

Hurricane Isabel generated an unusual fall bloom in Chesapeake Bay¹

¹Miller, W.D., L.W. Harding Jr., and J.E. Adolf . Hurricane Isabel generated an unusual fall bloom in Chesapeake Bay. *Geophysical Research Letters* 33, L06612, [doi:10.1029/2005GL025658].

Abstract

Ocean color measurements from aircraft revealed an unusually strong fall bloom of phytoplankton in Chesapeake Bay after passage of Hurricane Isabel in September 2003. Flights conducted before (11 September) and after (24 September) Isabel showed a two-fold increase of chlorophyll-*a* (Chl *a*) covering ~3000 km² of the mid- to lower Bay, with an abrupt return to long-term average (LTA) Chl *a* by early October. Wind mixing induced rapid de-stratification of the water column, injecting nitrogen (N) into the euphotic layer that supported a fall bloom of diatoms. Here I quantify a significant perturbation of the annual phytoplankton cycle in Chesapeake Bay, driven by Hurricane Isabel.

Introduction

Hurricane Isabel passed west of Chesapeake Bay on 18 September 2003, producing sustained southeasterly winds at 30 m s^{-1} , but relatively low precipitation of $\leq 5 \text{ cm}$. The storm disrupted vertical density stratification and thoroughly mixed the water column. Stratification was re-established 2-3 days after storm passage due to the strong horizontal salinity gradient from the head to the mouth of the estuary (Li et al., 2006).

Mid-Atlantic hurricanes typically produce high precipitation, freshwater flow, and nutrient loading, supporting increased phytoplankton biomass and shifts of floral composition over weeks to months (Paerl et al., 2001). Tropical Storm Agnes in June 1972 led to unprecedented freshwater flow and a protracted increase of phytoplankton biomass in Chesapeake Bay associated with a massive nutrient pulse (Zubkoff and Warinner, 1977). Phytoplankton responses to Isabel were distinct, occurring within days of storm passage by a mechanism described for the coastal ocean wherein hurricane energy erodes the pycnocline and injects nutrients to the surface mixed layer (Davis and Yan, 2004).

I draw on aircraft and shipboard observations before and after the storm to describe phytoplankton responses to Hurricane Isabel. The storm occurred during a ‘wet’ hydrologic year with higher-than-average phytoplankton biomass, making it essential to separate storm effects from prevailing climatic conditions of 2003 (Cloern et al., 2005). Multiple effects of Hurricane Isabel on Chesapeake Bay have been reported (Roman et al., 2005), including a brief description of phytoplankton responses. Here I expand on that treatment to show how biomass as chlorophyll (Chl

a), floral composition, and primary productivity (PP) were affected over a large area of the main stem Bay.

Effects of Hurricane Isabel were unique for the Bay: i) fall blooms of the areal extent and magnitude that occurred after the storm have not been documented previously; ii) wind-mixing supported the bloom rather than precipitation, flow, and nutrient loading more typical of mid-Atlantic hurricanes; iii) tropical systems in this region have been infrequent historically, but show a recent increase of activity with likely ecosystem consequences (Webster et al., 2005).

Methods

Phytoplankton biomass as Chl *a* was obtained from ocean color measurements with a multi-spectral radiometer (SAS III, Satlantic, Inc. Halifax, NS, Canada). SAS III was deployed on light aircraft at low altitude (~150 m) and speed (~50 m s⁻¹), following a defined set of flight lines traversing ~750 km (Chesapeake Bay Remote Sensing Program; <http://www.cbrsp.org>). I used a spectral curvature algorithm (Campbell and Esaias, 1983) to convert water-leaving radiances in the blue-green region of the spectrum (L_w443 , L_w490 , and L_w555) to Chl *a*. Comparisons of remotely sensed and shipboard data document the accuracy of Chl *a* retrievals for Case 2 waters of the Bay that contain significant chromophoric dissolved organic matter (CDOM) and suspended particulate material (Harding et al., 1994; 1995). Data were interpolated to a 1-km² grid using a 2D, inverse-distance-squared, octant search on log₁₀ Chl *a* to achieve normality. LTA Chl *a* for September was derived using data from 35 flights (n = 245,000 observations). Statistical analyses used SAS version 9.1 (Cary, NC); outputs were mapped in Surfer version 8.0 (Golden, CO).

Shipboard data for biological and hydrographic properties were obtained from EPA's Chesapeake Bay Program (CBP) monitoring cruises (<http://www.chesapeakebay.net>), mainly for eight stations in the central channel of the mid-Bay (39.0° to 37.9° N) visited 2-3 days before (15-16 September) and a week after (23-24 September) Isabel's passage (Fig. 5.1a). Storm conditions prevented sampling from 37.2° - 37.9° N latitude in the weeks surrounding Isabel. Water column structure was described by vertical density difference, $\Delta\sigma_t$ (kg m^{-3}), computed as bottom density minus surface density. The lower pycnocline depth from CBP was used to define the surface mixed layer. Simple, linear regressions of bathymetrically-weighted values of water-column Chl *a* on \log_{10} surface Chl *a* were applied to remotely-sensed Chl *a* to quantify water-column Chl *a* for each 1-km² grid cell (Harding et al., 1994). These outputs were summed to estimate total Chl *a*. PP was determined from a depth-integrated model applied to remotely sensed Chl *a* and ancillary data from the closest monitoring cruise (cf. Harding et al., 2002). Floral composition for the bloom region (38.4° – 37.2° N) was quantified from HPLC pigment reconstructions for major phytoplankton taxa as fractions of Chl *a* (Adolf et al., 2006). Sampling for pigments was conducted 25 days prior to the storm and 15 days after the storm.

Results

The LTA for Chl *a* in September shows a north to south decrease along the main axis of Chesapeake Bay (Fig. 5.1a). The Bay-wide mean Chl *a* one week prior to Hurricane Isabel was 8.7 mg Chl *a* m⁻³ with slightly elevated Chl *a* in the upper Bay (Fig. 5.1b). Six days after Isabel (13 d after the last flight), Chl *a* in the region

between the Patuxent (38.4° N) and York (37.2° N) river mouths increased to 200% of the LTA for a 900 km² area, and averaged 178% of the LTA for the entire 3232 km² bloom region (Fig. 5.1c). The mean Chl *a* increase between pre- and post-Isabel flights was ~ 4.7 mg m⁻³ (Table 5.1). Average Chl *a* in the bloom region was 13.7 mg m⁻³, the third highest of 35 flights conducted since 1990. Aircraft (2 October; Fig. 5.1d) and shipboard (2-4 October; not shown) Chl *a* documented a rapid decrease to average fall concentrations two weeks after Isabel (range 4.7-11.8 mg Chl *a* m⁻³; mean 7.7 mg Chl *a* m⁻³). PP was not exceptional for fall in the mid- to lower Bay prior to Isabel, but PP increased by 29% 13 days after the storm (Table 5.1).

Floral composition of the bloom region for fall is typically dominated by diatoms (56%) and cryptophytes (30%), with cyanobacteria (6%) and dinoflagellates (4%) making minor contributions (Fig. 5.2a). Three weeks prior to Isabel, a mixed community was observed including above-average dinoflagellates (39%) and cyanobacteria (23%; Fig. 5.2b). After Isabel, floral composition more closely resembled the LTA as diatoms were most prevalent (55%), followed by dinoflagellates (17%), cryptophytes (15%), and cyanobacteria (9%; Fig. 5.2c).

Multiple lines of evidence suggest the lower Bay was de-stratified by the passage of Isabel, mixing nutrients into the euphotic layer to support the rapid increase of Chl *a* I observed. Above-average concentrations of dissolved inorganic nitrogen (DIN = NO₂⁻ + NO₃⁻ + NH₄⁺) were evident in both surface (Fig. 5.3a) and bottom (Fig. 5.3b) layers of the northern half of the Bay (>38.5° N) in September 2003. However, surface DIN in the bloom region (hatched areas Figs. 5.3a, 5.3b) prior to the storm was near the LTA, whereas bottom layer DIN was higher-than-average. After Isabel,

surface DIN increased and bottom DIN decreased to average values. The vertical density gradient, $\Delta\sigma_t$, decreased appreciably following the hurricane, consistent with vertical mixing that would disperse high DIN from bottom waters throughout the water column (Fig. 5.3c; Table 5.1). Additional evidence includes significant increases of both the average depth of the pycnocline and surface salinity in the mid-Bay after the hurricane (Table 5.1), and a 15% increase in the proportion of NH_4^+ in DIN to 55% in the surface mixed layer.

Discussion

Physical forcing by Hurricane Isabel generated a rapid and extensive fall bloom in mid- to lower Chesapeake Bay, consisting of increased Chl *a*, a shift of floral composition toward diatoms, and increased PP commensurate with increased biomass (Figs. 5.1, 5.2; Table 5.1). Nutrients mixed into the surface layer by Isabel supported the bloom at a time N is often limiting seaward of the Patuxent River mouth (Fisher et al., 1992). Ample DIN was present in the upper Bay to support phytoplankton, but light-limitation precluded an increase of biomass in that region. The transition from light- to N-limitation along the Bay's axis in summer/fall is largely controlled by the magnitude of freshwater flow from the Susquehanna River (Harding, 1994). Hydrologic conditions (i.e., high precipitation and freshwater flow) in the months preceding Isabel delivered suspended material and CDOM into the upper Bay, producing a shallow euphotic layer that defined the northern limit of the bloom.

Floral composition prior to Isabel (Fig. 5.2b) consisted of a mixed community of several major taxa commonly observed in late summer for stratified waters of the mid- to lower Bay (Adolf et al., 2006). The 34% increase of diatoms after the storm

(Fig. 5.2c) coincided with an interruption of stratification and a pulse of nutrients to the euphotic layer. This change in community composition has implications for trophic transfer and organic matter cycling (Malone, 1992), manifested as an early onset of hypoxia in deep waters of the main stem Bay in 2004. Increased PP following Isabel (Table 5.1) is consistent with the findings of Yeager et al. (2005) who described elevated PP in the lower Bay in response to a wind event that delivered NH_4^+ to the surface layer.

Nutrient remineralization in the bottom layer and subsequent reintroduction to the surface layer support the annual PP maximum in summer, when freshwater flow is generally low (Malone, 1992). Data suggest an analogous process supported high Chl *a* and PP in the fall bloom after Isabel. Prior to the hurricane, bottom-layer DIN in the bloom region was higher than the LTA due to record flow that fertilized the mid- to lower Bay (Acker et al., 2005). Surface-layer DIN increased after Isabel, indicating nutrients at above-average concentrations in bottom waters were mixed into the surface layer (Fig. 5.3a, 5.3b). Increased surface salinities were consistent with mixing of high-salinity bottom water into the surface layer and an intrusion of ocean water from storm surge. I reason that the proportion of NH_4^+ in surface layer DIN points to bottom water as the predominant N source. DIN in runoff is mostly NO_3^- (Yeager et al., 2005), and delivery of DIN from a pulse of freshwater to the bloom area would have a time lag of weeks to months. The decrease of $\Delta\sigma_t$ after the storm (Table 5.1) is also consistent with mixing associated with Isabel's passage.

Water column stratification was strong ($\Delta\sigma_t = 7.7 \text{ kg m}^{-3}$) before Isabel because of high freshwater flow in spring and summer 2003 (Fig. 5.3c). Sustained, strong winds

from the south eroded stratification of the mid- to lower Bay. Shipboard observations conducted six days after the storm showed partial re-stratification in the bloom region, but hindcast simulations by Li et al. (2006) showed the water column was completely mixed by Isabel. Model outputs were also consistent with rapid restratification shortly after the hurricane due to large horizontal salinity gradients (Li et al., 2006). Vertical mixing was essential to provide DIN to the surface mixed layer and support the bloom I observed, and re-stratification was also critical to retain phytoplankton in well-illuminated surface waters. The rapid formation and cessation of the post-Isabel bloom, together with nutrient and water column properties, suggest a phytoplankton response that was fueled by, and quickly assimilated nutrients mixed into the euphotic layer.

The increase of Chl *a* was reconciled with DIN input by mixing to test the validity of our hypothesized mechanism for the bloom. I estimated an increase of 61.9 tons Chl *a* in the bloom area (3232 km²) that would require 192 mg N m⁻² assuming N:Chl *a* (w/w) = 10 (Malone, 1992). Based on pre-storm DIN profiles for the northern half of the bloom region (<37.9°N), complete mixing of the water column would inject 387 mg N m⁻² into a euphotic layer averaging 3.8 m. These calculations show that vertical mixing could provide sufficient N to support the observed Chl *a* increase, with new biomass accounting for about half the DIN input. Probable fates of DIN not drawn down by phytoplankton growth include export to the coastal ocean, uptake by bacteria, remaining DIN in the surface layer, and the fraction assimilated into zooplankton by herbivory.

The use of ocean color remote sensing to detect a significant perturbation of phytoplankton dynamics by passage of Hurricane Isabel draws on the unique capabilities of aircraft to give high-resolution, quasi-synoptic coverage of estuarine and coastal waters. The broader importance of our findings is a clear demonstration of how rapid response capabilities allow us to observe ecosystem-scale effects of climate forcing, using sustained, long-term observations of key ecosystem variables to provide the context needed to resolve these effects.

Conclusions

Hurricane Isabel evoked a rapid increase of phytoplankton biomass as Chl *a* covering ~3000 km² in the mid- to lower Chesapeake Bay. Wind mixing of bottom-water nutrients into the euphotic layer during a time of year that phytoplankton are N-limited supported this unusually strong fall bloom dominated by diatoms. This event constituted a rare perturbation of the annual phytoplankton cycle I observed as abrupt responses of Chl *a*, floral composition, and PP. Expectations of more frequent and intense hurricanes in the near future accentuate the need to understand biological responses to climatic perturbations such as those described here.

Acknowledgements. The authors thank Bill Boicourt, Jim Cloern, Ed Houde, Dave Kimmel, Ming Li, Mike Lomas, Mike Mallonee, Hans Paerl, and Mike Roman for helpful contributions. Support from NASA, NOAA, NSF, and EPA is gratefully acknowledged. WDM was supported by a NASA Earth System Science Fellowship. Contribution No. 3945 of the University of Maryland Center for Environmental Science.

References

- Acker, J.G., L.W. Harding, G. Leptoukh, T. Zhu, and S. Shen. 2005. Remotely-sensed chl a at the Chesapeake Bay mouth is correlated with annual freshwater flow to Chesapeake Bay. *Geophys. Res. Lett.*, 32, L05601, doi:10.1029/2004GL021852.
- Adolf, J.E., C.L. Yeager, W.D. Miller, M.E. Mallonee, and L.W. Harding Jr. 2006. Environmental forcing of phytoplankton floral composition, biomass, and primary productivity in Chesapeake Bay, USA. *Estuar. Coast. Shelf Sci.*, 67, 108-122.
- Campbell, J.W., and W.E. Esaias. 1983. Basis for spectral curvature algorithms in remote sensing of chlorophyll. *Appl. Opt.*, 22, 1084-1093.
- Cloern, J.E., T.S. Schraga, C.B. Lopez, N. Knowles, R. Grover Labiosa, and R. Dugdale. 2005. Climate anomalies generate an exceptional dinoflagellate bloom in San Francisco Bay. *Geophys. Res. Lett.*, 32, L14608, doi:10.1029/2005GL023321.
- Davis, A., and X.-H. Yan. 2004. Hurricane forcing on chlorophyll-a concentration off the northeast coast of the U.S. *Geophys. Res. Lett.*, 31, L17304, doi:10.1029/2004GL020668.
- Fisher, T.R., E.R. Peele, J.W. Ammermann, and L.W. Harding, Jr. 1992. Nutrient limitation of phytoplankton in Chesapeake Bay. *Mar. Ecol. Prog. Ser.*, 82, 51-63.
- Harding, Jr., L.W. 1994. Long-term trends in the distribution of phytoplankton in Chesapeake Bay: roles of light, nutrients, and streamflow. *Mar. Ecol. Prog. Ser.*, 104, 267-291.
- Harding, L.W., E.C. Itsweire, and W.E. Esaias. 1994. Estimates of phytoplankton biomass in the Chesapeake Bay from aircraft remote sensing of chlorophyll concentrations, 1989-92. *Remote Sen. Environ.*, 49, 41-56.
- Harding, L.W., E.C. Itsweire, and W.E. Esaias. 1995. Algorithm development for recovering chlorophyll concentrations in the Chesapeake Bay using aircraft remote sensing, 1989-91. *Photogramm. Eng. Remote Sens.*, 61, 177-185.
- Harding, Jr., L.W., M.E. Mallonee, and E.S. Perry. 2002. Toward a predictive understanding of primary productivity in a temperate, partially stratified estuary. *Est. Coast. Shelf Sci.*, 55, 437-463.
- Li, M., L. Zhong, W.C. Boicourt, S. Zhang, and D. Zhang. 2006. Hurricane induced storm surges, currents, and destratification in a semi-enclosed Bay. *Geophys. Res. Lett.*, 33, L02604, doi:10.1029/2005GL024992.

- Malone, T.C. 1992. Effects of water column processes on dissolved oxygen, nutrients, phytoplankton and zooplankton, p. 61-112. In D.E. Smith, M. Leffler, and G. Mackiernan [eds.]. *Oxygen Dynamics in the Chesapeake Bay: A Synthesis of Recent Research*. Maryland Sea Grant Program.
- Paerl, H.W., J.D. Bales, L.W. Ausley, C.P. Buzzelli, L.B. Crowder, L.A. Eby, J.M. Fear, M. Go, B.L. Peierls, T.L. Richardson, and J.S. Ramus. 2001. Ecosystem impacts of three sequential hurricanes (Dennis, Floyd, and Irene) on the United States' largest lagoonal estuary, Pamlico Sound, NC. *Proc. Natl. Acad. Sci.*, 98, 5655-5660.
- Roman, M.R., J.E. Adolf, J. Bichy, W.C. Boicourt, L.W. Harding, Jr., E.D. Houde, S. Jung, D.G. Kimmel, W.D. Miller, and X. Zhang. 2005. Chesapeake Bay plankton and fish abundance enhanced by Hurricane Isabel. *EOS Trans. AGU* 86, 261, 265.
- Webster, P.J., G.J. Holland, J.A. Curry, and H.-R. Chang. 2005. Changes in Tropical Cyclone Number, Duration, and Intensity in a Warming Environment. *Science* 309, 1844-1846.
- Yeager, C.L., L.W. Harding, Jr., and M.E. Mallonee. 2005. Phytoplankton production, biomass and community structure following a summer nutrient pulse in Chesapeake Bay. *Aquat. Ecol.*, 39, 135-149.
- Zubkoff, P.L., and J.E. Warinner III. 1977. The effect of Tropical Storm Agnes as reflected in chlorophyll a and heterotrophic potential of the lower Chesapeake Bay, p. 368-387. In J. Davis, B. Laird [eds.]. *The Effects of Tropical Storm Agnes on the Chesapeake Bay Estuarine System*. The Johns Hopkins University Press.

Table 5.1. Phytoplankton and hydrographic data before and after Hurricane Isabel.

Variable	Before	After	Difference
PP (mg C m ² d ⁻¹) ^a	914	1179	265*
Chla (mg m ⁻³) ^a	8.7	13.4	4.7*
Total Biomass (tons) ^a	179	241	62*
Salinity ^b	10.3	12.0	1.7*
Pycnocline (m) ^b	13.9	26.2	12.2*
$\Delta \sigma_t$ (kg m ⁻³) ^b	7.7	3.3	-4.3*

^a from aircraft remote sensing in bloom region

^b from CBP pre- and post Isabel monitoring

* significant at $p < 0.001$ (paired Student's t-test)

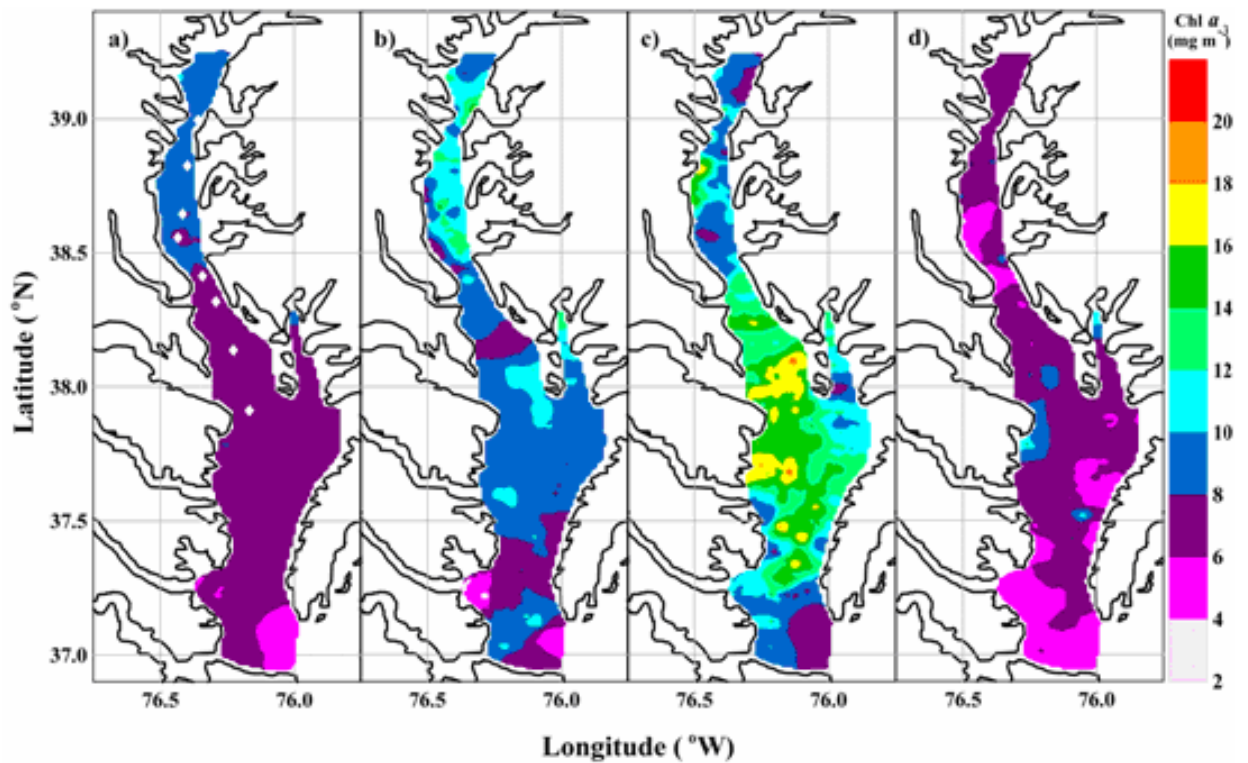
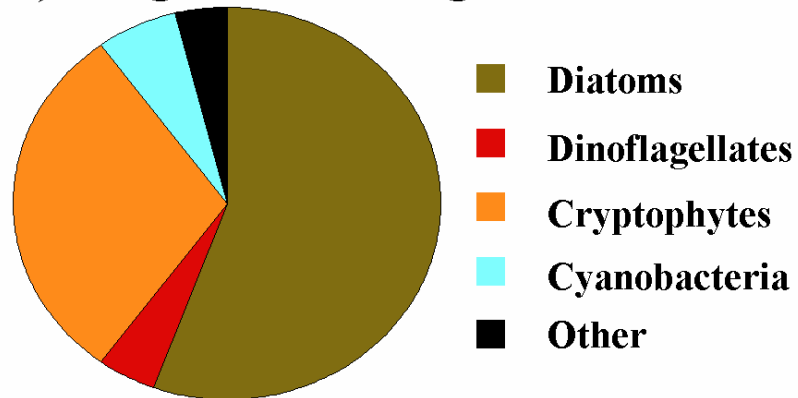
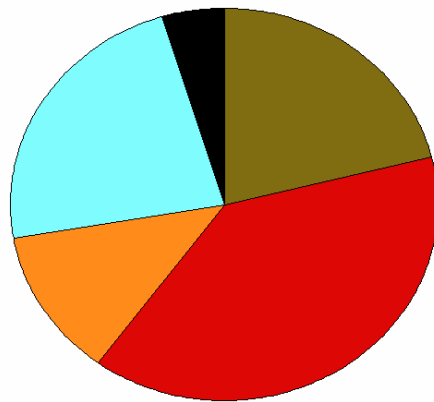


Fig. 5.1. Phytoplankton biomass as Chl*a*: a) LTA for September 1989-04; b) pre-Isabel, 11 September; c) post-Isabel, 24 September and d) two weeks post-Isabel, 2 October. Diamonds in first panel show CBP stations used in analyses.

a) Long-Term Average



b) Pre-Isabel



c) Post-Isabel

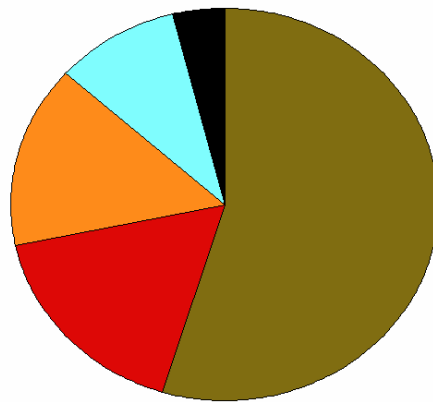


Fig. 5.2. Floral composition in bloom region as percent of Chla: a) LTA for fall (1995-2000); b) pre-Isabel (24 August); c) post-Isabel (3 October).

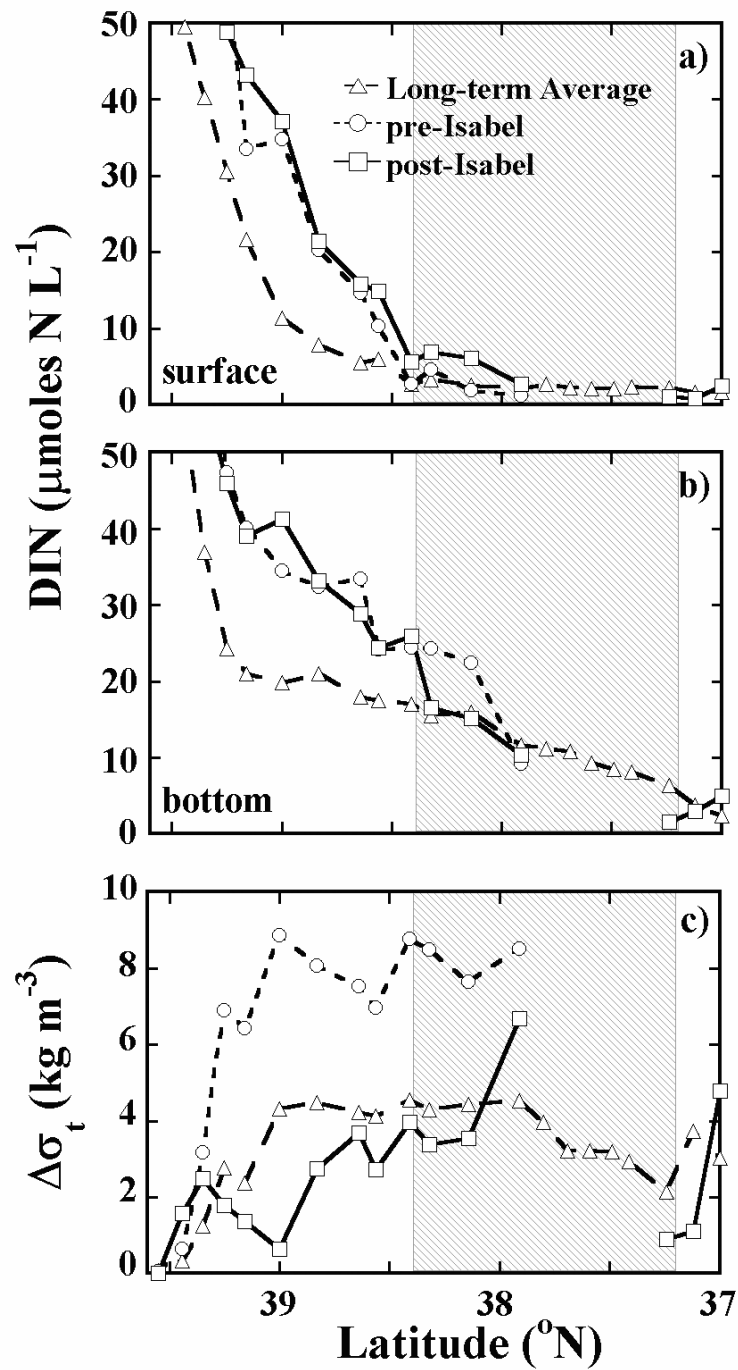


Fig. 5.3. a) DIN in the surface layer, and b) bottom layer; c) $\Delta\sigma_t$ from CBP cruises. Hatched area indicates bloom region.

Chapter 6

Conclusions

Several conclusions can be drawn from this Dissertation. First, climate is a strong regulator of ecosystem dynamics in Chesapeake Bay and regional-scale climate defined by a synoptic climatology successfully quantifies that variability. Second, characteristics of the spring phytoplankton bloom (timing, position, magnitude) can be predicted from winter weather conditions through their influence on precipitation and freshwater flow. Third, variability of summer and annual integral production can be explained by climate during the preceding winter-spring. These analyses of climate forcing of Chl *a* and PP support predictive models that explain significant amounts of the variance of these important ecosystem properties. Lastly, event-scale climate perturbations, such as hurricanes, can also have significant impacts on Chesapeake Bay phytoplankton dynamics with ramifications for seasonal and regional carbon cycling.

An essential component of this research was the availability of highly resolved Chl *a* and PP data. The time series of ocean color data collected from aircraft as part of the Chesapeake Bay Remote Sensing Program (CBRSP) is unique in its length of operation (1989-present), number of flights (>350 and counting), and spatial coverage (~7000 km²) (Harding et al., 2001). As retrievals from satellite remote sensing mature for the coastal zone through improved atmospheric correction and algorithms, a transition to space-based remote sensing should: (1) increase the frequency of repeat coverage (>80 scenes yr⁻¹); (2) expand the spatial scales over which measurements are made; (3) reduce the logistical and financial difficulties associated with maintaining an aircraft remote sensing program. Activities are currently underway to correct/reprocess SeaWiFS and MODIS data to achieve these goals and provide a

satellite-based time series back to August 1997. These time series offer the potential to explore climate forcing of the coastal ocean (Acker et al., 2005).

The use of synoptic climatology to describe climate variability and its impacts on ecosystems has increased in the last decade (Yarnal et al., 2001). By definition, synoptic climatology is the relationship between atmospheric circulation and the surface environment that includes a wide variety of physical, chemical, and biological variables (Yarnal, 1993). Outside of Chesapeake Bay, most applications have related atmospheric circulation to freshwater flow (Cayan and Peterson, 1993; Wilby, 1993) and other physical parameters, like air mass trajectories (Greene et al., 1999). Few have examined biological responses to atmospheric forcing. In Chesapeake Bay, this approach has been used to explain recruitment success of estuarine fishes that exhibit distinct spawning strategies (Wood, 2000), and to predict abundances and distributions of two ecologically important calanoid copepod species (Kimmel et al., 2006). The development and application of a synoptic climatology for the Chesapeake Bay region described in this Dissertation, including a reconciliation of weather patterns with precipitation and flow, and a detailed analysis of climate forcing of phytoplankton, significantly extends this approach. This is an area ripe for more interdisciplinary research to connect climate and biology.

I believe the regional synoptic climatology may prove useful to describe ecosystem responses in neighboring estuaries of the Mid-Atlantic, including Delaware Bay, Neuse River/Pamlico Sound, and the Hudson River. These estuaries are all similarly influenced by freshwater flow (Pennock, 1985; Rudek et al., 1991; Malone, 1977), and experience weather from the same general domain (25-50°N x

65-100°W) as the synoptic climatology developed in this Dissertation. Chapter 2 describes the methodology to develop a synoptic climatology centered on any area where data are available, making the approach adaptable and relevant. Surface sea-level pressure data are readily available for most of the northern hemisphere since 1950, so the limiting factor will often be time series for the surface environment, i.e., data for variables potentially subject to climate forcing. These types of comparisons should give us insight to the generality or specificity of regional-scale climate forcing of estuarine ecosystem dynamics.

I have documented climate forcing as a dominant source of seasonal and interannual variability of Chl *a* and PP in Chesapeake Bay. The relationships I report can be exploited to hindcast Chl *a* and PP for time periods for which I have less highly resolved data in a manner analogous to that described by Harding and Perry (1997), wherein present day salinity, temperature, and freshwater flow were used to model Chl *a*. These models were then applied to historical salinity, temperature, and freshwater flow data for periods when Chl *a* was infrequently collected to assess trends. Available data for those time periods were then compared to model results and discrepancies ascribed to the effects of nutrient overenrichment. Data used to determine atmospheric circulation from the synoptic climatology, i.e., surface sea-level pressures, are available from 1950 and possibly earlier for the region, making it feasible to hindcast Chl *a* and PP for periods when actual data were sparse. The resulting data could then be used to address questions of changing ecosystem responses to climate forcing and potentially to provide input data for fisheries production models.

The general appreciation of climate influences on estuarine, coastal, and oceanic ecosystems is documented by an increase in publications on the topic, most frequently in the context of climate change (Harley et al., 2006). While the physical changes associated with climate change are still highly uncertain for most regions (Najjar et al., 2000), it is prudent to understand the potential direction and magnitude of ecosystem responses to such perturbations. Using long-term observations for contrasting climatic extremes is an established way to quantify the potential ecosystem responses to hypothesized climate change (Cloern, 1991). The research I describe in this Dissertation provides a way to explore potential ecosystem responses. Chapters 3 and 4 highlighted the importance of winter-spring climate on seasonal to interannual variability of Chl *a* and PP. This is also the time frame expected to show the greatest response to climate change (Neff et al., 2000). Most climate change scenarios predict warmer and wetter conditions during the winter-spring (Najjar, 1999). These changes will translate to increased frequencies of warm/wet weather patterns (patterns 1, 3, 4, and 8). Warmer and wetter conditions during winter-spring generate increased spring Chl *a* covering a larger area, located farther down-estuary, and occurring later in the spring. These climate conditions would also likely result in high annual and summer integral production (AIP, SIP) in the absence of a declining trend in photic depth. As general circulation model (GCM) results converge on a single expected outcome, our ability to predict the phytoplankton response will also improve.

In addition to potential climate change, quantifying the effects of eutrophication will become increasingly difficult in highly dynamic estuarine environments that are

increasingly influenced by event-scale climate perturbations such as hurricanes (Paerl et al., 2001; 2006), that may be increasing in frequency in the Atlantic in coming decades (Webster et al., 2005). These perturbations can have lasting effects through changes in water residence time, inputs of organic matter from the watershed, and changes in distribution of ecologically important species (Paerl et al., 2001; Roman et al., 2005). Adequate characterization of how climate forces phytoplankton dynamics (event, seasonal, interannual) will be required if they are to be used as indicators of ecosystem status (Paerl et al., 2003).

Research on climate forcing of phytoplankton dynamics in Chesapeake Bay has been dominated by descriptions of Chl *a* and to a lesser degree PP (Malone et al., 1988; Jordan et al., 1991; Harding, 1994; Malone, 1992; Harding and Perry, 1997; Boynton and Kemp, 2000; Harding et al., 2002), while studies of climate forcing of floral composition (Marshall and Nesius, 1996; Adolf et al., 2006) and cell size structure are relatively sparse. Assimilating information on floral composition and size structure into our analyses of phytoplankton responses to climate forcing should improve our ability to accurately forecast effects of natural and anthropogenic perturbations (Cloern, 2001). In addition to climate forcing of phytoplankton dynamics that was the focus of my work, there is a large and growing literature on climate forcing of other trophic levels in Chesapeake Bay, including zooplankton (Kimmel and Roman, 2004; Kimmel et al., 2006), gelatinous zooplankton (Purcell and Decker, 2005), and fish (Wood, 2000; North and Houde, 2003). Our understanding of ecosystem responses to climate variability and change will assuredly benefit from a synthesis of these findings.

References

- Acker, J.G., L.W. Harding, G. Leptoukh, T. Zhu, and S. Shen. 2005. Remotely-sensed chl a at the Chesapeake Bay mouth is correlated with annual freshwater flow to Chesapeake Bay. *Geophys. Res. Lett.*, 32, L05601, doi:10.1029/2004GL021852.
- Adolf, J.E., C.L. Yeager, W.D. Miller, M.E. Mallonee, L.W. Harding Jr. 2006. Environmental forcing of phytoplankton floral composition, biomass, and primary productivity in Chesapeake Bay, USA. *Estuar. Coast. Shelf Sci.*, 67, 108-122.
- Boynton, W.R. and W.M. Kemp. 2000. Influence of river flow and nutrient load on selected ecosystem processes, p. 269-298. In J.E. Hobbie [ed.]. *Estuarine Science: A synthetic approach to research and practice*. Island Press.
- Cayan, D.R. and D.H. Peterson. 1993. Spring climate and salinity in the San Francisco Bay Estuary. *Water Resour. Res.*, 29, 293-303.
- Cloern, J.E., 1991. Annual variations in river flow and primary production in the south San Francisco Bay estuary, p. 91-96. In M. Elliot and D. Ducrotoy, [eds.]. *Estuaries and Coasts: Spatial and Temporal Intercomparisons*. Olsen and Olsen Publisher.
- Cloern, J.E. 2001. Our evolving conceptual model of the coastal eutrophication problem. *Mar. Ecol. Prog. Ser.*, 210, 223-253.
- Greene, J.S., L.S. Kalkstein, H. Ye, and K. Smoyer. 1999. Relationship between synoptic climatology and atmospheric pollution at four US cities. *Theoretical and Applied Climatology* 62, 163-174.
- Harding, Jr., L.W. 1994. Long-term trends in the distribution of phytoplankton in Chesapeake Bay: roles of light, nutrients, and streamflow. *Mar. Ecol. Prog. Ser.*, 104, 267-291.
- Harding, Jr., L.W. and E.S. Perry. 1997. Long-term increases of phytoplankton biomass in Chesapeake Bay, 1950-1994. *Mar. Ecol. Prog. Ser.*, 157, 39-52.
- Harding, Jr., L.W., W.D. Miller, R.N. Swift, and C.N. Wright. 2001. Aircraft remote sensing, p. 113-122. In J.H. Steele, S.A. Thorpe, and K.K. Turekian [eds.]. *Encyclopedia of Ocean Sciences*. Academic Press.
- Harding, Jr., L.W., M.E. Mallonee, and E.S. Perry. 2002. Toward a predictive understanding of primary productivity in a temperate, partially stratified estuary. *Est. Coast. Shelf Sci.*, 55, 437-463.

- Harley, C.D.G., A.R. Hughes, K.M. Hultgren, B.G. Miner, C.J.B. Sorte, C.S. Thornber, L.F. Rodriguez, L. Tomanek, and S.L. Williams. 2006. The impact of climate change in coastal marine systems. *Ecol. Lett.*, 9, 228-241.
- Jordan, T.E., D.L. Correll, J. Miklas, and D.E. Weller. 1991. Long-term trends in estuarine nutrients and chlorophyll, and short-term effects of variation in watershed discharge. *Mar. Ecol. Prog. Ser.*, 75, 121-132.
- Kimmel, D.G. and M.R. Roman. 2004. Long-term trends in mesozooplankton abundance in Chesapeake Bay, USA: influence of freshwater input. *Mar. Ecol. Prog. Ser.*, 267, 71-83.
- Kimmel, D.G., W.D. Miller, and M.R. Roman. 2006. Regional scale climate forcing of mesozooplankton dynamics in Chesapeake Bay. *Estuaries* (in press).
- Malone, T.C. 1977. Environmental regulation of phytoplankton productivity in the Lower Hudson estuary. *Est. Coast. Mar. Sci.*, 5, 157-171.
- Malone, T.C., L.H. Crocker, S.E. Pike, and B.W. Wendler. 1988. Influences of river flow on the dynamics of phytoplankton production in a partially stratified estuary. *Mar. Ecol. Prog. Ser.*, 48, 235-249.
- Malone, T.C. 1992. Effects of water column processes on dissolved oxygen, nutrients, phytoplankton and zooplankton, p. 61-112. In D.E. Smith, M. Leffler, and G. Mackiernan [eds.]. *Oxygen Dynamics in the Chesapeake Bay: A Synthesis of Recent Research*. Maryland Sea Grant Program.
- Marshall, H.G. and K.K. Nesius. 1996. Phytoplankton composition in relation to primary production in Chesapeake Bay. *Mar. Bio.*, 125, 611-617.
- Najjar, R.G. 1999. The water balance of the Susquehanna River Basin and its response to climate change. *J. Hydrol.*, 219, 7-19.
- Najjar, R.G., H.A. Walker, P.J. Anderson, E.J. Barron, R.J. Bord, J.R. Gibson, V.S. Kennedy, C.G. Knight, J.P. Megonigal, R.E. O'Connor, C.D. Polsky, N.P. Psuty, B.A. Richards, L.G. Sorenson, E.M. Steele, and R.S. Swanson. 2000. The potential impacts of climate change on the mid-Atlantic coastal region. *Clim. Res.*, 14, 219-233.
- Neff, R., H. Chang, C. G. Knight, R. G. Najjar, B. Yarnal, and H. Walker. 2000. Impact of climate variation and change on Mid-Atlantic region hydrology and water resources. *Clim. Res.*, 14, 207-218.
- North, E.W. and E.D. Houde. 2003. Linking ETM physics, zooplankton prey, and fish early-life histories to striped bass *Morone saxatilis* and white perch *M. Americana* recruitment. *Mar. Ecol. Prog. Ser.*, 260, 219-236.

- Paerl, H.W., J.D. Bales, L.W. Ausley, C.P. Buzzelli, L.B. Crowder, L.A. Eby, J.M. Fear, M. Go, B.L. Peierls, T.L. Richardson, and J.S. Ramus. 2001. Ecosystem impacts of three sequential hurricanes (Dennis, Floyd, and Irene) on the United States' largest lagoonal estuary, Pamlico Sound, NC. *Proc. Natl. Acad. Sci.*, 98, 5655-5660.
- Paerl, H.W., L.M. Valdes, J.L. Pinckney, M.F. Piehler, J. Dyble, and P.H. Moisander. 2003. Phytoplankton photopigments as indicators of estuarine and coastal eutrophication. *BioScience* 53, 953-964.
- Paerl, H.W., L.M. Valdes, B.L. Peierls, J.E. Adolf, and L.W. Harding Jr. 2006. Anthropogenic and climatic influences on the eutrophication of large estuarine ecosystems. *Limnol. Oceanogr.*, 51, 448-462.
- Pennock, J.R. 1985. Chlorophyll distributions in the Delaware Estuary: regulation by light limitation. *Est. Coast. Shelf Sci.*, 21, 711-725.
- Purcell, J.E. and M.B. Decker. 2005. Effects of climate on relative predation by scyphomedusae and ctenophores on copepods in Chesapeake Bay during 1987-2000. *Limnol. Oceanogr.*, 50, 376-387.
- Roman, M.R., J.E. Adolf, J. Bichy, W.C. Boicourt, L.W. Harding, Jr., E.D. Houde, S. Jung, D.G. Kimmel, W.D. Miller, and X. Zhang. 2005. Chesapeake Bay plankton and fish abundance enhanced by Hurricane Isabel. *EOS Trans. AGU* 86, 261, 265.
- Rudek J., H.W. Paerl, M.A. Mallin, and P.W. Bates. 1991. Seasonal and hydrological control of phytoplankton nutrient limitation in the lower Neuse River Estuary, North Carolina. *Mar. Ecol. Prog. Ser.*, 75, 133-142.
- Webster, P.J., G.J. Holland, J.A. Curry, and H.-R. Chang. 2005. Changes in Tropical Cyclone Number, Duration, and Intensity in a Warming Environment. *Science* 309, 1844-1846.
- Wilby, R.L. 1993. The influence of variable weather patterns on river water quantity and quality regimes. *Int. J. Climatol.*, 13, 227-241.
- Wood, R.J. 2000. Synoptic scale climate forcing of multispecies fish recruitment patterns in Chesapeake Bay. PhD. Dissertation. College of William and Mary.
- Yarnal, B. 1993. *Synoptic Climatology in Environmental Analysis*, Belhaven Press.
- Yarnal, B., A.C. Comrie, B. Frakes, and D.P. Brown. 2001. Developments and prospects in synoptic climatology. *Int. J. Climatol.*, 21, 1923-1950.